

2

D 10.75

WANL-PR(LL)-040
DECEMBER 1971



Westinghouse Astronuclear Laboratory

FINAL PROGRESS REPORT

CR-123600

Contract No. NAS-8-27047

Control No. DCN 1-1-80-00072

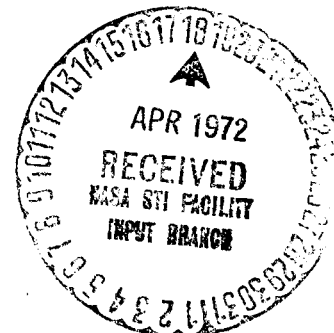
IMPLEMENTATION OF RADIATION SHIELDING CALCULATION METHODS

VOLUME 1

SYNOPSIS OF METHODS AND SUMMARY OF RESULTS

(NASA-CR-123600) IMPLEMENTATION OF RADIATION SHIELDING CALCULATION METHODS. VOLUME 1: SYNOPSIS OF METHODS AND SUMMARY OF RESULTS M.A. Capo, et al (Westinghouse Electric Corp.) Dec. 1971 173 p CSCL 18F G3/22	N72-24687 Unclas 27343
--	----------------------------------

Reproduced by
**NATIONAL TECHNICAL
INFORMATION SERVICE**
U S Department of Commerce
Springfield VA 22151



WESTINGHOUSE
ASTRONUCLEAR
LABORATORY

WANL-PR(LL)-040
DECEMBER 1971

FINAL PROGRESS REPORT

Contract No. NAS-8-27047
Control No. DCN 1-1-80-00072

IMPLEMENTATION OF RADIATION SHIELDING
CALCULATION METHODS

VOLUME 1

SYNOPSIS OF METHODS AND SUMMARY OF RESULTS

Prepared By:

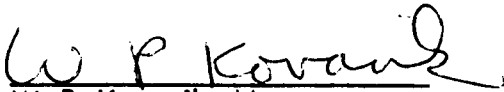


M. A. Capo
Nuclear Analysis Department



R. K. Disney
Nuclear Analysis Department

Approved By:



W. P. Kovacik, Manager
Nuclear Analysis Department

ACKNOWLEDGEMENT

The writers wish to acknowledge the technical guidance provided by Mr. Henry E. Stern and Dr. Martin O. Burrell of the Space Science Laboratory, George C. Marshall Space Flight Center, the technical monitors of this contract.

The writers also appreciate the able assistance and diligent effort of Mr. John Watts of the Space Science Laboratory in setting up, running, and preparing printed output of the numerous computer code jobs at MSFC.

ABSTRACT

This report is Volume 1 of two volumes of the final report on "Implementation of Radiation Shielding Calculation Methods". This volume summarizes the work performed under this contract in the following areas:

- (1) Analysis of realistic nuclear-propelled vehicle using the Marshall Space Flight Center computer code package. This code package includes one and two dimensional discrete ordinate transport, point kernel, and single scatter techniques, as well as, cross section preparation and data processing codes,
- (2) Development of techniques to improve the automated data transfer in the coupled computation method of the MSFC computer code package and improve the utilization of this code package on the MSFC UNIVAC-1108 computer system, and
- (3) Updating of the MSFC Master Data Libraries.

A brief description of the material employed during the MSFC Seminar/Workshop is included. This Seminar/Workshop provided detailed instructions on the application of the computer code package. Volume 2 of this report describes in detail the material employed during the Seminar/Workshop.

TABLE OF CONTENTS

<u>Section</u>		<u>Page</u>
1.0	Introduction	1-1
2.0	Summary and Recommendations	2-1
3.0	Analysis of a Realistic Nuclear-Propelled Vehicle Using the MSFC Computer Code Package (Task A)	3-1
3.1	Description of the Nuclear-Propelled Vehicle	3-1
3.2	Synopsis of Methods	3-2
3.2.1	Method of Analysis	3-2
3.2.2	Description of Computer Codes and Basic Data Libraries	3-5
3.3	Results of Analysis	3-17
3.3.1	Transport Analysis of the Nuclear Subsystem	3-17
3.3.2	External Radiation Environment	3-19
3.3.3	Crew Dose Analysis	3-21
4.0	Description of the Seminar/Workshop (Task B)	4-1
5.0	Techniques to Improve the Automated Coupling and Utilization of the MSFC Computer Code Package (Task C)	5-1
5.1	Modification of the APPROPOS Code	5-1
5.2	Modification to the ANISN-W Code	5-2
5.3	The CHEAPER Code	5-3
5.4	The LHAP Code	5-4
6.0	Updating of MSFC Master Libraries (Task D)	6-1
6.1	Update of Neutron Cross Section Data (Master Libraries 1, 2 and 3)	6-1
6.2	Update of Photon Production Library (Master Library 6)	6-3
6.2.1	Neutron Capture Photon Production Data	6-3
6.2.2	Neutron Inelastic Scatter Photon Production Data	6-4
7.0	References	

TABLE OF CONTENTS (CONT)

<u>Section</u>	<u>Page</u>
Appendix A - The CHEAPER Code	A-1
A.1 Computer Code Synopsis	A-1
A.2 Input Data Instructions	A-3
A.2.1 Input Format	A-3
A.2.2 Input Data Instructions	A-3
A.3 Detailed Input Data Instructions	A-3
A.3.1 Problem Size Determination	A-3
A.3.2 Discussion of Calculation Options	A-4
A.3.3 Other Useful Information	A-9
A.4 Problem Setup Information	A-9
A.4.1 Tape Assignments	A-9
A.4.2 Running Time	A-10
A.4.3 Core Storage Requirements	A-10
A.4.4 Error Messages	A-10
A.5 Description of Output	A-11
A.5.1 Printout	A-11
A.5.2 Punched Output	A-13
A.5.3 Output Flux Tape	A-13
Appendix B - The LHAP Code	B-1
B.1 Computer Code Synopsis	B-1
B.2 Input Data Description	B-3
B.2.1 Input Format	B-3
B.2.2 Input Data Instructions	B-7
B.3 Detailed Input	B-8

TABLE OF CONTENTS (CONT)

<u>Section</u>		<u>Page</u>
Appendix B (Cont)		
B.4	Problem Setup Information	B-8
B.4.1	Tape Assignments	B-8
B.4.2	Running Time	B-9
B.4.3	Error Messages	B-9
B.5	Method of Solution	B-10

LIST OF FIGURES

<u>Figure</u>		<u>Page</u>
3-1	Schematic Model of the Nuclear-Propelled Vehicle Geometry	3-26
3-2	Nuclear Subsystem R-Z Geometry Model	3-27
3-3	Analytical Procedure for Calculating the Radiation Environment Internal to and on the Surface of the Nuclear Subsystem	3-28
3-4	Analytical Procedure for Calculating External Environment and Crew Dose	3-29
3-5	Fast ($E > 1.0$ Mev) Neutron Flux Traverse on the Midplane of the Nuclear Subsystem	3-30
3-6	Intermediate ($0.3 \text{ ev} < E < 1.0$ Mev) Neutron Flux Traverse on the Nuclear Subsystem	3-31
3-7	Thermal ($E < 0.3 \text{ ev}$) Neutron Flux Traverse on the Midplane of the Nuclear Subsystem	3-32
3-8	Total Neutron Flux Traverse on the Midplane of the Nuclear Subsystem	3-33
3-9	Fast ($E > 1.0$ Mev) Neutron Flux Traverse Near the Centerline of the Nuclear Subsystem	3-34
3-10	Intermediate ($0.3 \text{ ev} < E < 1.0$ Mev) Neutron Flux Traverse Near the Centerline of the Nuclear Subsystem	3-35
3-11	Thermal ($E < 0.3 \text{ ev}$) Neutron Flux Traverse Near the Centerline of the Nuclear Subsystem	3-36
3-12	Total Neutron Flux Traverse Near the Centerline of the Nuclear Subsystem	3-37
3-13	Photon Flux Traverse on the Midplane of the Nuclear Subsystem as Calculated by the DOT-IIW Code	3-38
3-14	Photon Flux Traverse Near the Centerline of the Nuclear Subsystem as Calculated by the DOT-IIW Code	3-39

LIST OF FIGURES (CONT)

<u>Figure</u>		<u>Page</u>
3-15	Comparison Between MAP and KAP-VI Calculated Fast ($E > 1.0$ Mev) Neutron Flux on the Meridian Ring at 30 Feet from the Center of the Core	3-40
3-16	Comparison Between MAP and KAP-VI Calculated Photon Dose Rate on the Meridian Ring at 30 Feet from the Center of the Core	3-41
3-17	Photon Dose Rate on the Centerline at the Crew Compartment Versus Time Prior to Empty Tank	3-42
3-18	Comparison Between the MAP-SCAP and KAP-VI-SCAP Crew Dose Rate Due to the Nuclear Subsystem Sources	3-43
3-19	Photon Energy Flux of Single Scattered Radiation at the Crew Location	3-44
6-1	Neutron Cross Section Weighting Spectra-Number Flux Versus Lethargy	6-5
6-2	Neutron Cross Section Weighting Spectra-Differential Flux Versus Lethargy	6-6
B-1	LHAP Input Formats	B-18

LIST OF TABLES

<u>Table</u>		<u>Page</u>
3-1	Material Compositions Employed to Describe the Propellant Tank and Command Module Geometry	3-45
3-2	Element Atom Densities for the Nuclear Subsystem Model for the MSFC Seminar/Workshop	3-46
3-3	Summary of the Master Libraries	3-47
3-4	Photon Sources in the Nuclear Subsystem Calculated by the NAGS Code	3-48
3-5	Fast Neutron ($E > 1.0$ Mev) Flux on the Thirty Foot Meridian Ring Calculated by the DOT-IIW-MAP Technique	3-49
3-6	Contribution of Source Regions to the Gamma Ray Dose Rate on the Meridian Ring	3-50
3-7	Crew Dose on the Centerline of the Command Module	3-51
3-8	Crew Dose Versus Time Prior to Empty Tank Condition - NSS Sources Only	3-52
3-9	SCAP Calculated Scattered Radiation by Zone to the Crew Location on Axis - NSS Sources Only	3-53
3-10	Contribution of Source Regions to the Gamma Ray Dose Rate at the Tank Top and in the Crew Compartment	3-54
6-1	Summary of Master Libraries	6-7
6-2	Transport Corrected Neutron Cross Section Sets In Master Library 1	6-8
6-3	P_1 Neutron Cross Section Sets In Master Library 2	6-13
6-4	Thermal Neutron Capture Gamma Production Spectra for APPROPOS-NAGS	6-28

LIST OF TABLES (CONT)

<u>Table</u>		<u>Page</u>
6-5	Basic Data Source for Thermal Neutron Capture Photon Production Spectra Data	6-35
6-6	Neutron Inelastic Photon Production Spectra	6-37
A-1	Input Instructions for the CHEAPER Code	A-14
B-1	Input Data Instructions for the LHAP Code	B-11
B-2	LHAP Boundary Equation Numbers and Equations	B-17

1.0 Introduction

This report is Volume 1 of two volumes of the final report on "Implementation of Radiation Shielding Calculation Methods". This work was performed under Contract NAS 8-27047 by the Westinghouse Astronuclear Laboratory. Presented in this volume are:

- Results of analysis of a realistic nuclear-propelled vehicle using the MSFC computer code package.
- A synopsis of the MSFC radiation shielding computer code package.
- Improvements in the MSFC computer codes and basic data libraries.

The MSFC radiation shielding computer code package and basic data libraries were developed during previous contracts NAS-8-24919 and NAS-8-20414.⁽¹⁻⁴⁾ Included in this code package are the following programs:

- GAMLEG-W to provide multigroup, photon transport cross sections.
- APPROPOS to process and spectral-weight multigroup, neutron cross section data and to process reaction rate data.
- NAGS to process multigroup neutron and photon flux distribution data.
- SATURN to process neutron cross section data using a minimum amount of core storage.
- ANISN-W, a multigroup, one-dimensional discrete ordinate transport code.
- DOT-IIW, a multigroup two-dimensional discrete ordinate transport code.
- MAP to calculate the energy and angular dependent radiation transport external to a source.
- DOQ and ADOQ to calculate, respectively, symmetric and asymmetric quadrature coefficients for ANISN-W and DOT-IIW.

- KAP-VI, a point kernel code.
- SCAP, a single scatter analysis code.

As part of this contract, implementation of the MSFC code package in the analysis of a nuclear-propelled vehicle configuration was completed. The computer code techniques, the vehicle geometry, and the results of this analysis are presented in Section 3.0.

Several techniques to improve the automated data transfer in the coupled computation methods of the MSFC computer code package and improve the utilization of this code package on the MSFC UNIVAC-1108 computer system were also developed as described in Section 5.0.

The MSFC basic data libraries were updated in the areas of: (1) hydrogen microscopic neutron cross section data, and (2) photon production data for neutron capture and inelastic scatter. The updated library data are presented in Section 6.0.

In addition, a four day Seminar/Workshop was conducted at MSFC to provide practical experience in the application of the MSFC computer code package. Volume 2 of this report provides descriptive material employed during the Seminar/Workshop.

2.0 SUMMARY AND RECOMMENDATIONS

Under this contract, Westinghouse Astronuclear Laboratory has: (1) implemented the computer code package supplied to MSFC in contracts NAS-8-20414 and NAS-8-24919⁽¹⁻⁴⁾ in an analysis of a nuclear propelled vehicle, (2) prepared and presented a Seminar/Workshop demonstrating the use of the MSFC computer code package to MSFC, NASA, and NASA contractor personnel, and (3) modified or updated portions of the MSFC computer code package to provide improved utilization of the MSFC computer code package on the MSFC UNIVAC-1108 computer system.

WANL has performed the contracted work through the execution of the following four tasks:

Task A - Analysis of a Realistic Nuclear Propelled Vehicle Using the MSFC Computer Code Package

In this task, WANL selected with the concurrence of the MSFC contracting office representative (COR) a realistic nuclear propelled vehicle model. This model included the nuclear subsystem, the nozzle assembly and propellant lines radiation source (CRAM), the propellant tank, and the command and control module. This vehicle model was converted into the appropriate analytical models required for the computer codes in the MSFC computer code package. An analysis of the radiation environment at the command and control module was conducted to demonstrate the use of individual codes in an analysis and the linkage of the codes by data transfer on cards and/or magnetic tape. This analysis was performed to provide material for presentation in Task B of this contract.

Task B - Conduct a Four (4) Day Seminar/Workshop at MSFC

In Task B of this contract, WANL has prepared a set of detailed Seminar/Workshop notes describing the input data preparation and job setup of the computer codes in the Task A effort. These notes supplemented by opaque presentation material were presented by WANL personnel to MSFC, NASA, and NASA contractor personnel at a four (4) day Seminar/Workshop presented at MSFC. This Seminar/Workshop demonstrated the use and

capability of the MSFC computer code package in performing radiation analyses required for nuclear propelled vehicle design studies and the general radiation analysis capability of the MSFC computer code package.

Task C - Investigation of Techniques to Improve the Automated Coupling and Utilization of the MSFC Computer Code Package on the MSFC UNIVAC-1108 Computer System

The Task C effort of this contract involved the modification of the APPROPOS and ANISN-W codes to provide an automated tape and/or punched card linkage with fewer tapes on a specific job. The number of tapes required by an APPROPOS job was reduced to a maximum of five (5) and a minimum of two (2) tapes. These modifications will normally improve the job turnaround time on the MSFC UNIVAC-1108 computer. A second effort in Task C was the addition of the CHEAPER data processing code to improve the use of DOT-IIW scalar flux tape output and the addition of the LHAP code for liquid hydrogen capture gamma ray analysis.

Task D - Review and Update of Current Neutron and Photon Cross Section Information in the MSFC Computer Code Package

In Task D of this contract, WANL reviewed the use of existing neutron and photon cross section data libraries of the MSFC computer code package in Task A type analysis. An update of neutron cross sections to include additional hydrogen neutron cross section sets and an expansion of the neutron scattering data to a full scatter-transfer matrix was made to improve the data library. In addition, a new set of photon production data due to neutron capture and neutron inelastic scatter were placed in the MSFC computer code package. These new data were used in the Task A analysis.

Recommendations

On the basis of the completed effort in this contract and the types of analyses required in the design of nuclear propelled stages a number of future study programs or specific additions to the MSFC computer code package are recommended. These are summarized as follows:

- (1) Extend the library of gamma ray production data in the MSFC Master Library No. 6 to
 - (a) Include neutron energy dependent capture gamma ray spectral data,
 - (b) Include additional element data in the inelastic neutron scatter gamma ray production library;
 - (c) Expand the inelastic gamma ray production data to 52 neutron energy groups to match the fine-group neutron library data.
- (2) Modify the APPROPOS code to perform a group-collapse and spectral-weighting of the Master Library No. 6 data developed in (c) above. With this modification, any broad-group, neutron-energy group structure can be obtained in the coupling calculation in the APPROPOS code.
- (3) Investigate the use of adjoint kernel techniques in the analysis of external radiation environment. The use of adjoint kernel techniques to solve for the angular dependent, adjoint boundary source for use in a DOT-IIW problem is one possible application. In addition, the alternate technique of using an adjoint kernel technique to calculate the adjoint solution to each mesh cell within an r, z problem in combination with the use of a similar forward solution DOT-IIW problem is another area of interest. The use of adjoint kernels to the mesh cells provides a solution to the external environment of the radiation source distribution obtained from the integration of the forward solution.
- (4) Update the point kernel techniques to facilitate rapid, parametric analyses in the following areas:
 - (a) Recode the KAP-VI code using the flexible dimension feature of FORTRAN-IV,
 - (b) Expand the capabilities of the SCAP code in the areas of exclusion radii, albedo model, and numerical methods, and

- (c) Modify the SCAP code to include the KAP-VI code capability of assigning the ambiguity indices for each region boundary.
- (5) Incorporate into the MSFC code package the capability to perform activation analyses of the nuclear stage. This could be accomplished by utilizing the DOT-IIW-MAP technique to determine detailed group-wise neutron fluxes for input to an activation type program. An updated version of the ACT-II code or the NAP code (provided in the INAP code development work sponsored by MSFC) could be made operational on the MSFC UNIVAC-1108 computer system.

3.0 Analysis of a Realistic Nuclear-Propelled Vehicle Using the MSFC Computer Code Package (Task A)

In Task A of this contract, the MSFC computer code package was applied to the analysis of a realistic nuclear-propelled vehicle. The intent of this analysis was to demonstrate how the computer techniques could be applied rather than to generate detailed design results. In this section, the nuclear propelled vehicle is described, a synopsis of the computer techniques is given, and key results of the analysis are developed.

3.1 Description of the Nuclear-Propelled Vehicle

Figure 3-1 schematically illustrates the nuclear-propelled vehicle geometry employed in this study. The geometry consists of the propulsion module, the propellant module, and the command and control module. The command module selected for analysis is a modified Apollo module to accommodate a six-man crew.⁽⁵⁾ The overall weight of the command module is approximately 35,200 kilograms (16,000 pounds). The propellant module consists of a 660,000 kilogram (300,000 pound) capacity tank with a 10° half-angle conical bottom. The propulsion module includes a ~20900 kilogram (~9500 pound) capacity run tank. This propellant tank geometry is the Class I hybrid configuration selected by MacDonnell Douglas Company in Phase III of the Nuclear Shuttle System Definition Study.⁽⁶⁾

The compositions utilized in the computer code analysis to describe the propellant tank and command module geometries are given in Table 3-1. Generally, fifteen geometrical regions were employed to describe the command module and about twenty-five geometrical regions were employed to describe the propellant tank geometries, including the aluminum tank wall.

The geometry of the Nuclear Subsystem is shown schematically in Figure 3-2. This is a detailed, unclassified model of the NERVA Nuclear Subsystem (NSS).⁽⁷⁾ As shown in Figure 3-2, five zone loadings were employed in the reactor core. Surrounding the core in the radial direction are the following: a graphite "filler strip" region, aluminum structure, the beryllium reflector, and a region representing the control vanes. The major regions in

the axial direction include the core support plate, the BATH* and lead shield regions, and the dome plenum. The Nuclear Subsystem is enclosed by an aluminum pressure vessel. The dome of the NSS is actually elliptical in shape. However, for purposes of analysis, the dome is approximated in the R-Z geometry as shown in Figure 3-2.

Twenty-two geometrical regions were employed to describe the NSS in the computer codes employed in this study. The element atom densities for those regions are presented in Table 3-2.

Detailed descriptions of the geometries are presented in the eleven sections of Volume 2 of this report in which the computer code input data are described.

3.2 Synopsis of Methods

The MSFC computer code package provides various options for analysis of a nuclear propelled vehicle. One particular scheme, selected for the analysis performed in this task, is described in this section. A brief description of each computer code is also presented.

The following sources of radiation which contribute to the photon dose at the crew compartment were considered in this study: The Nuclear Subsystem; the nozzle, skirt, and skirt extension; the aluminum propellant discharge line; and, the liquid hydrogen in the propellant tanks.

3.2.1 Method of Analysis

Figures 3-3 and 3-4 illustrate the analytical procedure utilized to calculate the radiation environment internal and external to the Nuclear Subsystem, respectively. Referring to Figure 3-3, the starting point of the Nuclear Subsystem analysis is the SATURN code. The MSFC fifty-two group microscopic neutron cross section library data along with the atom densities for each geometric region are input to the SATURN problem. The SATURN code placed on tape, 52 group macroscopic neutron, P_0 , transport, region dependent cross

*BATH is the NERVA reference design shield material consisting of boron carbide, aluminum, and titanium hydride. The total weight of the shield assembly is ~ 2900 pounds.

sections for input to the ANISN-W code. Two ANISN-W problems were run--one describing the geometry of the Nuclear Subsystem in the radial direction and one in the axial direction. ANISN-W then provided 52 group neutron spectra for all mesh in the axial and radial geometries on two separate tapes. These two tapes along with the region dependent atom densities and the MSFC basic data library tapes were input to the APPROPOS code.

The APPROPOS code performs these functions: (1) 16 group macroscopic, region dependent, P_0 , transport corrected neutron cross sections (with upscatter removed) are provided as punched card output for input to the DOT-IIW neutron problems; the 16 group neutron cross sections were spectrally-weighted by region using the 52 group fluxes input from ANISN; (2) 13 group, P_1 , macroscopic, region dependent photon cross sections are provided as punched card output for input to the DOT-IIW photon problem, and (3) reaction rate data and other basic data are provided as punched card output for input to the NAGS data processing code.

Two neutron DOT-IIW problems were run to analyze the Nuclear Subsystem. The first problem was run as a fixed source problem. The fission source spatial distribution input to DOT-IIW was obtained from the axial and radial ANISN-W eigenvalue problems. The geometry for this problem extended in the axial direction from the bottom of the hot end hardware region to a few mean free paths into the BATH shield region (see Figure 3-2). A boundary source from this problem was input to the second DOT-IIW neutron problem.

This second problem extended in the axial direction from the bottom of the aluminum shield plate to the top of the pressure vessel dome. Both neutron problems employed an S₈ angular quadrature. Of course, both problems provided: (1) scalar fluxes in each mesh cell in the geometry, and (2) surface angular leakage tapes. The scalar flux tapes were input to the CHEAPER data processing code. This code combined the two scalar flux tapes into a mesh cell description for input to the NAGS code. The NAGS code provided: (1) the photon source data by mesh cell on tape for input to the DOT-IIW photon geometry problem, and

(2) photon source data on punched cards for input to the KAP-VI point kernel program. The S_g quadrature photon DOT-IIW problem provides the photon distribution internal to the Nuclear Subsystem, as well as, the angular leakage at the surface of the entire NSS geometry.

Figure 3-4 illustrates the technique employed to calculate the radiation environment external to the Nuclear Subsystem and the dose rate at the crew location. The radiation environment external to the NSS and at the crew locations were calculated by two different techniques. The first technique employed the MAP code, whereas, the second technique employed the KAP-VI code. The photon surface leakage flux tape from the DOT-IIW problem was input to the MAP code which calculated the photon levels on a meridian ring external to the NSS. These meridian ring flux data were input as punched card data to the SCAP code. The SCAP code calculates the direct and single scattered contributions of the NSS sources at the crew location. The punched NSS sources from the NAGS code were input to the KAP-VI point kernel code which also calculated the photon levels on a meridian ring external to the NSS. The radiation levels on the meridian were also input to the SCAP code as punched card data. The SCAP code was run with various levels of LH₂ in the propellant tanks--this yields dose rate versus run time data. This data is then integrated as a function of time to obtain the crew dose.

The energy and spatial distribution of sources in the nozzle, skirt, and skirt-extension were obtained from the March, 1970, Common Radiation Analysis Model (CRAM).⁽⁸⁾ These sources were input to the KAP-VI code to calculate: (1) the direct radiation at the crew location, and (2) the radiation levels on the meridian ring due to these sources. The latter data were then input to the SCAP code to obtain the scattered dose contribution.

The energy and spatial distribution of the photon sources in the pump discharge line (PDL) were also obtained from the CRAM. These sources were input directly to the SCAP code which calculated the direct and scattered dose components at the crew location.

The neutron surface leakage fluxes from the DOT-IIW problems were input to the MAP code to calculate the neutron fluxes on a meridian ring external to the NSS. The meridian ring neutron fluxes were input to the LHAP code to determine the contribution to the crew due to the secondary gamma ray source in the liquid hydrogen propellant.

3.2.2 Description of Computer Codes and Basic Data Libraries

The compilation of neutron and photon cross section data for MSFC has generated five Master Library Tapes and a deck of basic nuclear data as shown in Table 3-3. These libraries⁽⁴⁾ were developed under Contract NAS-8-24919 and updated under the present contract as described in Section 6.0.

Master Library Tape No. 1 contains 143 microscopic, transport corrected, neutron cross section sets for 38 elements for use in the ANISN-W, DOT-IIW, and APPROPOS codes. These data are in a 52 energy group structure. Master Library Tape No. 2 contains 445 microscopic, P_{λ} ($\lambda \leq 3$) neutron cross section sets for 38 elements for use in the ANISN-W, DOT-IIW, and APPROPOS codes. These data are also in a 52 energy group structure. Master Library Tape No. 3 contains 142 sets of reaction rate cross section data for use in the APPROPOS code. The data on Master Library Tapes No. 1, 2, and 3 are averaged over four representative, spatially dependent, neutron spectra obtained from current NERVA R-1 nuclear subsystem design work. These first three tapes are obtained in a manner consistent with each other and with the nuclear and radiation analysis procedures used in the radiation analysis of reactors at the Westinghouse Astronuclear Laboratory (WANL).⁽⁷⁾

Master Library Tape No. 4 contains 510 microscopic, P_{λ} , gamma ray cross section sets for 51 elements for use in the ANISN-W, DOT-IIW, and APPROPOS codes. These data, which are in a 13 energy group structure, are averaged over a source spectrum of prompt gamma ray energy emitted from the fission of ²³⁵Uranium. Master Library Tape No. 5 contains the pair-production and photo-electric gamma ray cross section data used

in the KAP-VI, SCAP, MAP, and GAMLEG-W codes. Again, the data on Tapes 4 and 5 are obtained in a manner consistent with each other and with the radiation analysis procedures used in the radiation analysis of reactors at WANL.

Finally, a basic set of nuclear data (Master Library 6) is provided for use in the complete package of codes.

The GAMLEG-W Code

The GAMLEG-W code provides multigroup, photon transport cross sections for use in multigroup, discrete ordinate transport or Monte Carlo transport codes. The code is designed to provide photon transport cross sections in a maximum of 100 groups with scatter transfer cross sections represented as a Legendre expansion (P_l) of arbitrary order. The code performs a numerical integration with a user specified weighting function to obtain multigroup absorption and scatter-transfer cross sections. Absorption cross sections are obtained from pointwise, photoelectric and pair-production data on punched data cards or magnetic tape, and Compton absorption from the Klein-Nishina equation for the inelastic scattering of a photon with a free electron. Scatter-transfer cross sections are obtained from the differential form of the Klein-Nishina equation for the inelastic scattering of a photon with a free electron.

The code can, at option, provide photon transport cross section data for use in energy flux or particle flux calculations. Production of a pair of 0.511 MeV photons due to pair production annihilation can be included in the energy scatter-transfer or particle scatter-transfer cross section data.

Output data from the GAMLEG-W code are compatible with the ANISN-W or DOT-IIW computer codes and are placed on either punched data cards or magnetic tape.

The GAMLEG-W code, as it is in production use on the UNIVAC-1108 at MSFC, is fully documented in Reference 4, Volume 3.

The APPROPOS Code

In the analysis of nuclear reactor systems, an efficient technique for preparing multigroup, cross section data in the required format for discrete ordinate transport as well as Monte Carlo computer codes is required. The APPROPOS code provides this needed technique. APPROPOS prepares multigroup, simultaneous, neutron-photon cross section data and neutron reaction cross section data for radiation transport codes.

The APPROPOS code processes multigroup, neutron cross section data and multigroup, neutron reaction cross section data (e.g., radiative capture, fission, inelastic scatter, and elastic scatter) to provide spectral-weighted, neutron cross section data in a reduced number of energy groups. These data are then processed with input specified elemental atom densities, gamma ray production data due to neutron reactions, and photon cross section data to provide macroscopic, coupled, neutron-photon cross section data, neutron cross section data, and photon cross section data. Output data from the APPROPOS code are placed on punched cards and/or magnetic tape for use in the ANISN-W, DOT-IIW, or NAGS codes.

The APPROPOS code, as it is in production use on the UNIVAC-1108 at MSFC, is fully documented in Reference 4, Volume 3.

The NAGS Code

When the vast amount of data handling required in a complete two-dimensional radiation analysis of a nuclear system is considered, the need for an automated, data processing link between discrete ordinates transport techniques and both point kernel and Monte Carlo techniques is evident. The NAGS code provides this needed link. NAGS processes multigroup, neutron and photon flux distributions for one-dimensional, slab or cylinder geometry models, or two-dimensional r, z or r, θ geometry models. Flux input data to the NAGS code are obtained by magnetic tape or disk from the ANISN-W or DOT-IIW discrete ordinate transport codes. Additional input data required by the NAGS code are prepared by the

APPROPOS code. The NAGS code provides: (1) neutron and photon source data for use in point kernel, Monte Carlo, or discrete ordinate transport analyses, (2) neutron and photon dose rates, and (3) nuclear energy deposition data (neutron and photon) for use in subsequent thermal and hydraulic design analyses. Source distribution data are generated, on punched data cards for input into the KAP-VI code and on magnetic tape for use in ANISN-W or DOT-IIW codes.

The NAGS code, as it is in production use on the UNIVAC-1108 at MSFC, is fully documented in Reference 4, Volume 3.

The SATURN Code

In certain calculations using the ANISN-W and DOT-IIW discrete ordinates transport codes with a large number of input cross section data, execution of the calculation is sometimes terminated because of insufficient core storage to process the cross section data. To alleviate this situation, the SATURN code was developed. SATURN processes P_x or transport corrected cross section data using a minimum amount of core storage to produce multigroup cross section data tapes in two formats for use in the ANISN-W or DOT-IIW codes. The two formats are the normal, group-dependent data tape or the specially prepared, group-independent data tape.

The data processing functions and options performed by the SATURN code are as follows:

- (1) Preparation of group-dependent and/or group-independent cross section data on magnetic tape or disk file and/or punched cards,
- (2) Inclusion of transverse leakage corrections to the macroscopic cross section data,
- (3) Preparation of macroscopic cross sections using mixing table operations,
- (4) Adjoint reversal of the cross section data, and
- (5) Output tape labeling and relabeling.

These operations are performed in the SATURN code as a sequence of logical steps to minimize the core storage required to prepare cross section data.

The SATURN code is an auxiliary code and should only be used for those situations where the DOT-IIW or ANISN-W codes cannot process the cross section data or for problems that require special, transverse leakage corrections, or group-independent tapes.

The SATURN code, as it is in production use on the UNIVAC-1108 at MSFC, is fully documented in Reference 4, Volume 3.

The ANISN-W Code

ANISN-W is a multigroup, discrete ordinate transport code that solves the energy dependent, one-dimensional, Boltzmann transport equation with general anisotropic scattering for slab, cylindrical or spherical geometries. The code solves forward or adjoint, homogeneous or inhomogeneous problems. The method is applicable to both neutron and gamma transport problems. Inhomogeneous problems may have a fixed volume distributed source, or a specified angular-dependent shell source at any mesh interval; fissions may be included for a subcritical system. Vacuum, reflective, periodic, white, or albedo boundary conditions may be specified. Time absorption calculations, concentration searches, outer radius searches, buckling searches, or zone thickness searches are also solved. Cross sections may be input from a library tape and/or from punched cards; multigroup flux distributions may be used to perform a group reduction of the cross section data. The code also includes space point scaling to accelerate the flux solution on inner iterations.

To provide a more efficient tool, the ANISN-W code has been improved over the original ANISN code⁽⁹⁾ to provide for the inclusion of automated tape linkage of input and output data and for the capability to input a distributed or shell source from magnetic tape and/or punched cards. Microscopic and/or macroscopic cross section data may be input to ANISN-W from cards and/or a library tape. Cross sections from tape can be input from a microscopic library data tape (the mixing table option in ANISN-W can be employed to calculate macroscopic cross sections) or from a SATURN prepared, group-dependent or group-independent, cross section tape.

The ANISN-W computer code, as it is in production use on the UNIVAC-1108 at MSFC, is fully documented in Reference 4, Volume 4.

The DOT-IIW Code

DOT-IIW is an implementation of the discrete ordinates transport technique. This code solves the two-dimensional, energy dependent, linear Boltzmann transport equation with general anisotropic scattering for $x, y; r, z;$ and r, θ geometries. The code solves forward or adjoint, homogeneous or inhomogeneous problems. The method is applicable to both neutron and gamma ray transport problems. Inhomogeneous problems may have a fixed volume distributed source, or a specified angular dependent boundary source at the right or top boundaries; fissions may be included for a subcritical system. Vacuum, reflective, periodic, white, or albedo boundary conditions may be specified. Time absorption calculations, concentration searches, or zone thickness searches are also solved. Cross sections may be input from a library tape and/or from punched cards. Asymmetric or symmetric quadrature calculations may be performed. The code includes a choice of Gaussian Iteration, Successive Overrelaxation, Space Point Scaling, or Chebyshev Acceleration to achieve a flux solution on inner iterations.

The version of the DOT-IIW code provided to Marshall Space Flight Center has been changed from the original version of DOT-II to be consistent with the nuclear and radiation analysis methods provided MSFC, and to incorporate state-of-the-art features of the current DOT-IIW code as released by RSIC (with the exception of a polynomial source option). The major improvements in DOT-IIW are the inclusion of acceleration techniques on the group flux solution, improved convergence logic, asymmetric quadrature capability, and improved tape operations.

Microscopic and/or macroscopic cross section data may be input to DOT-IIW from magnetic tape and/or punched cards. Cross sections from tape can be input from a microscopic library data tape (the mixing table option in DOT-IIW can be employed to calculate macroscopic cross sections) or from a SATURN prepared, group-dependent or group-independent, cross section tape.

The DOT-IIW computer code, as it is in production use on the UNIVAC-1108 at MSFC, is fully documented in Reference 4, Volume 5.

The MAP Code

The MAP code solves for the energy-dependent radiation transport external to a nuclear radiation source. The code uses as energy- and angular-dependent, surface source data the multigroup, angular-dependent surface leakage fluxes, as calculated by an r, z geometry discrete ordinate transport calculation. The capabilities of the MAP code include:

- (1) Two techniques of treating symmetric quadrature, discrete ordinate transport, angular-dependent, leakage fluxes to provide a continuous variation of flux with angle;
- (2) Techniques to use generalized quadrature, discrete ordinate transport, angular-dependent leakage fluxes (including asymmetric sets) at both the source surface and detector surface;
- (3) Techniques to produce magnetic data tapes of angular-dependent flux data for use as boundary-source input into subsequent, discrete ordinate transport problems; and
- (4) Techniques to calculate the uncollided radiation as well as estimates of the collided radiation (using point kernel techniques) reaching detector surfaces in a geometry described by intersecting, quadratic surfaces.

Cross section data are obtained from (1) internal calculations of point value data from Klein-Nishina relationships and data tables for photons, or (2) input values of macroscopic cross sections for materials in zones.

This code provides techniques which circumvent the use of discrete ordinate transport codes in calculating radiation transport through voids or near voids. MAP provides accurate results in areas where "ray effects"⁽¹⁰⁾ due to discrete direction angular flux solutions produce anomalous results and provides for extended use of the discrete ordinate transport technique. MAP provides this capability without using high orders of angular quadrature or conventional symmetric quadrature techniques in discrete ordinate transport codes.

The MAP radiation transport code, as it is in production use on the UNIVAC-1108 at MSFC, is fully documented in Reference 4, Volume 5.

The DOQ Code

The ANISN-W one-dimensional and DOT-IIW two-dimensional discrete ordinates transport codes require as input data the discrete directions for which solutions are desired. These discrete directions cannot be chosen arbitrarily. Because the energy-angle relationship of the scatter cross sections used by these transport codes are represented by Legendre polynomials, quadrature sets that correctly integrate Legendre polynomials are required for particle conservation. In addition, symmetry conditions on discrete directions are important. The ANISN-W and DOT-IIW codes perform specific checks on these quadrature data to insure consistency. At least seven significant digits of precision for the input quadrature coefficients are required.

The DOQ Discrete Ordinates Quadrature code* was developed to assist the user in the preparation of these input coefficients to the transport codes. The DOQ code computes the discrete ordinates quadrature coefficients (direction cosines and weights) given the point coordinates and symmetry conditions. A generalized technique using the method of moments is used. The code prints out and punches on cards the quadrature coefficients in a format appropriate for direct input to the ANISN-W and DOT-IIW codes. Output from

*Originally developed as the SNAFU code by R. G. Rodgers, F. R. Mynatt, and W. W. Engle, Jr., of the Computer Technology Center, Oak Ridge, Tennessee.

the DOQ code may also be used as input data to the ADOQ asymmetric quadrature code. The DOQ code utilizes the variable dimensioning technique of FORTRAN-IV to allow the calculation of high orders of quadrature by efficient use of core memory storage.

The DOQ computer code, as it is in production use on the UNIVAC-1108 at MSFC, is documented in Reference 4, Volume 5.

The ADOQ Code

The importance of accurately predicting the nuclear radiation environment and radiation transport external to a nuclear reactor system has necessitated the development of asymmetric quadrature techniques for use in discrete ordinate transport analyses. These two-dimensional, transport theory techniques have significantly reduced "ray effects" and have provided increased angular resolution of the spatially attenuated nuclear subsystem leakage spectrum. When conventional symmetric quadrature transport techniques are used to calculate the radiation transport through low-scattering media or voids, "ray effects" are observed with low order quadratures. These "ray effects", or anomalous computational results, are due to the discrete representation of the angular variable in discrete ordinate transport theory approximations and predict preferential radiation streaming along the discrete directions of angular quadrature chosen.

Accurate angular resolution of the spatially attenuated leakage spectrum at locations far removed from the nuclear system is also important in the prediction of neutron thermalization in local media for the calculation of secondary gamma ray sources.

Analytical radiation transport techniques have been developed to satisfy both of these requirements. The method consists of (1) the development of asymmetric quadrature data using the DOQ and ADOQ computer codes to achieve a high degree of angular resolution along the axis and in the solution plane of interest; (2) the modification of the DOT two-dimensional, discrete ordinate transport code to use these data; and (3) the development and coding of the MAP code to reconstruct the angular and energy dependence of the neutron or photon flux as a function of position external to the nuclear system using the reactor surface angular fluxes from the DOT code as input data.

In addition, techniques in the MAP code for processing asymmetric quadrature data at the surface and providing asymmetric quadrature angular flux at the surface of a succeeding DOT problem of a medium separated from the reactor have been developed.

The ADOQ code is a technique for (1) combining asymmetric quadrature data with symmetric quadrature data in one hemisphere of the unit S_n sphere, (2) adjusting the level weights of the last asymmetric level to match the symmetric level, and (3) verifying the various relationships these data must satisfy. ADOQ prints out and punches on cards the quadrature coefficients (direction cosines and weights) in a format appropriate for direct input to the DOT-IIW code.

The ADOQ computer code, as it is in production use on the UNIVAC-1108 at MSFC, is documented in Reference 4, Volume 5.

The KAP-VI Code

KAP-VI is a point kernel code designed to calculate the radiation level at detector points located within or outside a complex radiation source geometry. This geometry can be described by a combination of quadratic surfaces with a maximum of six boundary surfaces per zone. The code evaluates the material thicknesses intercepted along the line-of-sight from the source point to the detector point. These material thicknesses (or path lengths) are then employed in attenuation functions to calculate the flux, dose rate, or heating rate at the detector. The attenuation function for gamma rays employs exponential attenuation with a buildup factor. Three optional neutron attenuation functions are included: (1) a modified Albert-Welton function for calculating fast neutron dose rate using removal cross sections; (2) a bivariate polynomial expression for computing neutron spectra using infinite media moments data; and (3) a monovariate polynomial for computing neutron spectra using infinite media moments data.

The KAP-VI code handles cylindrical, spherical, disc, line, or point sources. Separate source distributions may be employed for neutrons and gamma rays with a variety of available options for describing the source distributions. Radiation source distributions are

assumed to be separable energy- and spatial-distributions. Internally calculated normalization is included to provide a volumetric source in cylindrical and spherical coordinates. An option is also provided to describe an azimuthal source density variation by specifying input data for discrete point sources.

The KAP-VI code, as it is in production use on the UNIVAC-1108 at MSFC, is fully documented in Reference 4, Volume 6.

The SCAP Code

SCAP is a point kernel code employing energy-dependent single- or albedo-scatter methods to calculate the radiation level at a detector point located within or outside a complex scattering geometry. This geometry can be described by a combination of quadratic surfaces. The code evaluates the material thickness and scatter points in materials intercepted along the lines-of-sight from an anisotropic energy-dependent, source point. The material thicknesses (or path lengths) to each scatter point are used in an exponential attenuation function to calculate the radiation level at each scatter point.

Three options exist in the treatment of particle scattering to a detector point. Photon scattering from the scatter point to the detector point can be treated as a Compton scatter event using the differential form of the Klein-Nishina equation for the inelastic scattering of a photon with a free electron, or as a simple, albedo-scatter event at the surface of a geometric zone. Neutron scattering from the scatter point to the detector point can be treated only as an albedo-scatter event at the surface of the geometric zone. The attenuation function for the scattered particle (photon or neutron) on the scatter leg to the detector point is an exponential attenuation function with a buildup factor for photons only.

The code handles a series of anisotropic energy-dependent point sources. These anisotropic point sources are described with pointwise, energy-dependent distributions as a function of polar angle on a meridian.

Point source distribution data can be supplied on punched cards from the KAP-VI and MAP codes as anisotropic, energy-dependent source data for input to the SCAP code.

The SCAP code, as it is in production use on the UNIVAC-1108 computer system at MSFC, is fully documented in Reference , Volume

The CHEAPER Code

As part of this contract, the CHEAPER code was added to the MSFC computer code package. A user's manual describing the code is given in Appendix A to Volume 1 of this report.

A typical radiation analysis of a nuclear subsystem may consist of two neutron, and possibly three photon DOT-IIW problems. From these problems as many as 2.4×10^5 scalar fluxes are obtained as output data. Reducing this large volume of data to a readily useable form is both time consuming and subject to error. The CHEAPER program was coded to rapidly process these scalar fluxes.

The CHEAPER code performs several operations on DOT scalar flux tapes, such as, linking two flux tapes, modifying the flux tapes so that they may be used as flux guesses in problems of differing geometry, adding two tapes together, inverting the fluxes, etc. CHEAPER also calculates flux-response data as transverses or at discrete data points.

The LHAP Code

As part of this contract, the LHAP code was added to the MSFC computer code package. A user's manual describing the code is given in Appendix B to Volume 1 of this report.

The LHAP code is a modified version of the SCAP code to calculate by a simple approximation the secondary gamma rays due to neutron capture in liquid hydrogen or in a thin wall neutron capture medium. The code accepts as input data the neutron flux levels at an arbitrary meridian ring as polar angle energy dependent data. These data can easily be obtained from either the KAP-VI or MAP codes. The LHAP code calculates the uncollided flux at an arbitrary capture point determined by the entry point into an absorbing region. An energy dependent flux and dose rate, with and without buildup on the secondary leg are computed as a function of source angle and capture zone.

3.3 Results of Analysis

This section describes some of the key results obtained from application of the techniques described above to the analysis of the nuclear-propelled vehicle. Results are discussed in three areas: (1) internal to the Nuclear Subsystem, (2) external to the NSS (meridian ring), and (3) at the crew location.

3.3.1 Transport Analysis of the Nuclear Subsystem

A total of nine computer problems were run to analyze accurately the radiation environment internal to and at the surface of the Nuclear Subsystem. The sequence of this analysis was previously outlined in Figure 3-3 and described in Section 3-2.

The neutron environment as calculated by the discrete ordinates technique internal to the Nuclear Subsystem is illustrated in Figures 3-5 through 3-12. The fast ($E > 1.0$ Mev), intermediate ($0.3 \text{ ev} \leq E \leq 1.0$ Mev), thermal ($E < 0.3 \text{ ev}$), and total neutron fluxes on the core midplane and near the core centerline are presented. The DOT-IIW and ANISN-W calculated fluxes are compared. In the DOT-IIW problems, the 16 group, P_0 transport corrected cross sections (with upscatter removed) from the APPROPOS code were employed. In the ANISN-W problems, the 52 group, P_0 transport corrected (with upscatter) cross sections from the SATURN code were employed. The DOT-IIW problems employed an S_8 quadrature and the ANISN-W problems employed an S_4 quadrature. Forty radial mesh and essentially 87 axial mesh were employed in both problems. The DOT-IIW analysis was run in two problems as described previously. In the reactor geometry portion of the DOT-IIW problem 50 axial mesh were employed, and in the shield geometry problem, 47 axial mesh were employed.

Figures 3-5 through 3-8 present the neutron flux transverses on the core midplane as a function of radial distance from the center of the core to the outer surface of the pressure vessel. The ratio of the DOT-IIW to the ANISN-W data is approximately a factor of 1.5 for all groups and at most radial locations. This ratio is typical of the centerline

to average ratios observed in the two-dimensional analysis. Hence, for this geometric situation the one and two dimensional values are in good agreement.

The shape of fast and intermediate neutron fluxes in the radial direction display a typical fall-off as a function of radius. The thermal flux (Figure 3-7) displays the typical shape for the NSS, i.e., a rapid increase near the edge of the core due to the thermalization by the beryllium reflector.

Figures 3-9 through 3-12 present the neutron flux transverses near the core centerline as a function of axial location. The data are obtained at the center of the first mesh interval in the transport problems, i.e., 1.5 cm. Excellent agreement between the one and two dimensional neutron fluxes is observed except for the case of the thermal flux in the dome plenum. From Figure 3-11, it is noted that the DOT-IIW thermal flux in the dome plenum (~210 cm) is roughly an order of magnitude lower than the ANISN-W 52 group calculated flux. It should be pointed out that no transverse leakage correction was used in the ANISN-W problems in the low density plena regions. In an attempt to understand the cause for the large difference between the DOT-IIW and the ANISN-W results in the dome plenum region, an ANISN-W problem was run in which the same 16 group neutron cross sections employed in the DOT-IIW problem were also input to an ANISN-W problem. As shown in Figure 3-11, the results are in much better agreement with the DOT-IIW fluxes in the plenum region. It is postulated that the major difference in the thermal flux calculation in the liquid hydrogen plenum region was not due to the change in group structure, but was due to the inclusion of upscatter in the highly thermalizing liquid hydrogen region in the 52 group ANISN-W problem.

The shape of the fast and intermediate neutron fluxes shown in Figures 3-9 and 3-10 are typical of the NERVA Nuclear Subsystem. In the core region, between 5 and 130 cm, the flux displays a cosine distribution which is essentially the same as the fission distribution. The rapid fall-off of the flux in the BATH shield region is also observed as expected.

The shape of the thermal flux shown in Figure 3-11 is also typical. In the core region, the thermal flux is higher at the core inlet (120 cm) than at the core exit (5 cm) due to the reflection and thermalization in the core plenum. The rapid increase due to thermalization in the core support plate region is noted. The thermal flux falls off rapidly across the BATH shield region and then again increases due to the thermalization in the liquid hydrogen in the dome plenum.

The comparisons between the one and two dimensional discrete ordinates calculations described above provide the user with some insight into the differences that can be expected in the application of both techniques.

Figures 3-13 and 3-14 illustrate, respectively, the midplane radial and centerline axial distribution of the total photon flux in the Nuclear Subsystem as calculated by the DOT-IIW code. Thirteen group photon sources generated by the NAGS code were employed as input to the DOT-IIW problem. An S_8 quadrature was used. Thirty-four radial and 58 axial mesh were employed in the DOT-IIW problem. The thirteen group photon analysis employed P_1 transport cross sections. Figure 3-14 shows the typical cosine shape in the reactor core and the rapidly decreasing flux across the shield region.

Of major importance in the analysis of the Nuclear Subsystem is the development of the photon source for use in the DOT-IIW and KAP-VI problems. The source by region in the NSS as calculated by the NAGS code is presented in Table 3-4. The contribution of these sources to the dose rate external to the Nuclear Subsystem is discussed below in Sections 3.3.2 and 3.3.3.

3.3.2 External Radiation Environment

Two techniques were demonstrated to calculate the radiation environment on a meridian ring external to the Nuclear Subsystem. In the first technique, the angular leakage fluxes at the surface of the NSS calculated by the DOT-IIW code were input via tape to the MAP point kernel code. In the second technique, the NAGS calculated sources

internal to the NSS were input via punched cards to the KAP-VI point kernel code. Both the MAP and KAP-VI codes were run to compute the neutron flux and photon dose rates at twenty-one "detector points" on a meridian ring located 30 feet from the center of the reactor core. Results of both techniques are compared in Figures 3-15 and 3-16.

Specifically, Figure 3-15 compares the MAP and KAP-VI calculated fast ($E > 1.0$ Mev) neutron flux as a function of polar angle on the meridian ring. These comparisons are typical of previous NERVA analysis utilizing both methods.⁽⁴⁾ At the dome end (shielded end), the KAP-VI flux is a factor of 2.5 higher than the MAP calculations. It is believed that the "exact" answer is somewhere between the two extremes. However, at polar angles near 20° , the MAP calculated flux is as much as a factor of 5 greater than the KAP-VI calculation. In this polar angle region, the MAP calculation is believed to be the more correct solution since the KAP-VI technique of applying the infinite media carbon moments data does not adequately account for the true scattering component in the reflector regions. At polar angles between 60° and 180° , both techniques show reasonably good agreement as expected.

Table 3-5 illustrates the contribution of the side leakage flux component at several selected polar angles as calculated by the MAP program. It should be recalled that two neutron DOT-IIW problems were run--one describing the reactor geometry and one describing the shield geometry. Thus, two MAP problems must be run to obtain a complete mapping of the meridian ring as shown in Table 3-5. At the polar angle of 15° , the reactor side leakage component accounts for 72% of the total fast neutron flux.

Figure 3-16 compares the MAP and KAP-VI calculated photon dose rate on the meridian ring as a function of polar angle. Again, the KAP-VI data are higher than the MAP calculation at the dome end ($\alpha = 0^\circ$) by about a factor of two. Due to the use of the infinite media buildup factor, the KAP-VI results are thought to be slightly conservative and the "exact" answer is somewhere between the two calculations. The two techniques show good agreement at the side of the reactor ($\alpha = 90^\circ$).

Table 3-6 illustrates the contribution of various source regions in the NSS to the photon dose rate on the meridian ring as calculated by the KAP-VI point kernel code. The dose rate, as well as the percent of the total dose rate, at polar angles of 0° (dome end), 80° (side), and 180° (aft end) are presented. It is interesting to note that at $\alpha = 0^\circ$, the reactor core contributes only 28.5% to the total dose rate, although from Table 3-4 it was noted that the core represents 95% of the total photon source in the NSS. Also, at $\alpha = 0^\circ$, the support plate region contributes about 32% of the total dose rate. The core sources are, of course, shielded by the support plate, the shield and other hardware in the axial (forward) direction. The photon sources in the support plate region have a "harder" spectrum than those in the core and are shielded only by the internal shield in the axial direction. The secondary sources in the BATH shield region contribute less than 10% to the total dose rate on the centerline since a large fraction of the source in this region is due to the 0.5 Mev gamma ray accompanying the (n, α) reaction in the boron in the BATH material.

At the side and aft end of the NSS, the reactor core contributes more than 80% of the total dose rate as expected.

3.3.3 Crew Dose Analysis

The following sources of radiation which contribute to the photon dose at the crew compartment were considered to demonstrate the application of the MSFC computer code package: the Nuclear Subsystem; the nozzle, skirt, and skirt extension; the aluminum propellant discharge line; and, the liquid hydrogen in the propellant tanks. The calculational procedure was shown in Figure 3-4 and was described in Section 3.2. It should be recalled that two techniques were employed to evaluate the NSS source contribution: (1) the MAP calculated energy fluxes on the meridian ring were input to the SCAP single scatter code, and, (2) the KAP-VI calculated energy fluxes on the meridian ring were input to the SCAP single scatter code. For comparison purposes, the KAP-VI code was also employed to calculate the direct radiation component at the crew location.

In this section the following nomenclature is used throughout: scattered dose rate is defined as the radiation component that has undergone scattering in the propellant tanks and crew compartment; direct dose rate is defined as the radiation component that has undergone scattering only in the Nuclear Subsystem.

The SCAP code analysis was limited to the calculation of the dose rate on the centerline of the crew compartment, since the off-axis calculations require significantly more computer time. The KAP-VI analysis, which is less costly, was however, performed off-axis both in the crew compartment and at the top of the propellant tank.

In the SCAP and KAP-VI problems, the detector point representing the "crew compartment" was located 246.54 centimeters above the top of the tank on the centerline. The location can be visualized by referring to Figure 3-1. The details of the crew compartment geometry are presented in Sections 9.0 and 10.0 of Volume 2 of this report.

Figure 3-17 shows the photon dose rate on the centerline at the crew location versus time prior to empty tank. To obtain the curve of dose rate versus time, four SCAP problems were run as follows:

- (1) The small "run tank" filled with ~9500 pounds of LH_2 , i.e., 104 seconds prior to empty tank condition,
- (2) The small run tank filled with LH_2 plus LH_2 in the propulsion module to -1500 cm (see Figure 10-1, Section 10.0, Volume 2), i.e., 135 seconds prior to empty tank.
- (3) The small run tank filled with LH_2 plus LH_2 in the propulsion module to -1717 cm, i.e., 262 seconds prior to empty tank,
- (4) The small run tank filled with LH_2 , plus LH_2 in the propulsion module to -2542.54 cm, i.e., 1072 seconds prior to empty tank.

Figure 3-17 includes the scattered and direct radiation components from the NSS, nozzle and PDL sources, and the LH_2 secondary radiation component. The total

dose rate from the NSS source is also plotted. This NSS total is essentially the grand total since the other radiation components did not contribute appreciably to the dose rate at the crew location.

Figure 3-18 compares the photon dose rate on the centerline at the crew location due to the NSS sources as calculated by the two techniques, i.e., the MAP meridian ring data input to the SCAP code and the KAP-VI meridian ring data input to the SCAP code. The MAP-SCAP results are roughly a factor of 2.5 lower than the KAP-SCAP data. These results are as expected if one refers back to Figure 3-16 which compares the two sets of meridian ring data. Near the centerline, the MAP calculation is about a factor of two lower than the KAP-VI results.

The photon dose rate data presented in Figures 3-17 and 3-18 were integrated as a function of time in order to obtain the total crew dose. The results are presented in Table 3-7. These data apply to a total burn time of about 46 minutes with approximately 9500 pounds of residual propellant remaining in the small run tank. Both the MAP-SCAP and the KAP-VI-SCAP data are presented in Table 3-7. These results show that the total dose is due mainly to the NSS sources. The direct and scattered NSS components are roughly equal.

It should be noted that the data in Figures 3-16 and 3-17 were extrapolated as a function of time so that an integration for a total of 46 minutes of burn time could be obtained.

Table 3-8 illustrates how the crew dose due to the NSS sources is accumulated as a function of burn time. This table presents the NSS direct, scattered, and total dose as a function of time prior to empty tank conditions in increments of 100 seconds up to 1000 seconds and then from 1000 to 2880 seconds. These data show that 43 percent of the total dose due to the NSS source is received at the crew location in the last 200 seconds of burn time, i.e., between 100 and 300 seconds prior to the tank empty condition.

Included in the SCAP code printed output data is the contribution of the scattered radiation by zone. These data can aid the user to determine if the results are reasonable, and possibly may assist in determining where shielding might be required. A portion of the SCAP output data is summarized in Table 3-9. Table 3-9 shows the contribution by scatter zone to the scattered dose rate at the crew location and the percent contribution to the scattered dose rate. The direct and direct plus scattered dose rate is also given in this table. Data are presented for two SCAP problems: (1) 104 seconds prior to an empty tank condition, i.e., with only the run tank filled with LH₂, and, (2) 1072 seconds prior to an empty tank condition. For the 104 second case, nearly half of the scattered radiation is due to scattering from the LH₂ (zones 8, 9 and 10 as shown in Figures 10-1 and 10-2 of Section 10.0, Volume 2) in the small run tank, and the remainder (~40%) is due to scattering in the zone representing the retro rocket in the command module. However, for the 1072 second case, only 23% of the scattered radiation is due to scattering in the LH₂ zones in the run tank since this "source" is now attenuated by the LH₂ in the large propellant module. For this same case, nearly 60% of the scattered radiation is due to the LH₂ in the large propellant tank as expected. For the 104 second case, scattered and direct contributions are roughly equal. For the 1072 second case, the scattered dose rate is about twice as important as the direct component since more of the direct radiation is now being attenuated by the LH₂ in the large propellant tank.

The SCAP code also prints out the photon energy flux at the detector location due to the scattered radiation. Typical data are shown in Figure 3-19 for the condition of 104 seconds prior to empty tank. Data for the NSS sources are shown both with and without buildup on the scattered leg. The predominance of the high energy flux can be noted.

The SCAP code also calculates the radiation heat deposition in the propellant tank. The results of this calculation due to the NSS sources are: 4.4 kilowatts based on the KAP-VI meridian ring input data and 3.0 kilowatts based on the MAP meridian ring input data.

As part of this study, the use of the KAP-VI code to compute the direct photon dose rate at the crew location was also demonstrated (see Section 9.0, Volume 2). Four detector points were run in the KAP-VI problem for the case with the small run tank filled with ~9500 pounds of LH_2 : (1) on the centerline at the top of the propulsion tank, (2) at a radius of 300 cm at the top of the propellant tank, (3) on the centerline at the crew location, and (4) at a radius of 148 cm in the crew compartment. Table 3-10 summarizes the KAP-VI results at each of the four detector points. Presented in Table 3-10 is the contribution of each source region to the total direct dose rate, as well as the percent of the total.

The data in Table 3-10 show that regardless of the detector point location the reactor core contributes roughly 15% of the total dose rate, the support plate contributes about 40%, and the reflector regions contribute about 15%.

No significant change in dose rate is observed between the tank top centerline and the tank top outer radius as expected. However, there is about a factor of 2 increase in dose rate between the centerline location in the crew compartment and at the 148 cm radius of the crew compartment. This occurs because the latter detector point is no longer "shielded" by the material in the retro rocket region. Thus, it is difficult to assess an overall attenuation factor for this particular crew compartment geometry.

The KAP-VI calculated dose rate at the crew location on the centerline of 6.9×10^2 (Table 3-10) can be compared to the SCAP calculation (Table 3-9) of 5.5×10^2 . This is good agreement considering the difference in the geometries, i.e., SCAP utilized an anisotropic equivalent point source as input, whereas, the KAP-VI code used volume distributed sources throughout the NSS geometry.

FIGURE 3-1
SCHEMATIC MODEL OF THE NUCLEAR PROPELLED VEHICLE GEOMETRY

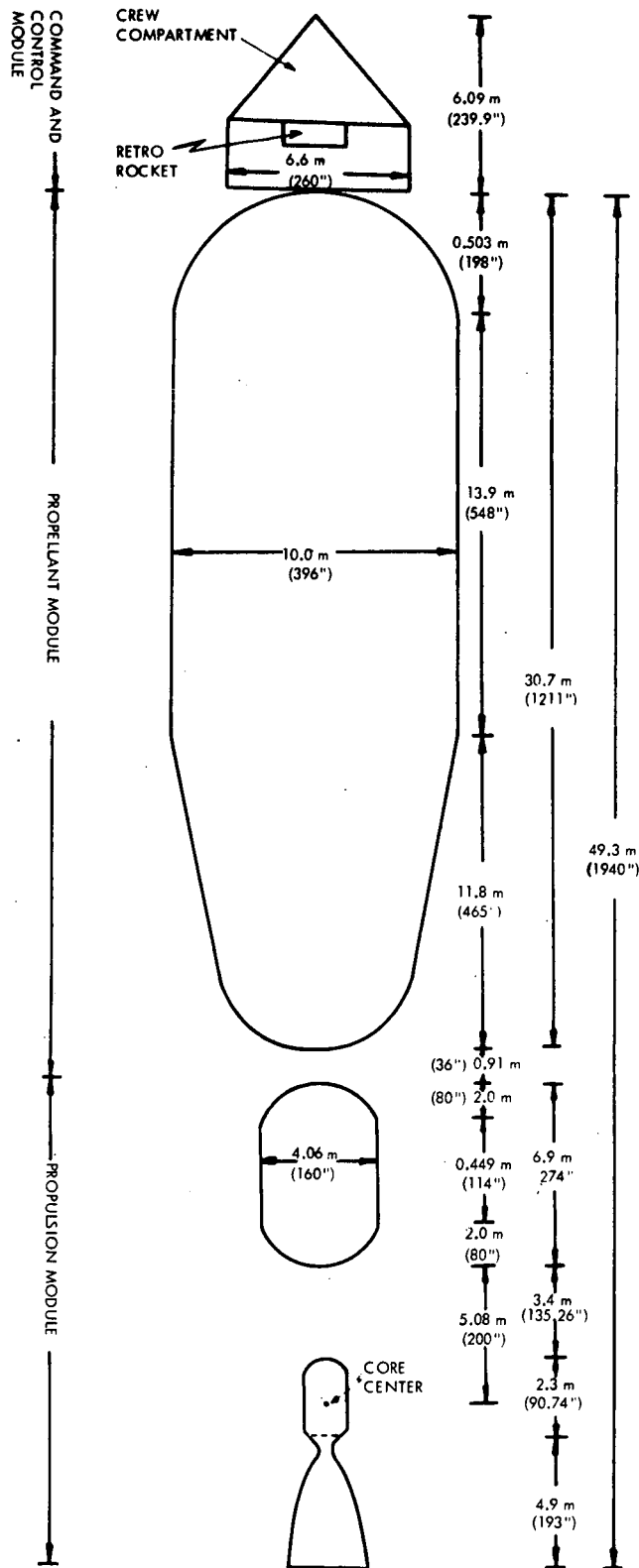
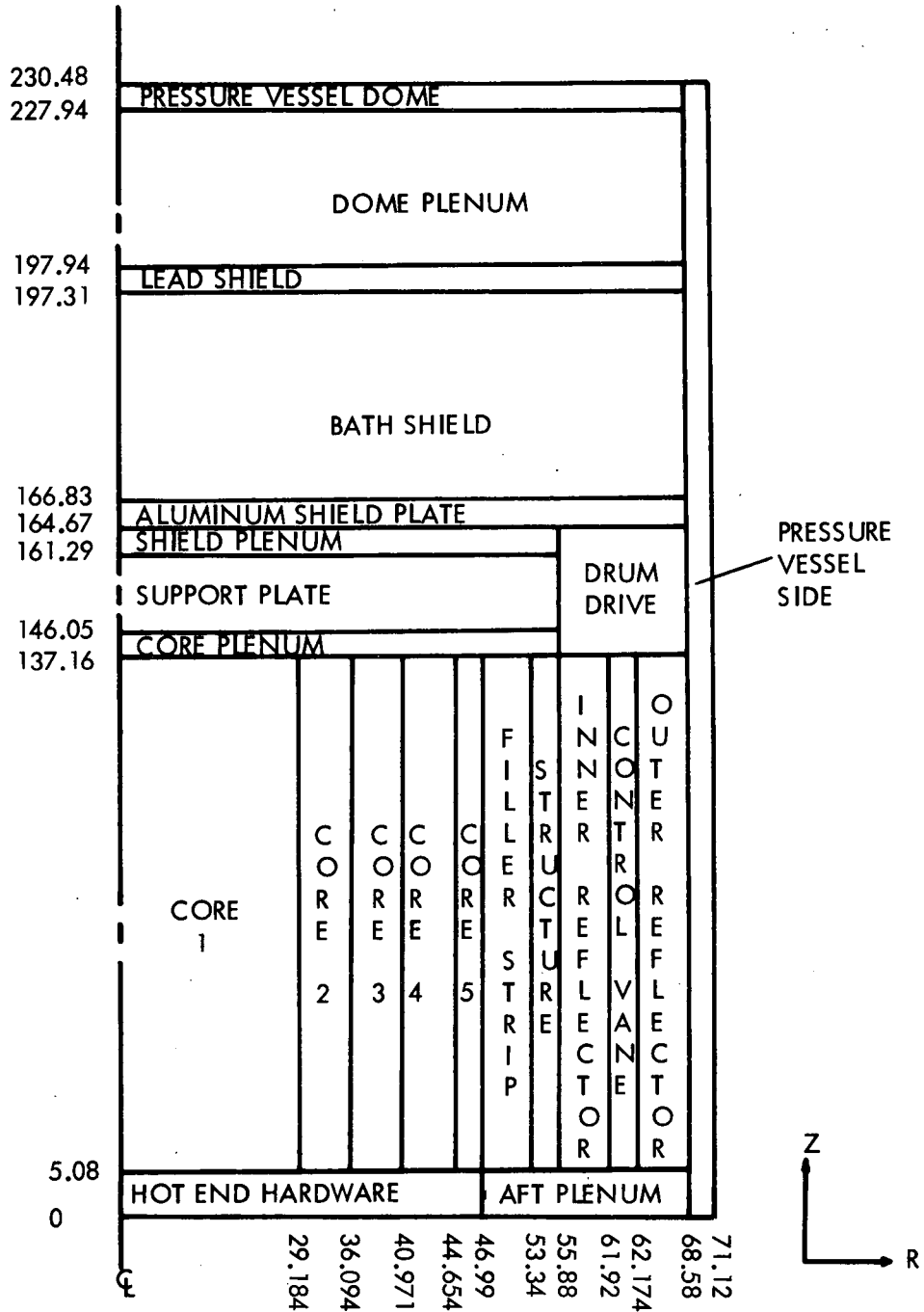


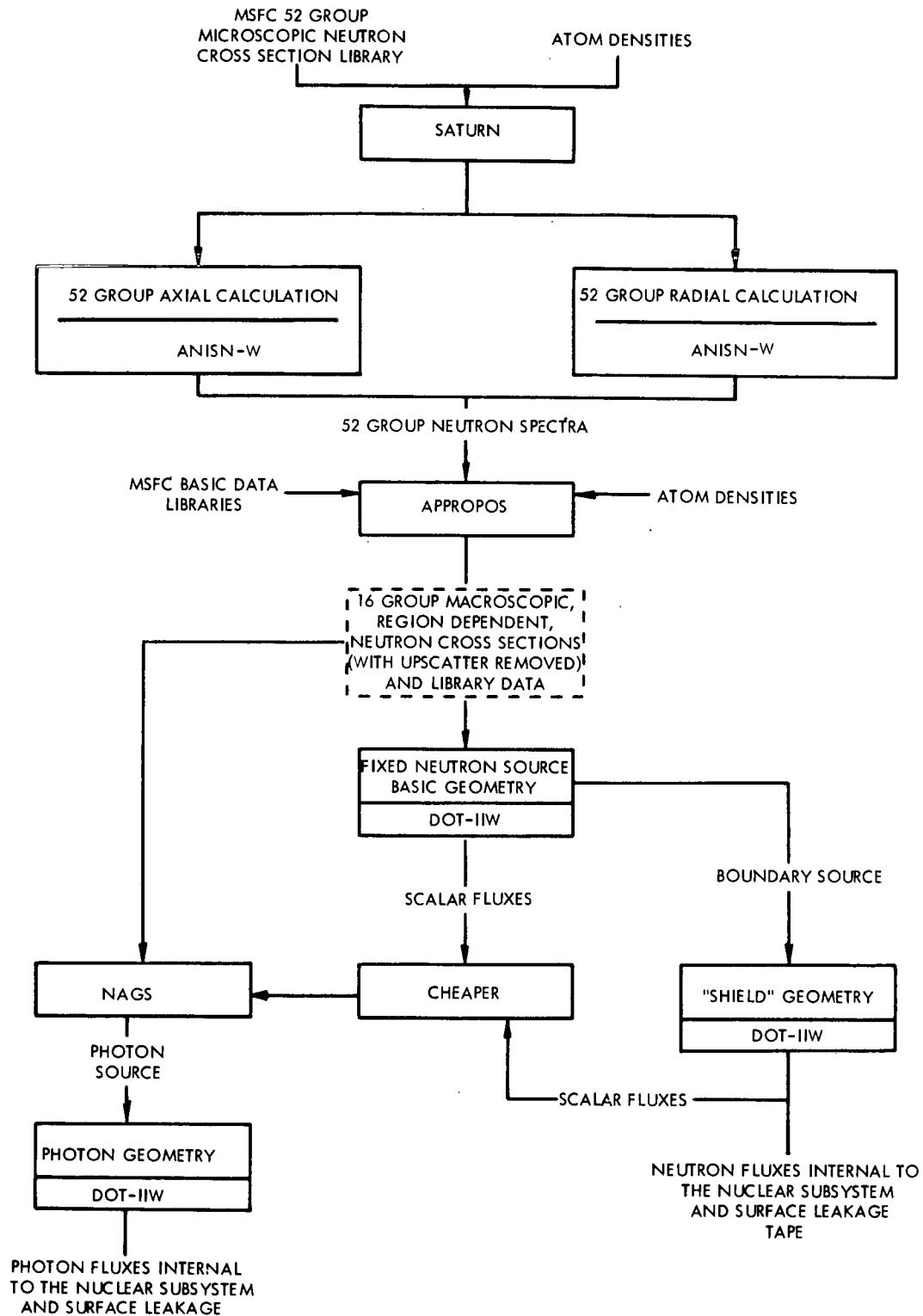
FIGURE 3-2

NUCLEAR SUBSYSTEM R-Z GEOMETRY MODEL



NOTE: DRAWING NOT TO SCALE. DIMENSIONS IN CENTIMETERS.

FIGURE 3-3. ANALYTICAL PROCEDURE FOR CALCULATING THE RADIATION ENVIRONMENT INTERNAL TO AND ON THE SURFACE OF THE NUCLEAR SUBSYSTEM



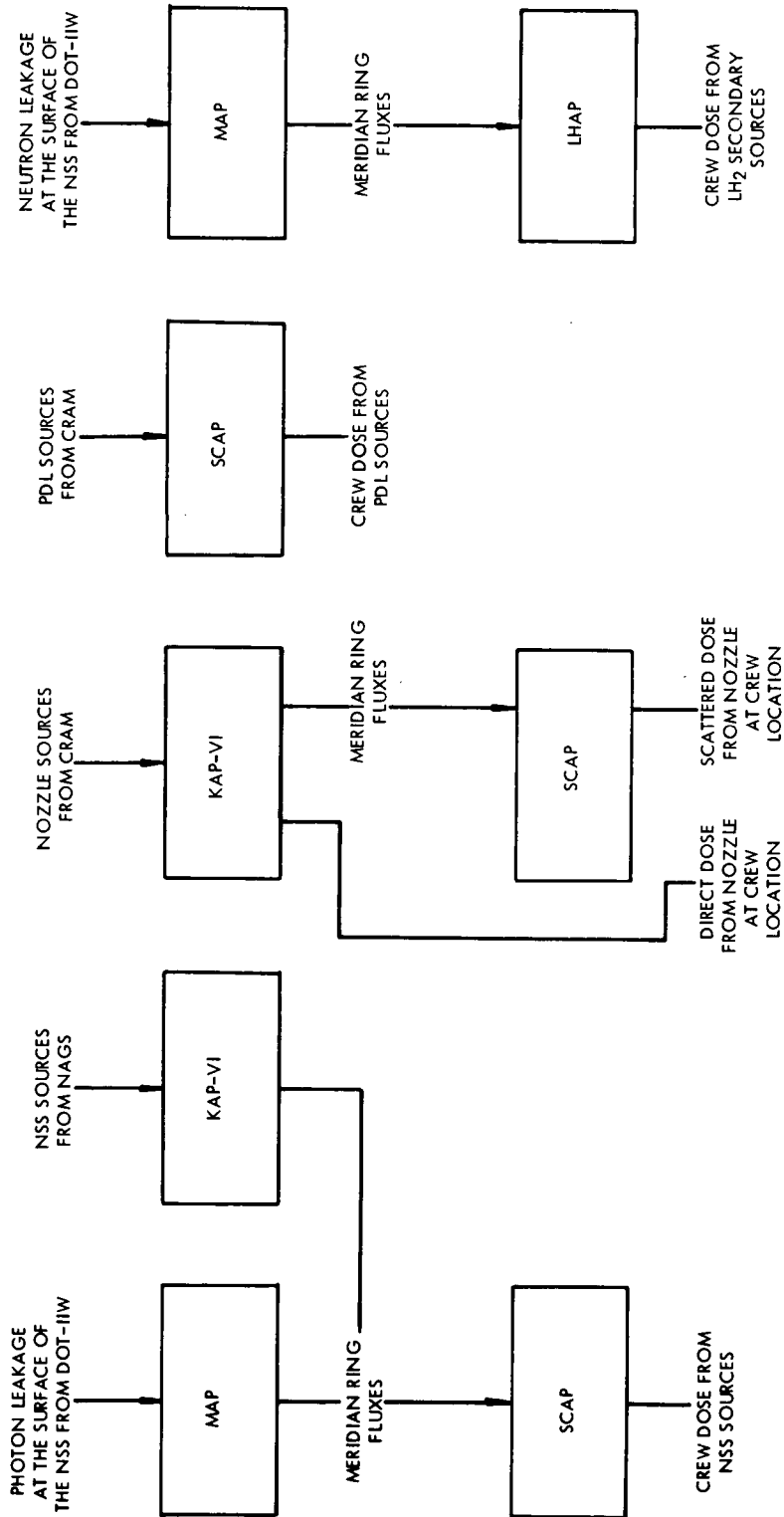


FIGURE 3-4. ANALYTICAL PROCEDURE FOR CALCULATING EXTERNAL ENVIRONMENT AND CREW DOSE

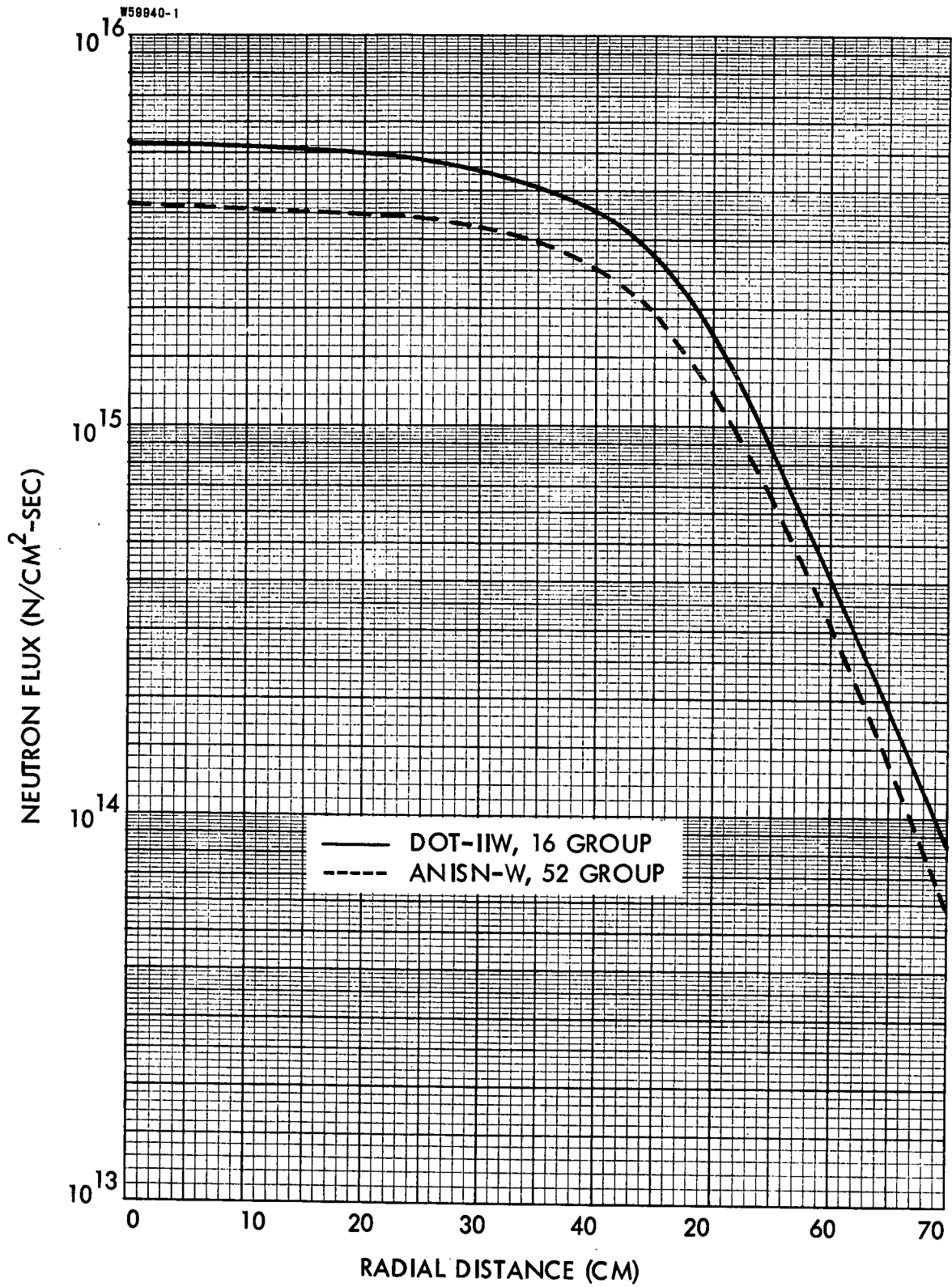


FIGURE 3-5. FAST ($E > 1.0$ MEV) NEUTRON FLUX TRAVERSE ON THE MIDPLANE OF THE NUCLEAR SUBSYSTEM

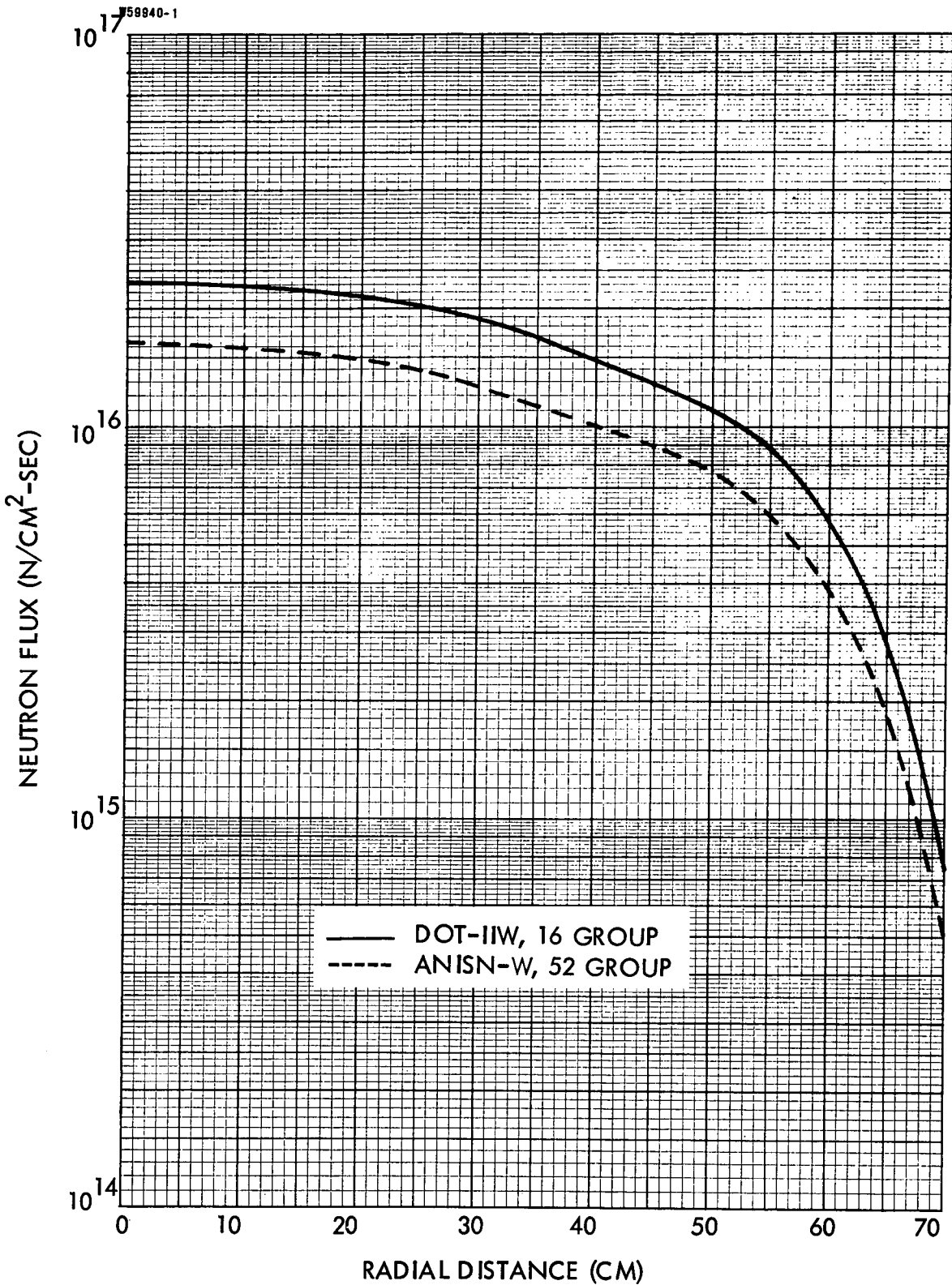


FIGURE 3-6. INTERMEDIATE ($0.3 \text{ eV} < E < 1.0 \text{ MEV}$) NEUTRON FLUX TRAVERSE ON THE MIDPLANE OF THE NUCLEAR SUBSYSTEM

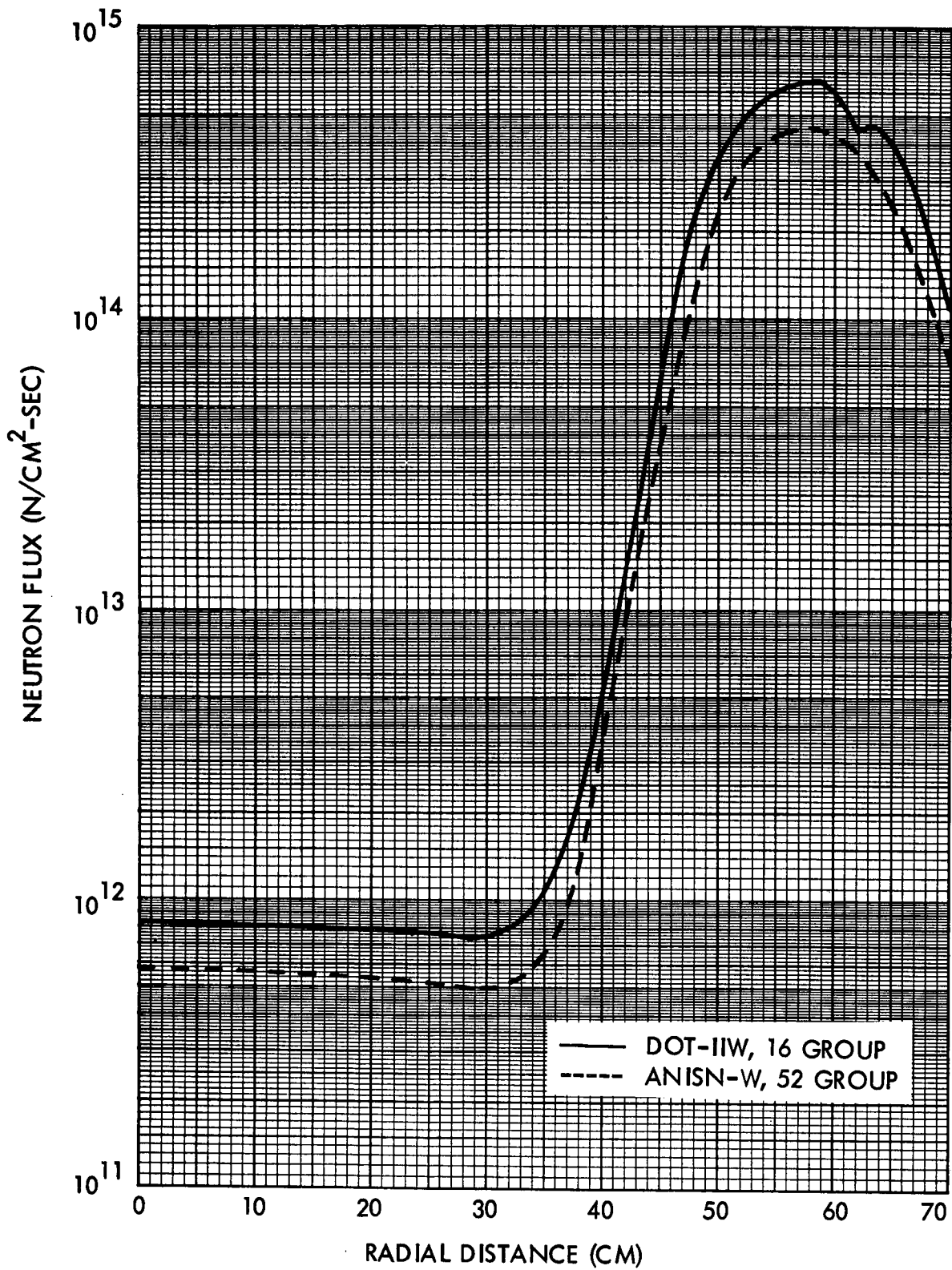


FIGURE 3-7. THERMAL ($E < 0.3$ EV) NEUTRON FLUX TRAVERSE ON THE MIDPLANE OF THE NUCLEAR SUBSYSTEM

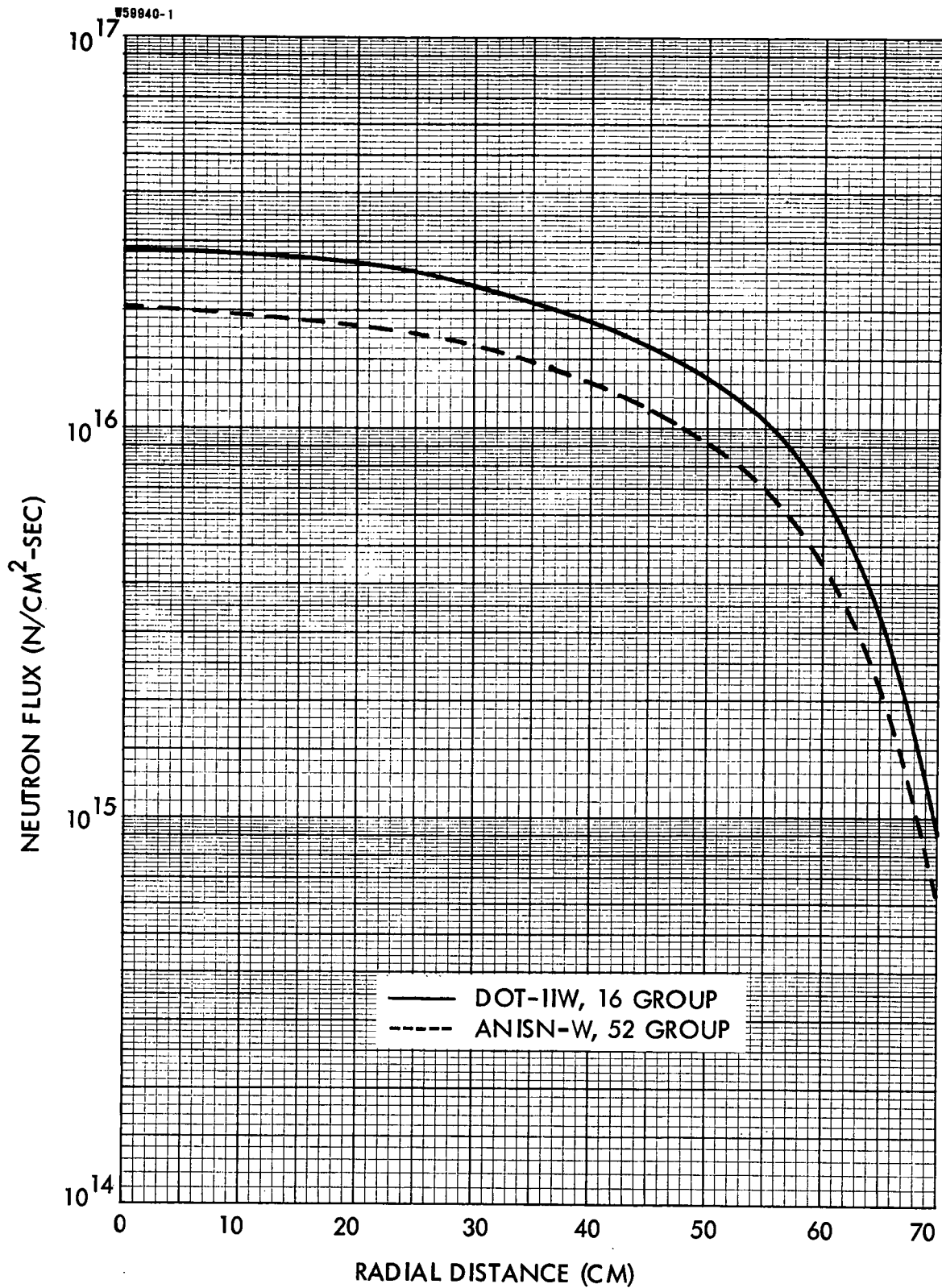


FIGURE 3-8. TOTAL NEUTRON FLUX TRAVERSE ON THE MIDPLANE OF THE NUCLEAR SUBSYSTEM

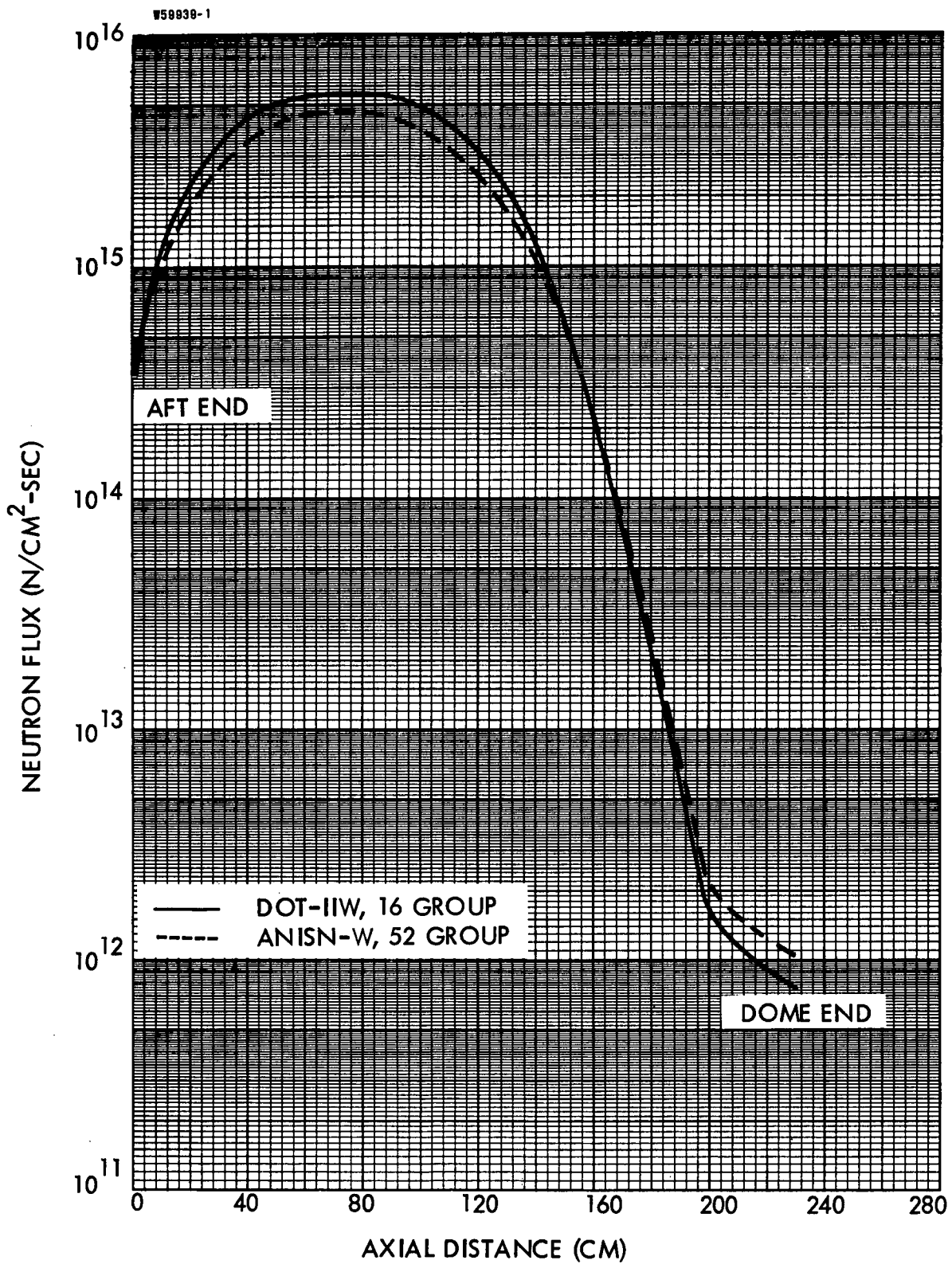


FIGURE 3-9. FAST ($E > 1.0$ MEV) NEUTRON FLUX TRAVERSE NEAR THE CENTERLINE OF THE NUCLEAR SUBSYSTEM

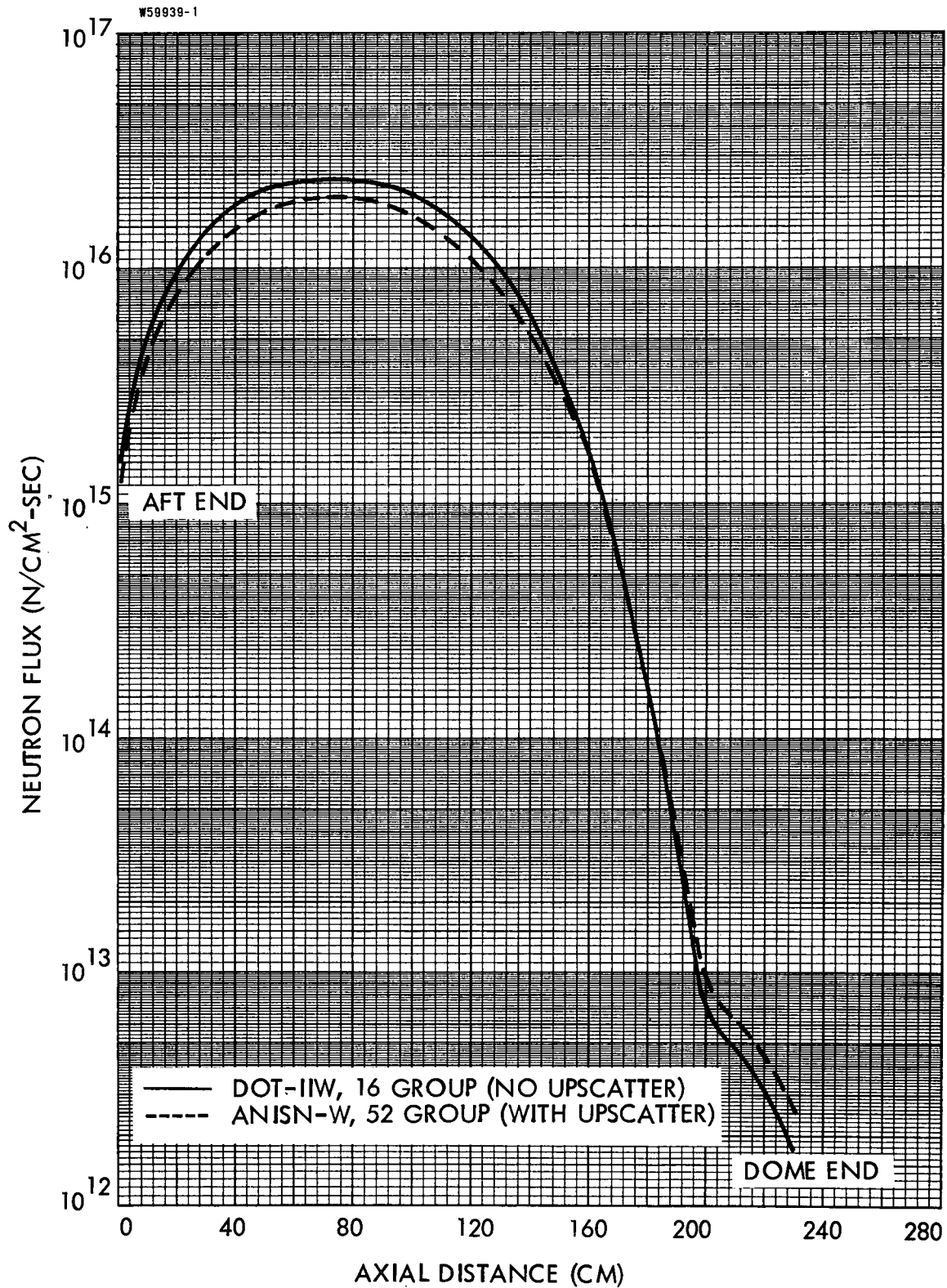


FIGURE 3-10. INTERMEDIATE (0.3 eV < E < 1.0 MEV) NEUTRON FLUX TRAVERSE NEAR THE CENTERLINE OF THE NUCLEAR SUBSYSTEM

W59838-1

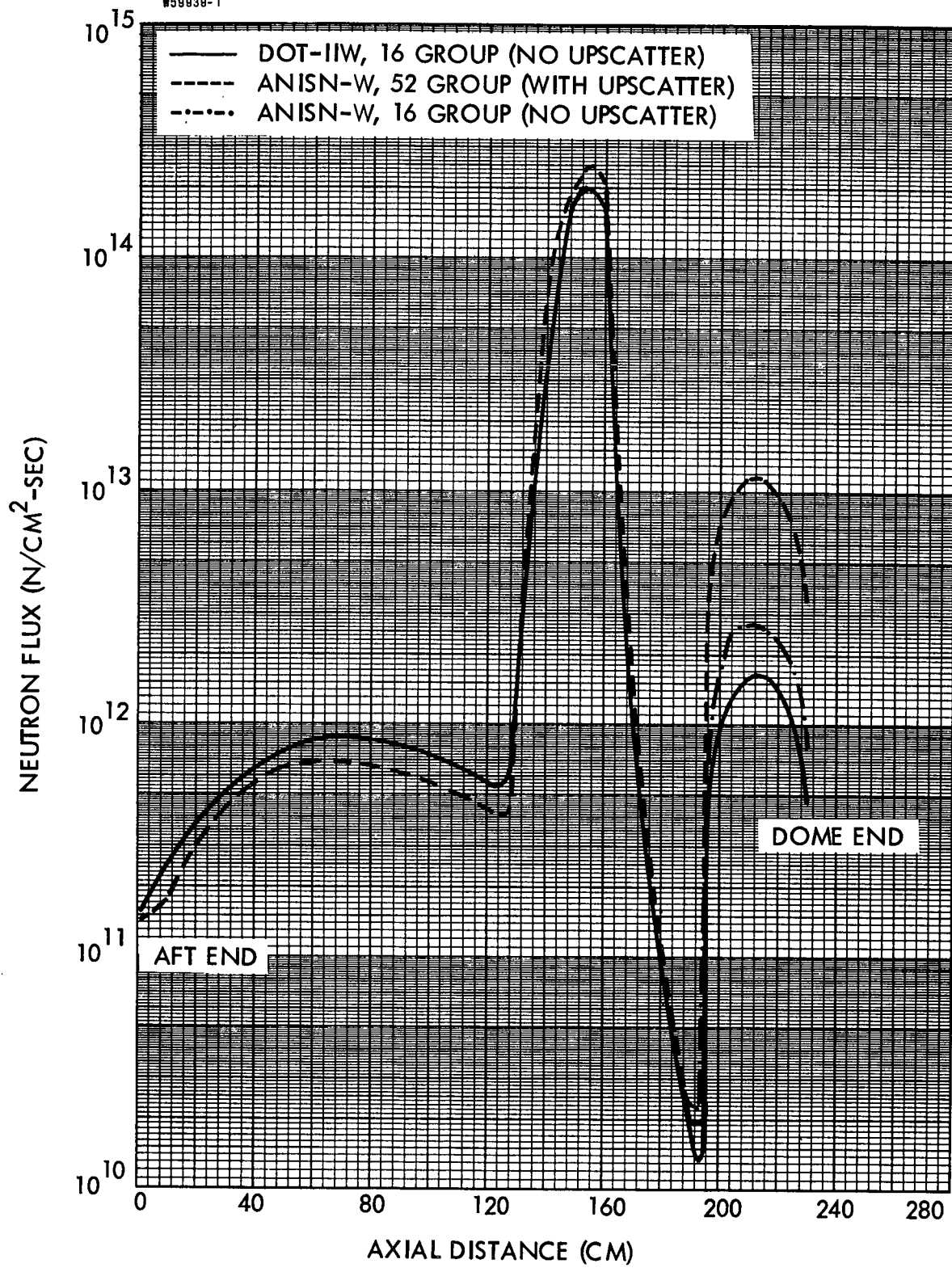


FIGURE 3-11. THERMAL (E < 0.3 EV) NEUTRON FLUX TRAVERSE NEAR THE CENTERLINE OF THE NUCLEAR SUBSYSTEM

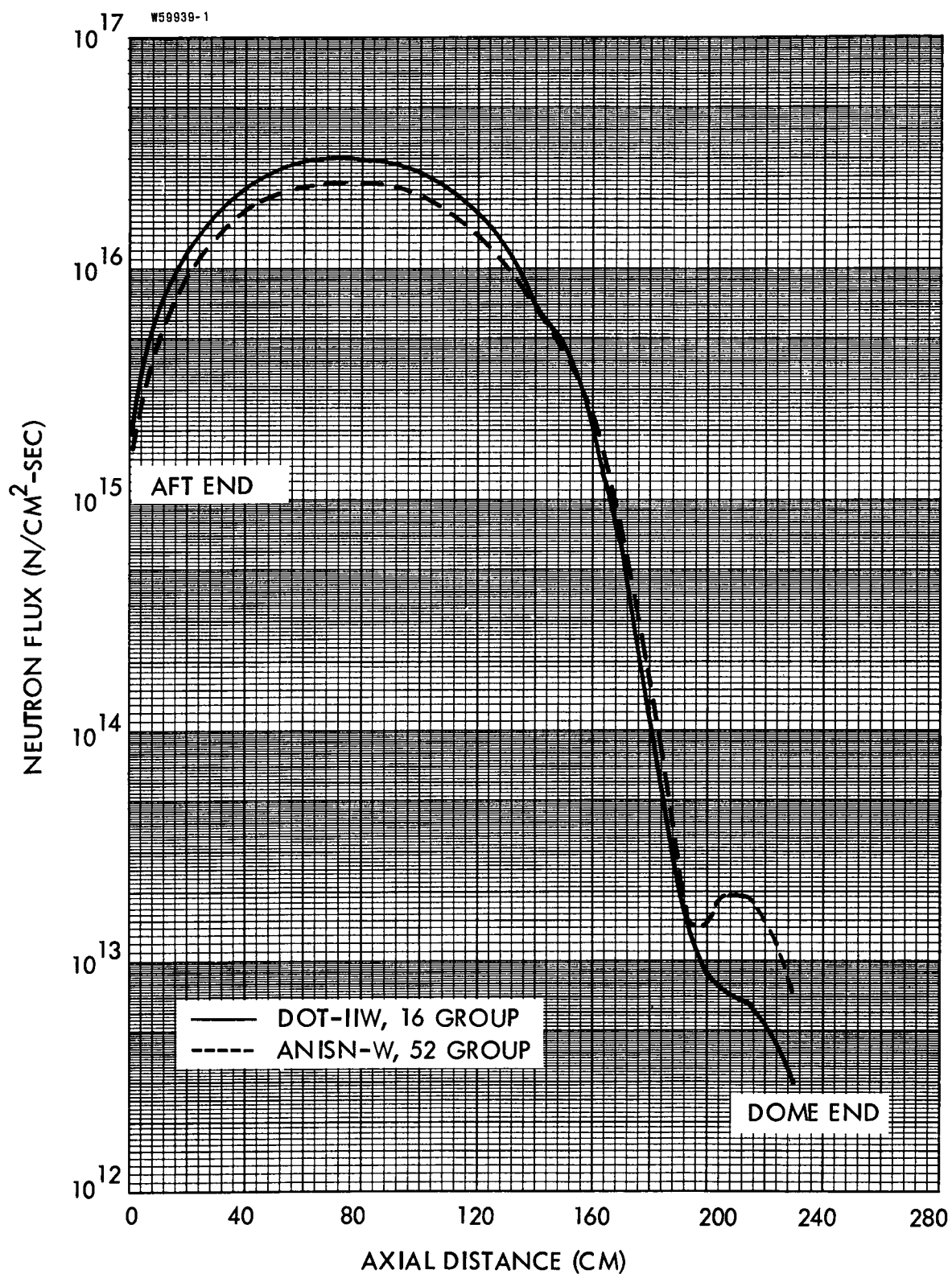


FIGURE 3-12. TOTAL NEUTRON FLUX TRAVERSE NEAR THE CENTER-LINE OF THE NUCLEAR SUBSYSTEM

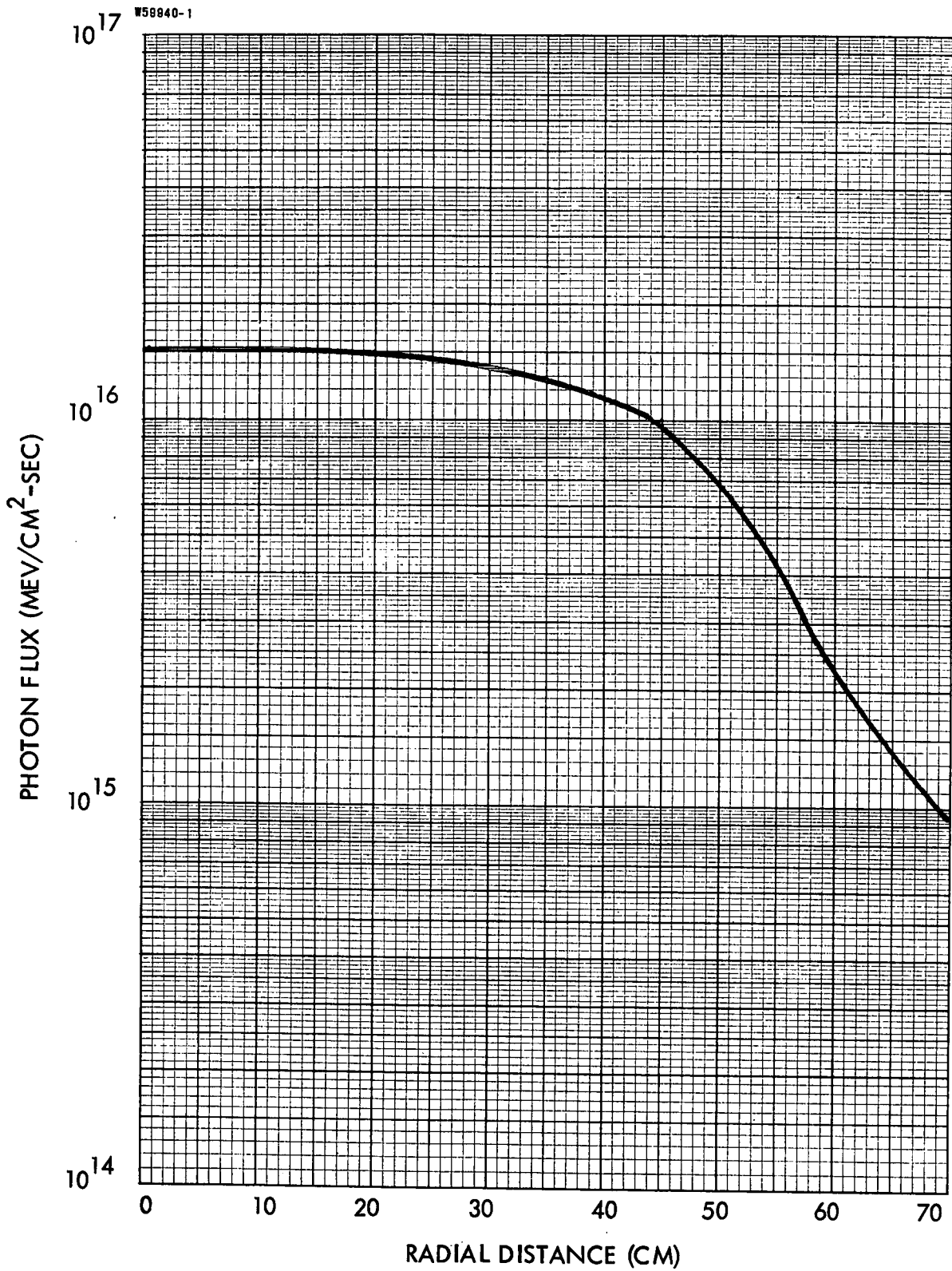


FIGURE 3-13. PHOTON FLUX TRAVERSE ON THE MIDPLANE OF THE NUCLEAR SUBSYSTEM AS CALCULATED BY THE DOT-IIW CODE

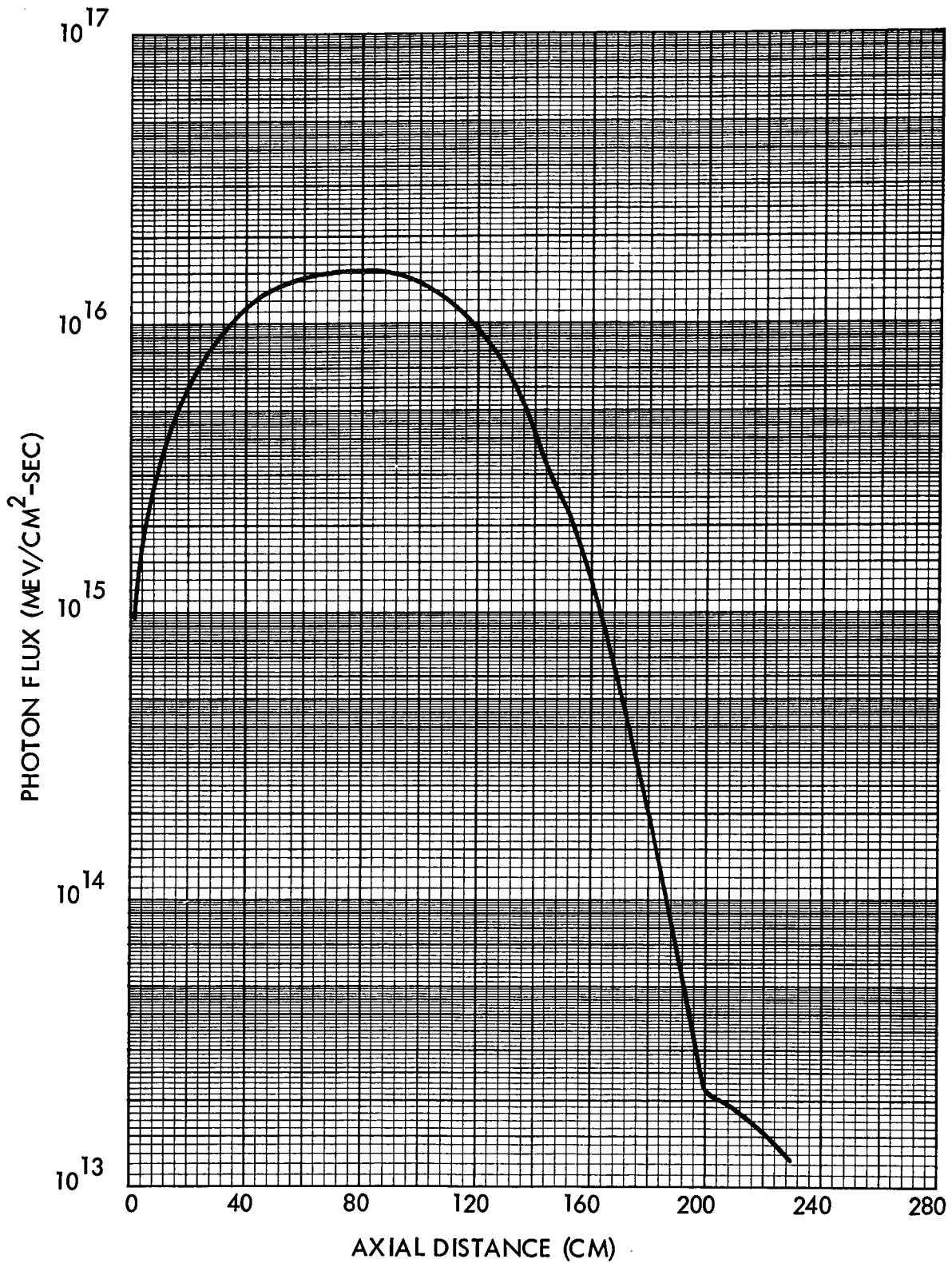


FIGURE 3-14. PHOTON FLUX TRAVERSE NEAR THE CENTERLINE OF THE NUCLEAR SUBSYSTEM AS CALCULATED BY THE DOT-IIW CODE

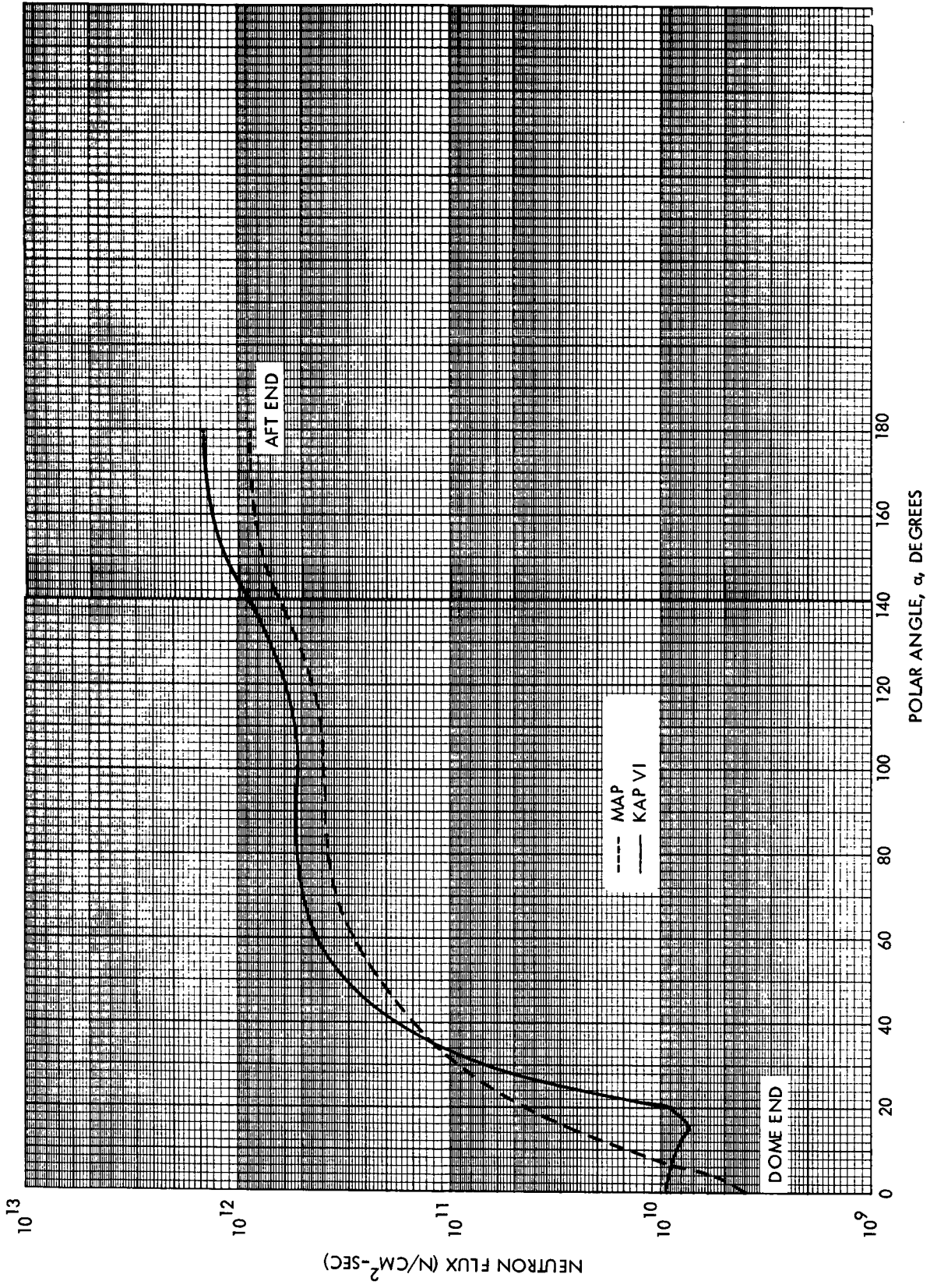


FIGURE 3-15. COMPARISON BETWEEN MAP AND KAP VI CALCULATED FAST ($E > 1.0$ MEV) NEUTRON FLUX ON THE MERIDIAN RING AT 30 FEET FROM THE CENTER OF THE CORE

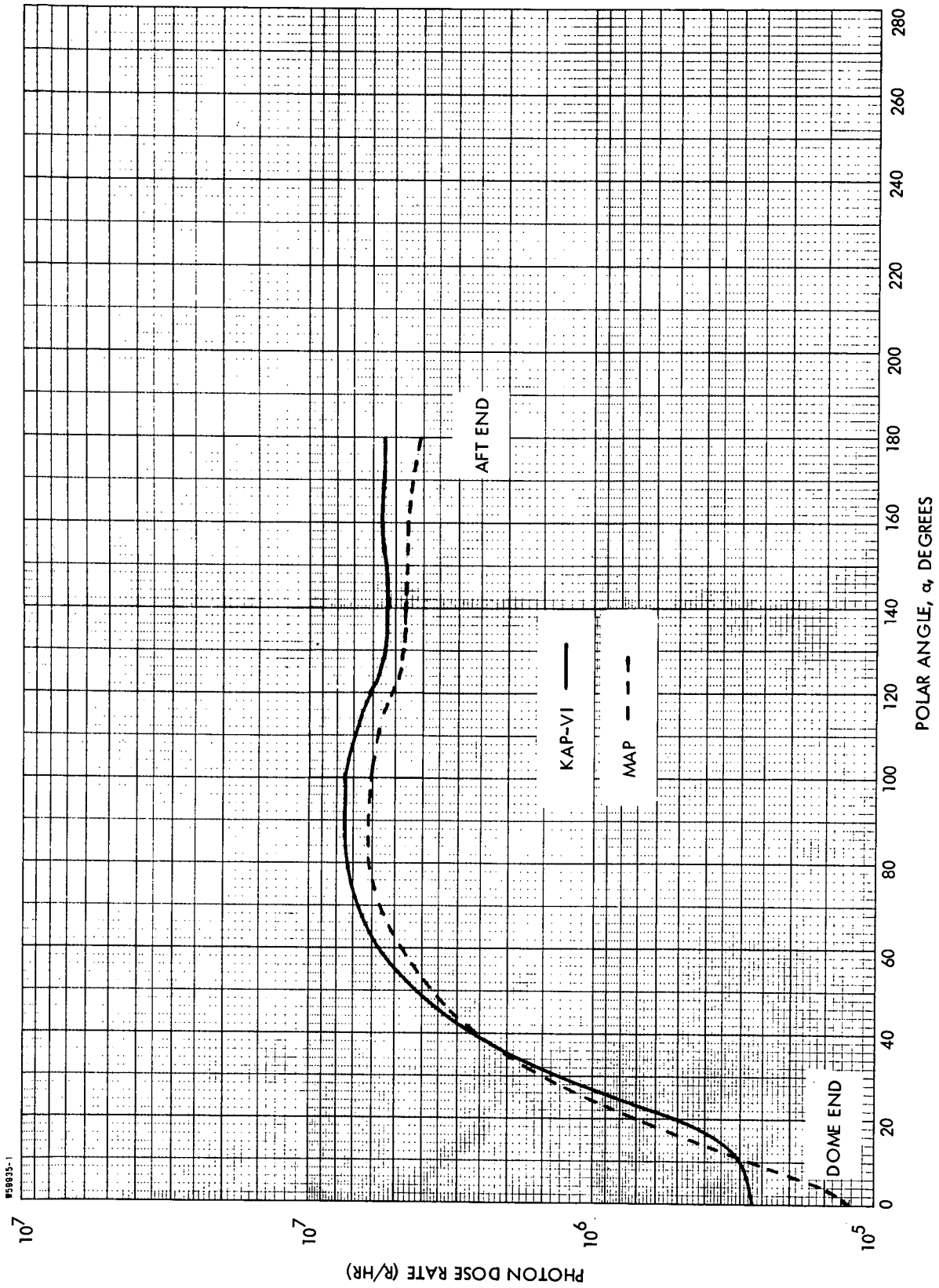


FIGURE 3-16. COMPARISON BETWEEN MAP AND KAP-VI CALCULATED PHOTON DOSE RATE ON THE MERIDIAN RING AT 30 FEET FROM THE CENTER OF THE CORE

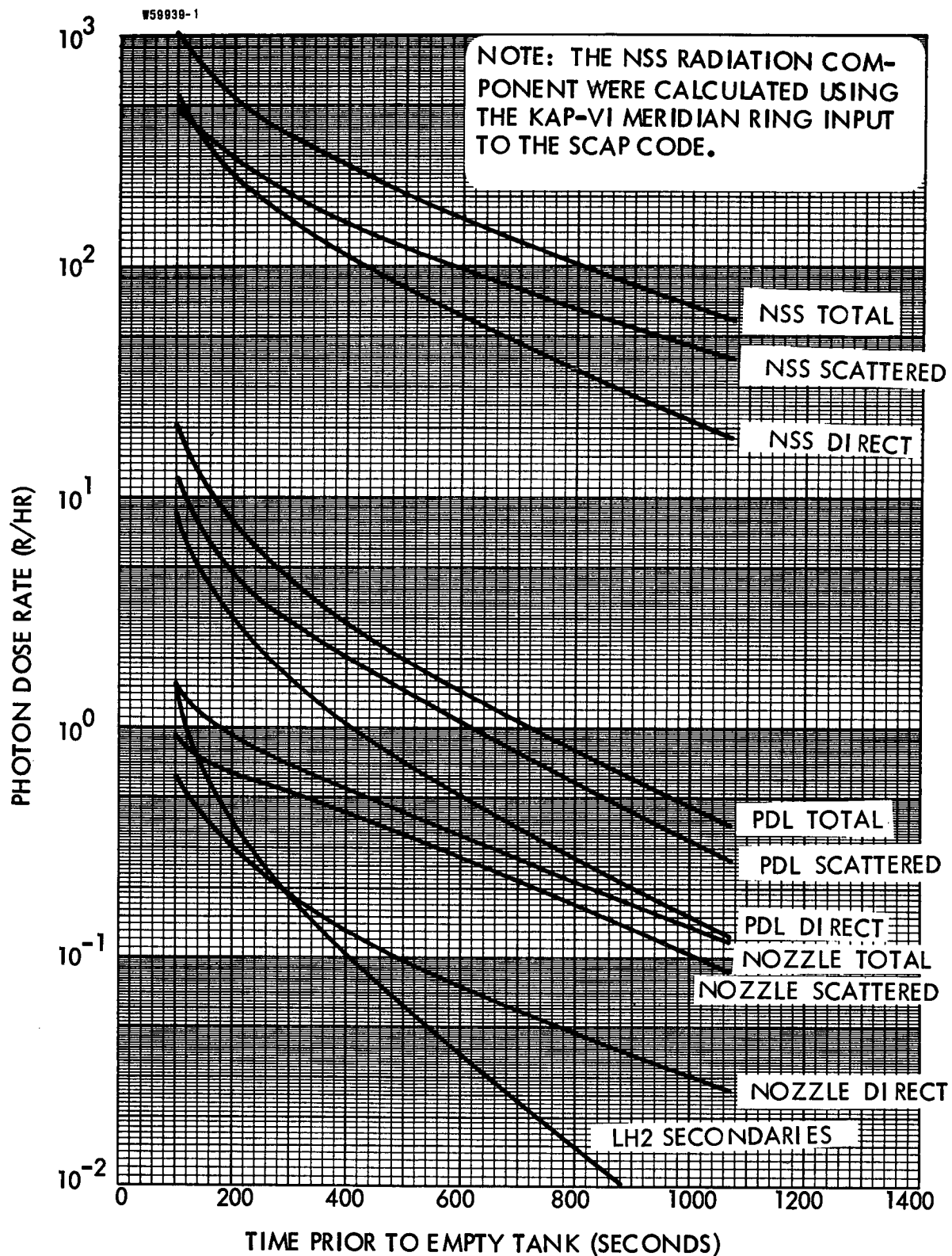


FIGURE 3-17. PHOTON DOSE RATE ON THE CENTERLINE AT THE CREW COMPARTMENT VERSUS TIME PRIOR TO EMPTY TANK

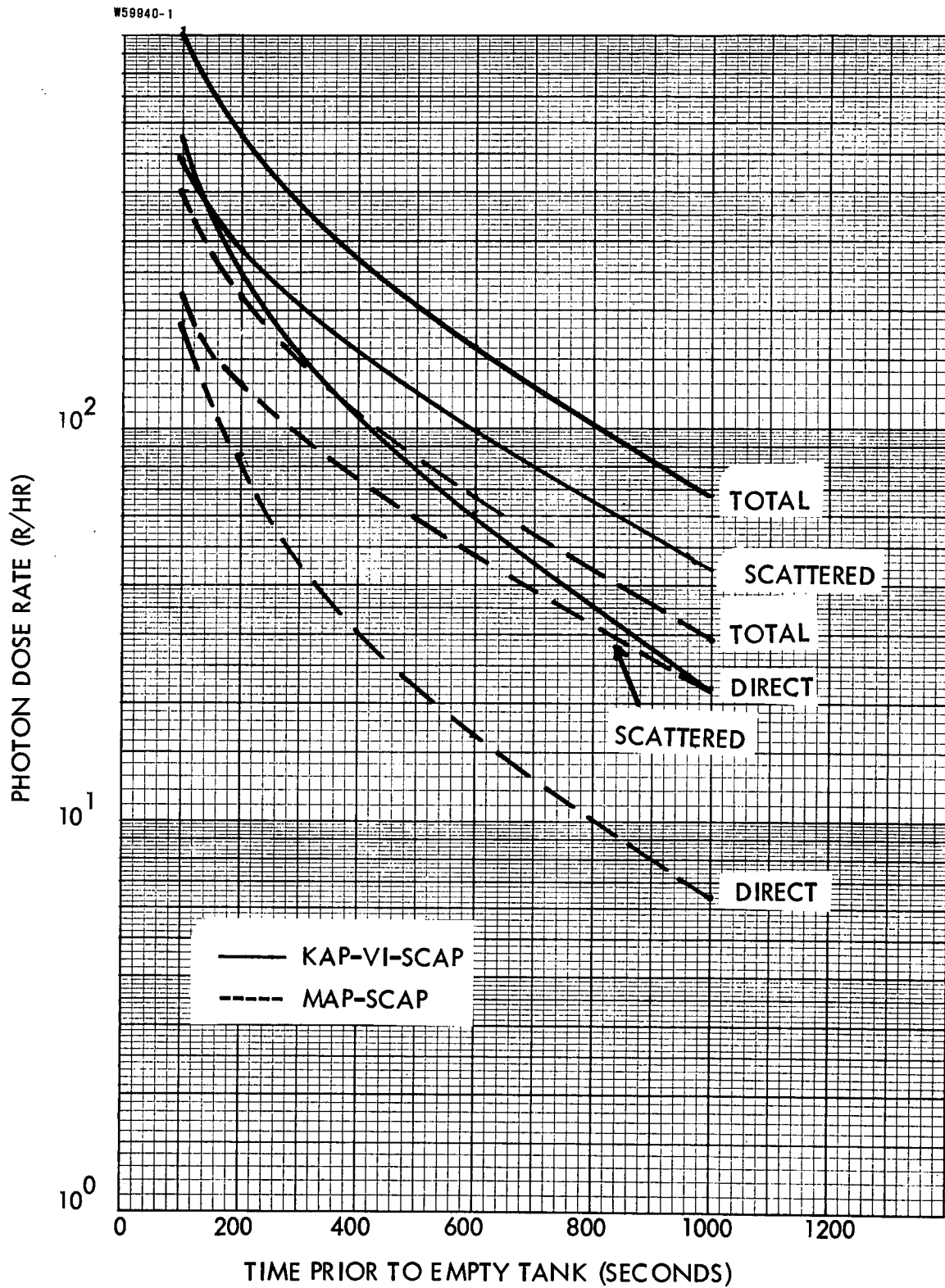


FIGURE 3-18. COMPARISON BETWEEN MAP-SCAP AND KAP-VI-SCAP CREW DOSE RATE DUE TO THE NUCLEAR SUBSYSTEM SOURCES

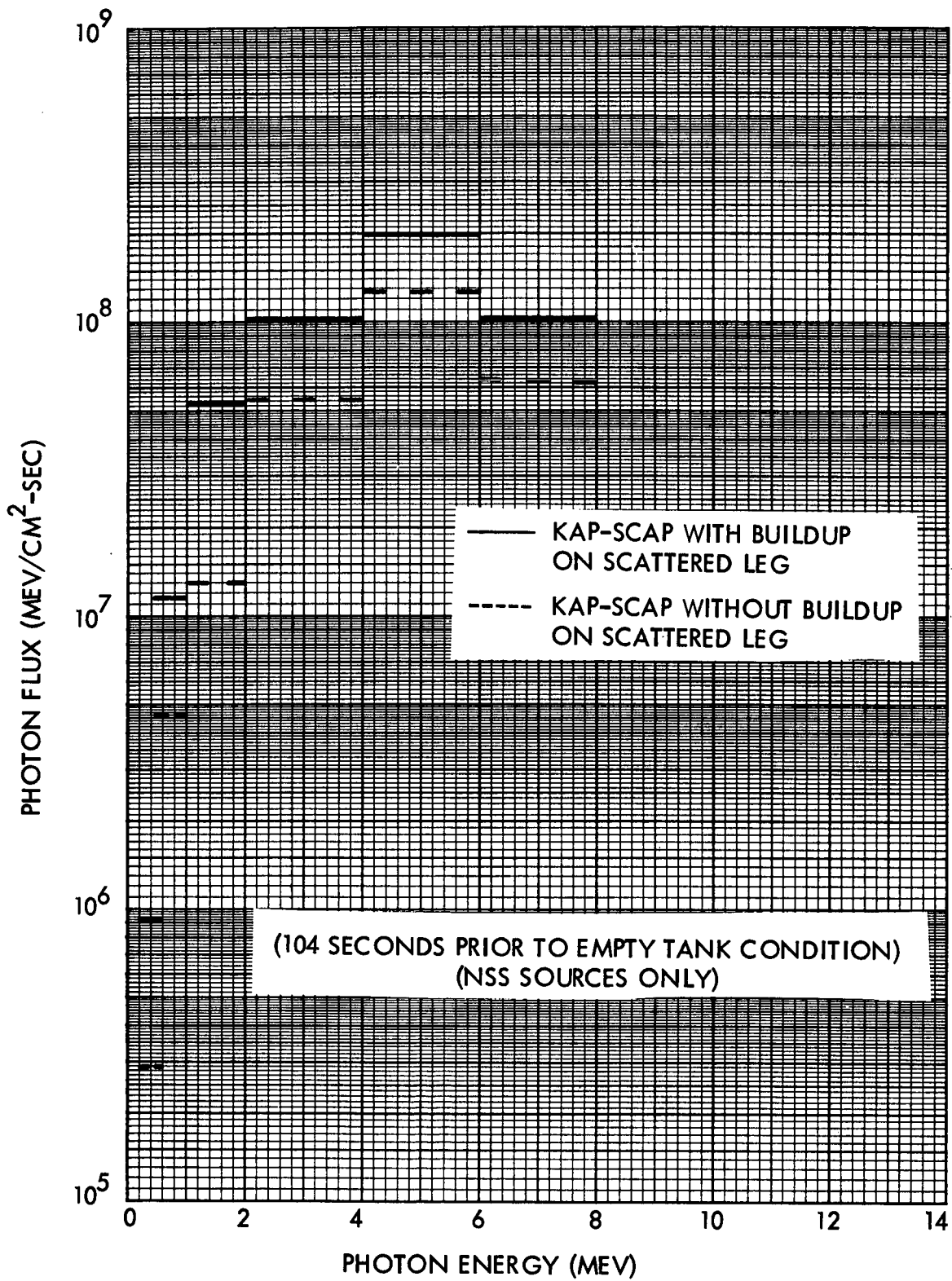


FIGURE 3-19. PHOTON ENERGY FLUX OF SINGLE SCATTERED RADIATION AT THE CREW LOCATION

TABLE 3-1
 MATERIAL COMPOSITIONS EMPLOYED TO DESCRIBE THE PROPELLANT TANK
 AND COMMAND MODULE GEOMETRY
 (GM/CC)

Composition Description	Element						
	H	C	N	O	Al	Cl	
Tank Wall	-	-	-	-	2.7	-	-
Liquid Hydrogen	0.07	-	-	-	-	-	-
Gaseous Hydrogen	0.00088	-	-	-	-	-	-
Retro Propellant	0.0101	0.0484	0.0323	0.1425	-	-	0.0582
Air	0.000011	-	0.000028	0.000404	-	-	-
Epoxy	0.0387	0.3642	0.0283	0.1294	-	-	-
Capsule Wall	-	-	-	-	0.072	-	-

TABLE 3-2
ELEMENT ATOM DENSITIES (N/cc) FOR THE NUCLEAR SUBSYSTEM MODEL FOR THE MSFC SEMINAR WORKSHOP

Region No.	Region Description	H	C	Mn	Cr	Ni	Fe	Ta	Al	Zr	U ²³⁵	U ²³⁸	Ti	Be	Pb	B	W
1	Core 1	.000342	.04461	.0000137	.0001418	.0002039	.0004805	.00001	-	.007325	.0007942	.00005767	-	-	-	-	-
2	Core 2	.000342	.04474	.0000149	.0001542	.0002218	.0005226	.00001	-	.007311	.000992	.00007203	-	-	-	-	-
3	Core 3	.000342	.04468	.0000144	.0001495	.000215	.0005066	.00001	-	.007314	.001065	.00007731	-	-	-	-	-
4	Core 4	.000342	.04488	.0000165	.000171	.0002458	.0005791	.00001	-	.007283	.001026	.00007447	-	-	-	-	-
5	Core 5	.000342	.04542	.0000216	.0002238	.0003219	.0007584	.00001	-	.007217	.0007736	.00005618	-	-	-	-	-
6	Filler Strip	.0000285	.05578	-	-	-	-	-	-	-	-	-	-	-	-	-	-
7	Structure	.000299	-	-	.0003446	.0005278	.00117	-	.05842	-	-	-	.0005322	-	-	-	-
8	Inner Reflector	.00151	-	-	.0001862	.0002851	.000632	-	.004998	-	-	-	.00002875	.07969	-	-	-
9	Vane	-	-	-	-	-	-	-	-	-	-	-	-	-	-	-	-
10	Outer Reflector	.00151	-	-	.000574	.0008791	.001949	-	.005312	-	-	-	.00008864	.08085	-	-	-
11	Pressure Vessel Side	.00158	-	-	-	-	-	-	.0502	-	-	-	-	-	-	-	-
12	Cluster Hardware	.000955	.00647	.0000829	.000860	.00128	.00298	-	-	-	-	-	.000126	-	-	-	.00765
13	Plenum and Hardware	.00587	-	.000363	.000409	.000596	.00288	-	.0229	-	-	-	.0000601	-	-	-	-
14	Core Plenum	.00334	-	.000262	.00261	.00157	.00904	-	-	-	-	-	.00621	-	.000252	-	-
15	Support Plate	.00561	-	.000161	.00162	.000813	.00554	-	.03147	-	-	-	.0000126	-	-	-	-
16	Shield Plenum	.00501	-	.000208	.00207	.000934	.00708	-	-	-	-	-	-	-	-	-	-
17	Drum Drive	.00579	-	.000127	.000624	.000534	.00244	-	.00368	-	-	-	.0000377	-	-	-	-
18	Aluminum Shield Plate	.000657	-	-	-	-	-	-	.0507	-	-	-	-	-	-	-	-
19	BATH Shield	.0182	.00142	-	-	-	-	-	.0369	-	-	-	.00992	-	-	.00568	-
20	Lead Shield	.000657	-	-	-	-	-	-	-	-	-	-	-	.0275	-	-	-
21	Dome Plenum	.00776	-	-	-	-	-	-	-	-	-	-	-	-	-	-	-
22	Pressure Vessel	-	-	-	-	-	-	-	.0610	-	-	-	-	-	-	-	-

* x 10²⁴

TABLE 3-3
 SUMMARY OF MASTER LIBRARIES

<u>MSFC Master Library Number</u>	<u>Description</u>
1	Microscopic, 52 Group, Transport Corrected Neutron Cross Section Sets for Use in the ANISN-W, DOT-IIW, and APPROPOS Codes
2	Microscopic, 52 Group, P_0 , Neutron Cross Section Sets for Use in the ANISN-W, DOT-IIW, and APPROPOS Codes
3	Microscopic, 52 Group, Reaction Rate Cross Section Sets for Use in the APPROPOS Code
4	Microscopic, 13 Group, P_0 , Gamma Ray Cross Section Sets for Use in the ANISN-W, DOT-IIW, and APPROPOS Codes
5	Pair-Production and Photo-Electric Gamma Ray Cross Sections for Use in the KAP-VI, SCAP, MAP, and GAMLEG-W Codes
6*	Gamma Ray Production Data Due to Thermal Neutron Capture and Inelastic Scatter, Selected Nuclear Parameters, and Other Related Data.

*On Cards

TABLE 3-4

PHOTON SOURCES IN THE NUCLEAR SUBSYSTEM
CALCULATED BY THE NAGS CODE

<u>NSS Region*</u>	<u>Photon Source (Mev/Sec)</u>
Core	9.13×10^{20}
Filler Strip	6.60×10^{17}
Structure	9.61×10^{18}
Reflector	1.50×10^{19}
Pressure Vessel (Side)	1.33×10^{18}
Hot End Hardware	2.39×10^{18}
Aft Plenum	3.49×10^{17}
Core Plenum	5.93×10^{18}
Support Plate	9.99×10^{18}
Shield Plenum	6.35×10^{17}
Drum Drive	1.25×10^{18}
Shield Plate	1.59×10^{17}
BATH Shield	1.53×10^{18}
Lead Shield	4.87×10^{14}
Dome Plenum	1.56×10^{15}
Pressure Vessel (Dome)	1.68×10^{15}
TOTAL	9.63×10^{20}

*See Figure 3-2 for region location.

TABLE 3-5

FAST NEUTRON ($E > 1.0$ MEV) FLUX ON THE THIRTY FOOT MERIDIAN RING
CALCULATED BY THE DOT-IIW-MAP TECHNIQUE

Polar Angle (Degrees)	Flux ($n/cm^2\text{-sec}$)				Total
	Reactor Side*	Reactor Bottom	Shield Side*	Shield Top	
0	-	-	-	4.05(9)	4.05(9)
4	-	-	-	5.98(9)	5.98(9)
8	4.23(9)	-	9.39(7)	7.07(9)	1.14(10)
11	7.67(9)	-	5.02(7)	6.71(9)	1.45(10)
15	1.72(10)	-	1.03(9)	5.77(9)	2.40(10)
30	6.83(10)	-	1.26(10)	1.94(9)	8.28(10)
80	3.75(11)	-	3.47(9)	4.89(6)	3.78(11)
120	2.06(11)	2.53(11)	7.78(8)	-	4.59(11)
180	-	8.76(11)	-	-	8.76(11)

*The term reactor refers to the reactor geometry DOT-IIW problem leakage data; the term shield refers to the shield geometry DOT-IIW problem leakage data.

NOTE: Numbers in parentheses refer to powers of ten.

TABLE 3-6

CONTRIBUTION OF SOURCE REGIONS TO THE GAMMA RAY DOSE RATE
(REM/HOUR) ON THE MERIDIAN RING

Source Region	$\alpha = 0^\circ$ (Dome End)		$\alpha = 80^\circ$ (Side)		$\alpha = 180^\circ$ (Aft End)	
	Dose Rate	% of Total	Dose Rate	% of Total	Dose Rate	% of Total
Core 1	3.05(4)	11.8	6.62(5)	8.9	1.91(6)	34.7
Core 2	1.45(4)	5.6	8.50(5)	11.4	9.23(5)	16.8
Core 3	1.15(4)	4.5	1.22(6)	16.3	7.52(5)	13.6
Core 4	9.83(3)	3.8	1.69(6)	22.6	6.66(5)	12.1
Core 5	7.19(3)	2.8	1.76(6)	23.6	5.15(5)	9.4
Total Core	7.36(4)	28.5	6.18(6)	82.8	4.76(6)	86.6
Filler Strip	4.42(2)	0.2	1.59(4)	0.2	1.30(4)	0.2
Structure	3.63(3)	1.4	2.61(5)	3.5	1.19(5)	2.2
Inner Reflector	6.86(3)	2.7	1.93(5)	2.6	9.67(4)	1.8
Outer Reflector	1.55(4)	6.0	3.53(5)	4.7	9.13(4)	1.7
Pressure Vessel (Side)	2.63(3)	1.0	7.31(4)	1.0	1.74(4)	0.3
CHESH	1.33(-1)	<.1	1.39(4)	0.2	2.94(5)	5.3
Aft Plenum	5.89(0)	<.1	1.08(4)	0.1	3.86(4)	0.7
Core Plenum	2.26(4)	8.8	1.17(5)	1.6	2.12(2)	<.1
Support Plate	8.33(4)	32.2	1.63(5)	2.2	3.96(2)	<.1
Shield Plenum	8.78(3)	3.4	7.75(3)	0.1	9.88(-1)	<.1
Drum Drive	1.37(4)	5.3	5.92(4)	0.8	8.48(2)	<.1
Shield Plate	2.14(3)	0.8	1.93(3)	<.1	1.32(1)	<.1
BATH Shield	2.46(4)	9.5	1.51(4)	0.2	2.34(1)	<.1
Lead Shield	6.74(1)	<.1	8.69(0)	<.1	1.41(-3)	<.1
Dome Plenum	2.40(2)	0.1	1.73(2)	<.1	3.65(-4)	<.1
Pressure Vessel (Dome)	2.61(2)	0.1	2.25(1)	<.1	4.28(-3)	<.1
Total Non-Core	1.84(5)	71.5	1.28(6)	17.2	7.37(5)	13.4
Grand Total	2.58(5)	100.0	7.47(6)	100.0	5.50(6)	100.0

NOTE: Numbers in parentheses refer to powers of ten.

TABLE 3-7

CREW DOSE ON THE CENTERLINE OF THE COMMAND MODULE

 (Total Burn: ~46 Minutes)
 (Residual LH₂: ~9500 Pounds)

<u>Radiation Source</u>	<u>Dose (Rem)</u>
<u>Nuclear Subsystem</u>	
Direct	30.1 (13.5)*
Scattered	43.1 (19.6)*
<u>PDL</u>	
Direct	0.31
Scattered	0.55
<u>Nozzle</u>	
Direct	0.04
Scattered	0.10
LH ₂ Secondaries	0.04
TOTAL	74.24 (34.14)*

*Numbers in parentheses are results of MAP-SCAP analysis. Other NSS data are results of KAP-SCAP analysis.

TABLE 3-8

CENTERLINE CREW DOSE (REM) VERSUS TIME PRIOR TO EMPTY TANK
CONDITION - NSS SOURCES ONLY*

(Total Burn Time: ~46 Minutes)
(Residual Propellant: ~9500 Pounds)

<u>Time Prior to Empty Tank (Seconds)</u>	<u>NSS Direct (Rem)</u>	<u>NSS Scattered (Rem)</u>	<u>NSS Total (Rem)</u>
100 - 200	9.64	9.82	19.46
200 - 300	5.37	6.82	12.19
300 - 400	3.66	5.01	8.67
400 - 500	2.67	3.82	6.49
500 - 600	1.98	3.03	5.01
600 - 700	1.49	2.47	3.96
700 - 800	1.12	2.02	3.14
800 - 900	0.86	1.63	2.49
900 - 1000	0.69	1.35	2.04
1000 - 2880	2.61	7.12	9.73
TOTAL	30.09	43.09	73.18

*NSS contribution as calculated by the KAP-VI-SCAP technique.

TABLE 3-9
SCAP CALCULATED SCATTERED RADIATION BY ZONE TO THE CREW LOCATION
ON AXIS - NSS SOURCES ONLY

SCAP Zone Number	Zone Description	104 Seconds Prior to Empty		1072 Seconds Prior to Empty	
		Scattered Dose Rate (R/hr)	% of Total Scatter	Scattered Dose Rate (R/hr)	% of Total Scatter
5	Wall of Run Tank	7.16(-1)	0.1	2.57(-2)	<.1
7	Wall of Run Tank	9.49(-1)	0.2	4.12(-2)	<.1
8	LH ₂ - Run Tank	8.49(1)	17.6	3.23(0)	8.2
9	LH ₂ - Run Tank	1.20(2)	24.8	5.02(0)	12.7
10	LH ₂ - Run Tank	1.87(1)	3.9	8.74(-1)	2.2
11	GH ₂ - Run Tank	3.82(-1)	<.1	1.99(-2)	<.1
13	Wall of Large Tank	2.01(0)	0.4	9.26(-2)	<.1
16	GH ₂ /LH ₂ *	4.44(-1)	<.1	1.79(0)	4.5
17	GH ₂ /LH ₂ *	1.23(0)	0.3	4.43(0)	11.2
18	GH ₂ /LH ₂ *	1.69(0)	0.3	5.68(0)	14.4
19	GH ₂ /LH ₂ *	3.53(0)	0.7	1.04(1)	26.3
20	GH ₂	7.46(0)	1.5	2.36(-1)	0.6
21	GH ₂	3.49(0)	0.7	1.04(-1)	0.3
22	GH ₂	4.18(0)	0.9	1.24(-1)	0.3
23	Wall of Large Tank	5.43(0)	0.6	3.34(-1)	0.8
24	Wall of Large Tank	3.35(0)	0.7	9.66(-2)	<.1
26	Wall of Large Tank	5.87(0)	1.2	6.39(-1)	1.6
30	Instrumentation	6.67(0)	1.4	1.94(-1)	0.5
32	Instrumentation	7.38(0)	1.5	2.14(-1)	0.5
35	Retro Rocket	1.92(2)	39.8	5.62(0)	14.2
37	Instrumentation	3.29(-1)	<.1	8.02(-3)	<.1
38	Epoxy	9.52(0)	1.9	2.59(-1)	0.2
39	Capsule Wall	1.46(0)	0.3	3.93(-2)	<.1
41	Air	1.24(-2)	<.1	3.10(-4)	<.1
42	Air	2.52(-3)	<.1	6.19(-5)	<.1
43	Capsule Wall	8.70(-2)	<.1	2.08(-3)	<.1
Total Scattered		4.83(2)	100.0	3.95(1)	100.0
Direct		5.48(2)	-	1.88(1)	-
Direct + Scattered		1.03(3)	-	5.83(1)	-

*For the 104 second case, these regions contain GH₂. For the 1072 second case these regions contain LH₂. Numbers in parentheses refer to powers of ten.

TABLE 3-10

CONTRIBUTION OF SOURCE REGIONS TO THE GAMMA RAY DOSE RATE
(REM/HOUR) AT THE TANK TOP AND IN THE
CREW COMPARTMENT
(KAP-VI CALCULATIONS)

Source Region	Tank Top, R = 0		Tank Top, R = 300 cm		Crew, R = 0		Crew, R = 148 cm	
	Dose Rate	% of Total	Dose Rate	% of Total	Dose Rate	% of Total	Dose Rate	% of Total
Core 1	1.18(2)	6.9	1.16(2)	6.4	4.10(1)	6.0	9.86(1)	6.9
Core 2	5.54(1)	3.3	5.47(1)	3.0	1.91(1)	2.8	4.62(1)	3.2
Core 3	4.38(1)	2.6	4.33(1)	2.4	1.50(1)	2.2	3.65(1)	2.5
Core 4	3.74(1)	2.2	3.71(1)	2.1	1.28(1)	1.8	3.12(1)	2.2
Core 5	2.81(1)	1.7	3.33(1)	1.9	9.69(0)	1.4	2.44(1)	1.7
Total Core	2.83(2)	16.7	2.85(2)	15.8	9.76(1)	14.2	2.37(2)	16.5
Structure	1.99(1)	1.2	3.61(1)	2.0	8.59(0)	1.3	1.89(1)	1.3
Inner Reflector	1.08(2)	6.4	9.07(1)	5.0	4.80(1)	7.0	8.57(1)	6.0
Outer Reflector	1.50(2)	8.8	1.50(2)	8.3	6.68(1)	9.7	1.24(2)	8.6
Pressure Vessel (Side)	1.03(1)	0.6	1.29(2)	7.2	4.12(0)	0.6	2.21(1)	1.5
Core Plenum	1.84(2)	10.8	1.82(2)	10.1	5.74(1)	8.3	1.55(2)	10.7
Support Plate	6.62(2)	38.9	6.56(2)	36.3	2.86(2)	41.5	5.61(2)	39.0
Shield Plenum	7.64(1)	4.5	7.58(1)	4.2	3.41(1)	5.0	6.48(1)	4.5
Drum Drive	1.21(2)	7.1	1.17(2)	6.5	5.37(1)	7.8	1.02(2)	7.1
Shield Plate	1.37(1)	0.8	1.36(1)	0.8	5.71(0)	0.8	1.16(1)	0.8
BATH Shield	6.81(1)	4.0	6.77(1)	3.8	2.64(1)	3.8	5.71(1)	4.0
Total Non-Core	1.41(3)	83.1	1.52(3)	84.2	5.91(2)	85.8	1.202(3)	83.5
Grand Total	1.70(3)	100.0	1.805(3)	100.0	6.886(2)	100.0	1.439(3)	100.0

NOTE: Data apply at 104 seconds prior to tank empty condition. Numbers in parentheses refer to powers of ten.

4.0 Description of the Seminar/Workshop (Task B)

In Task B of the contract effort, the preparation of Seminar/Workshop material on the use of the MSFC computer code package and the presentation of this material at MSFC was completed. The purpose of the Seminar/Workshop was to demonstrate the implementation of the MSFC computer code package in the analysis of the radiation environment of a nuclear propelled vehicle. The analysis of the radiation environment of a typical nuclear propelled stage was performed in Task A of this contract and the techniques used and results obtained are described in Section 3.0. The Seminar/Workshop material is based on this analysis and consists of written material describing the input data preparation of each computer code problem in the analysis along with the punched card input deck listings. Printed output from the various problems were not included in the Seminar/Workshop material but were available in multiple copies during the Seminar/Workshop at MSFC.

The Seminar/Workshop conducted at MSFC consisted of a description of:

- (1) The computer codes included the MSFC computer code package,
- (2) The linkage by magnetic tape and/or punched cards of the various computer codes,
- (3) The contents and use of the Master Libraries of the MSFC computer code package,
- (4) The numerical solution employed in each code,
- (5) The computer code logic used in each computer code,
- (6) The input data preparation for each code and its relationship to the analytical model of the nuclear propelled stage,
- (7) The input and output magnetic tape operations necessary in the use of each computer code,

- (8) The output data and the format of output data tapes, and
- (9) The intercomparison and interpretation of computer code results.

The majority of this descriptive material is contained in the Seminar/Workshop notes (Volume 2 of WANL-PR(LL)-040) and the remainder was presented verbally by WANL personnel as opaque projection material.

5.0 Techniques to Improve the Automated Coupling and Utilization of the MSFC Computer Code Package (Task C)

In Task C of this contract an investigation of techniques to improve the use of the MSFC computer code package on the MSFC UNIVAC-1108 was conducted. This effort was primarily directed toward: (1) providing additional computer codes, (2) altering the use of magnetic tapes in existing computer codes, and (3) altering punched card output of codes. The various tasks completed are described in the following sections.

5.1 Modification of the APPROPOS Code

A series of modifications were made to the APPROPOS code in order to reduce the number of magnetic tapes required for an APPROPOS job. These modifications were made to improve the computer job turnaround time on the MSFC UNIVAC-1108 computer system. The original APPROPOS code supplied to MSFC required the following tapes for a job:

- (1) The APPROPOS code (optional, but desirable),
- (2) Master Library 1 or 2,
- (3) Master Library 3 and 6,
- (4) Master Library 4,
- (5) One or two tapes containing flux data for cross section weighting, and
- (6) An output tape.

This results in a total of seven tapes required for certain APPROPOS jobs. In order to reduce the number of tapes required, two changes were made. The APPROPOS code logic for using Master Libraries 3, 6 and 4 was changed from requiring two magnetic tapes to a single input tape. This tape contains the Master Library data in the order of Master Library 3, Master Library 4, and Master Library 6, and this tape is mounted on tape unit 10. This combined library tape was generated by copying Master Library 3, Master Library 6, and Master Library 4 to a single tape using the UNIVAC-1108 utility routines. The second modification to APPROPOS was the use of ANISN-W output tapes. In certain APPROPOS jobs, ANISN-W tapes from radial and axial geometries problems were required input on

tape units 17, and 18. The code logic was changed to require these two sets of data on a single tape mounted on tape unit 17. This APPROPOS change requires that the user run the two ANISN-W problems in the same job (ANISN-W will place the two sets of data on a single tape) or the user must copy the two sets of ANISN-W data onto a single tape. This tape copying of ANISN-W data is a simple procedure using the UNIVAC-1108 utility routines since the ANISN-W tapes always contain $4 \cdot \text{IGM} + 11$ logical records. In the use of Master Libraries 1 or 2 in ANISN-W this results in 219 logical records ($4 \cdot 52 + 11$) on the ANISN-W flux output tapes.

The two modifications to APPROPOS described above result in a total of 5 magnetic tapes for certain jobs with the number cut to 2 or 3 tapes if card input or output is used. The APPROPOS code will use only 2 input tapes if the APPROPOS FORTRAN source cards, and flux spectra punched cards are input, and the cross section output is on punched cards. Modification to ANISN-W described below provide flux spectra punched cards for use in APPROPOS.

5.2 Modification to the ANISN-W Code

The ANISN-W code supplied to MSFC in the previous contract had the capability to produce punched card output at option. This data consisted of the right and left leakage (neutrons/second) from each zone, the volume integral of flux (neutrons-centimeter/second) in each zone, the flux distribution, and the fission neutron distribution. This data was obtained for each group in the order described in Section 2.5.3 of the ANISN-W user's manual (Volume 4 of WANL-PR(LL)-034). This punched card output from ANISN-W was not directly useable in APPROPOS and therefore the ANISN-W code logic was changed to provide a direct punched card linkage of ANISN-W and APPROPOS and further reduce the number of magnetic tapes required by APPROPOS if desired by the APPROPOS user.

The modifications to ANISN-W provides the following punched card output:

- (1) Optional if $\text{ID2} = 2$ or 3 , the ANISN-W problem title card,

- (2) Optional if ID2 = 2 or 3,
 - (a) 3U card,
 - (b) Scalar fluxes by interval and group with each group starting on a new card,
- (3) Optional if ID2 = 2 or 3, three blank cards,
- (4) Two blank cards,
- (5) Zone average flux (neutrons/cm²-second) by group and zone with each set of zone data starting on a new card (This is APPROPOS input data),
- (6) Two blank cards,
- (7) Optional if ID2 = 2 or 3,
 - (a) 2U card,
 - (b) Source neutron density (neutrons/cm²-second) by interval.

As noted above the zone average fluxes are punched output from every ANISN-W problem and the APPROPOS code will accept these cards as input for the cross section weighting spectra.

5.3 The CHEAPER Code

In this contract, the addition of the CHEAPER code to the MSFC computer code package was completed. This code processes DOT-IIW scalar flux data to provide magnetic tapes for use as input to other codes or provides flux-response data. A user's manual for the CHEAPER code is in the Appendix of Volume 1 of this report and one use of the CHEAPER code is described in the Seminar/Workshop notes of Volume 2.

The CHEAPER code performs several useful operations using as input data one or more DOT-IIW scalar flux output tapes. The CHEAPER operations are:

- (1) The addition by mesh cell of the multigroup scalar flux output of DOT-IIW to produce a single output tape,

- (2) The linking of two DOT-IIW scalar flux output tapes to provide a single output tape,
- (3) The modifying of a DOT-IIW scalar flux tape by extrapolation or interpolation of input data to provide an output tape,
- (4) The inversion by mesh row of an input DOT-IIW scalar flux tape to provide an output tape,
- (5) The calculation of multigroup flux traverses at input specified axial or radial coordinates,
- (6) The calculation of multigroup flux-response data at specified axial or radial coordinates,
- (7) The calculation of multigroup scalar flux and flux-response at specified r , z coordinate points, and
- (8) The modifying of a DOT-IIW scalar flux tape by mesh row or mesh column deletions to produce a revised output tape.

In addition to the above CHEAPER capabilities the code contains the option to plot the scalar flux or flux-response traverses as a function of the radial or axial coordinate.

The CHEAPER code operations described in the preceding sections are limited to the multigroup scalar flux output of the DOT-IIW code. The principal use of CHEAPER is in the manipulation of one or more DOT-IIW output tapes to provide results on a complete system and these capabilities are necessary when a limited core memory storage in DOT-IIW requires a coupled analysis.

5.4 The LHAP Code

The addition of the LHAP code to the MSFC code package was performed in this contract to provide a capability to rapidly evaluate the effect of liquid hydrogen capture

gamma sources in propellant tanks on the nuclear stage radiation environment. The LHAP code employs an anisotropic point source representation of the nuclear subsystem neutron leakage to calculate the liquid hydrogen capture gamma source in the propellant tanks. These sources are then used in a point kernel technique to calculate the dose rate at a detector point in the complex geometry describing the nuclear stage. The capture gamma source calculation is a simple approximation which assumes a fraction of the neutron flux to be absorbed at the point of incidence to an absorbing zone.

The LHAP code is similar to the SCAP code described in Volume 6 of WANL-PR(LL)-034 and uses the same geometry capability. The LHAP code user's manual is in the Appendix of Volume 1 of this report. The use of the LHAP code in the analysis of a nuclear stage is demonstrated in the Seminar/Workshop notes of Volume 2 of this report.

6.0 Updating of MSFC Master Libraries (Task D)

Task D of the contract effort involved the review and update of the MSFC Master Libraries. In the previous contract effort, NAS-8-24919, WANL had supplied six Master Libraries on magnetic tape or punched cards. These Master Libraries were for use in the various computer codes and contained the information detailed in Table 6-1.

The review of the contents of these libraries involved the use of the data in Task A analysis as well as comparisons of these data to more recent compilations. The review and update of the Master Libraries was limited to Master Libraries 1, 2, 3 and 6. Master Libraries 4 and 5 were not changed since the data contained in Master Library 5 is of recent origin and Master Library 4 is derived from Master Library 5. The updates of Master Libraries 1, 2, 3, and 6 are described in the following sections.

6.1 Update of Neutron Cross Section Data (Master Libraries 1, 2 and 3)

The library data contained on Master Libraries 1, 2 and 3 are derived from the same data source (for details see Volume 2 of WANL-PR(LL)-034) and must be updated or added to consistently. The revisions to these library data consisted of the addition of a limited number of hydrogen neutron cross section data and the update of all existing cross section data to an expanded format.

The neutron cross sections provided in the MSFC computer code package are weighted over four representative spectra. These spectra are relative neutron flux spectra in four zones of a NERVA reactor model and are the reactor core center, reactor core edge, beryllium reflector, and BATH shield spectra. These spectra are plotted in Figures 6-1 and 6-2. The data in Figure 6-1 is the flux spectra in the four zones plotted versus lethargy and the data in Figure 6-2 is the differential flux spectra in the same four zones. These are 52 group data obtained from radial and axial ANISN-W problems.

The revisions and updates of the Master Libraries 1, 2 and 3 data are:

- (1) The addition of hydrogen cross section data based on different thermal neutron scattering law data. The new hydrogen data is based on hydrogen gas kernel scattering data at 150 and 275 degrees Kelvin. This results in 8 new cross section sets in Master Library 1, 32 new cross section sets in Master Library 2, and 8 new cross section sets in Master Library 3. The updated listing of the contents of Master Library 1 is in Table 6-2 and an updated listing of the contents of Master Library 2 is in Table 6-3. These listings in Table 6-2 and 6-3 are updates of Tables 3-6 and 3-7 of Volume 2, WANL-PR(LL)-034. Master Library 3 contains the same data as Master Library 1 with the exception of set number 3839.
- (2) The update of all other cross section data to a full scattering matrix. In the original MSFC Master Library the downscatter was limited to 20 groups (i.e., neutron scattering from groups g to group g' where g' is less than or equal to $g + 20$). Upscatter was limited to 10 groups (i.e., neutron scattering from group g to group g' where g' is greater than or equal to $g - 10$). This resulted in a total of 34 types of cross sections in each of 52 groups. This limited scattering matrix was expanded to 51 downscatter and 19 upscatter to accommodate hydrogen scattering. The 51 downscatter provides a scatter-transfer from any group to any other group and the 19 upscatter provides scatter transfer from any group with an energy less than 1.86 eV to any other group with energy of less than 1.86 eV. There are 20 arrays in the 52 group energy structure with energies less than 1.86 eV. This expansion of the scattering matrix resulted in the update of all existing hydrogen cross section data in the MSFC Master Libraries and the expansion of all other data to the full scattering matrix. These updates result in cross section sets with 74 types of cross sections in each group of 52 groups.

The revisions and updates of Master Libraries 1, 2, and 3 were made after initial calculations in Task A of this contract. These calculations were performed with low (20.4 degrees Kelvin) temperature and high (2500 degrees Kelvin) temperature cross section data in the appropriate zones of the NSS geometry model. These 52 group data were used in ANISN-W to solve for radial and axial zone spectra. These zone spectra were then used

in APPROPOS to weight the 52 group data down to 16 group data with upscatter cross sections removed by conserving scatter-transfer rates. These upscatter-removed cross sections were required in DOT-IIW calculations to limit the use of computer time (a DOT-IIW problem with upscatter requires multiple outer iterations to converge the upscatter source).

When the analysis was run with the low and high temperature data the conservation of scatter-transfer rates in upscatter removal resulted in negative downscatter cross sections in certain zone cross section sets. These negative values caused negative flux solutions in the DOT-IIW neutron problems. These problems resulted in the update of the MSFC library to include the new hydrogen data and a full scattering matrix. A rerun of the DOT-IIW neutron problems was made with the 275 degree Kelvin hydrogen cross section data with all positive flux solutions.

6.2 Update of Photon Production Library (Master Library 6)

The update of the photon production data for neutron radiative capture and neutron inelastic scatter was based on recent reviews of data conducted in the NERVA program at WANL. These reviews involved the original MSFC library data supplied in the previous contract, NAS-8-24919, (see Section 6.0 of Volume 2, WANL-PR(LL)-034, and more recent computations. This review resulted in the selection of a new set of photon production data for neutron capture and a revised set of photon production data for neutron inelastic scatter. These data were used to update Master Library 6 of the MSFC computer code package.

6.2.1 Neutron Capture Photon Production Data

The spectrum of gamma ray energy due to neutron capture is listed for 41 elements or isotopes in Table 6-4. For certain elements, as noted in the Table 6-4, the photon production spectrum is due to (n, p, γ) , (n, α, γ) , or (n, t, γ) reactions. The basic data source for each set of data is listed in Table 6-5. The data in Table 6-4 is the photon energy production due to neutron capture. A 13 group photon energy structure is used in compiling the data. These data are spectrum due to thermal neutron capture and are used in the MSFC

computer code package to compute the photon source spectrum due to capture of all energies of neutrons. Recent compilations of selected epithermal neutron capture data have been made available but this data is not included in this compilation.

6.2.2 Neutron Inelastic Scatter Photon Production Data

The spectrum of gamma ray energy due to the (n, n', γ) reaction for 18 elements or isotopes is listed in Table 6-6. The basic data source for each element or isotope is noted in the title of each set and the APPROPOS reference is to the original MSFC data library as supplied in contract NAS-8-24919 and documented in Section 6.0 of Volume 2, WANL-PR(LL)-034. These photon production spectra or cross sections were primarily obtained from the POPOP-4 computer code in a group structure compatible with the 52 neutron groups of the MSFC libraries. These data were then spectral weighted to 6 group data compatible with the 16 groups used in the MSFC computer code package. The neutron and photon group structures are noted in Table 6-6.

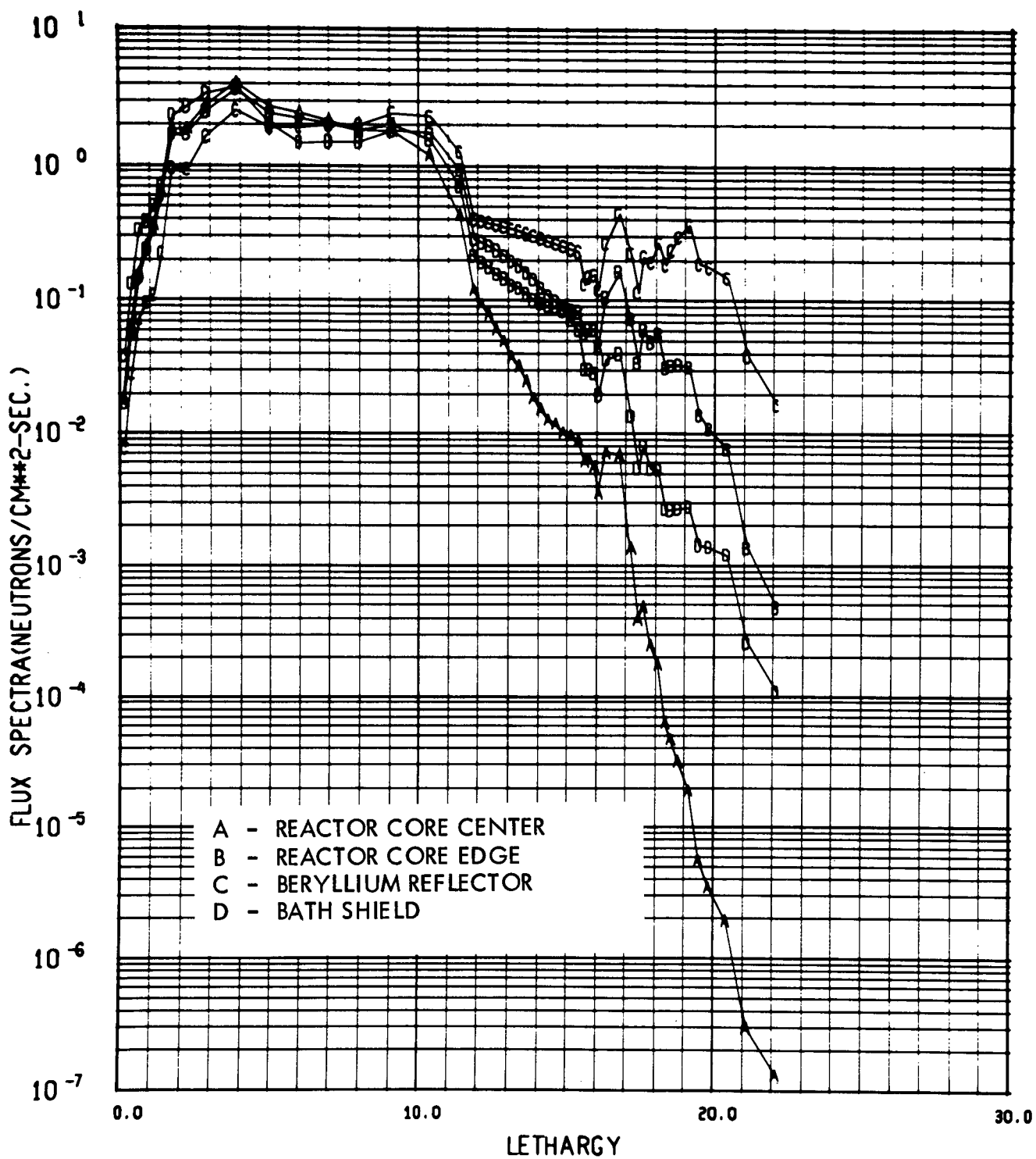


FIGURE 6-1. NEUTRON CROSS SECTION WEIGHTING SPECTRA

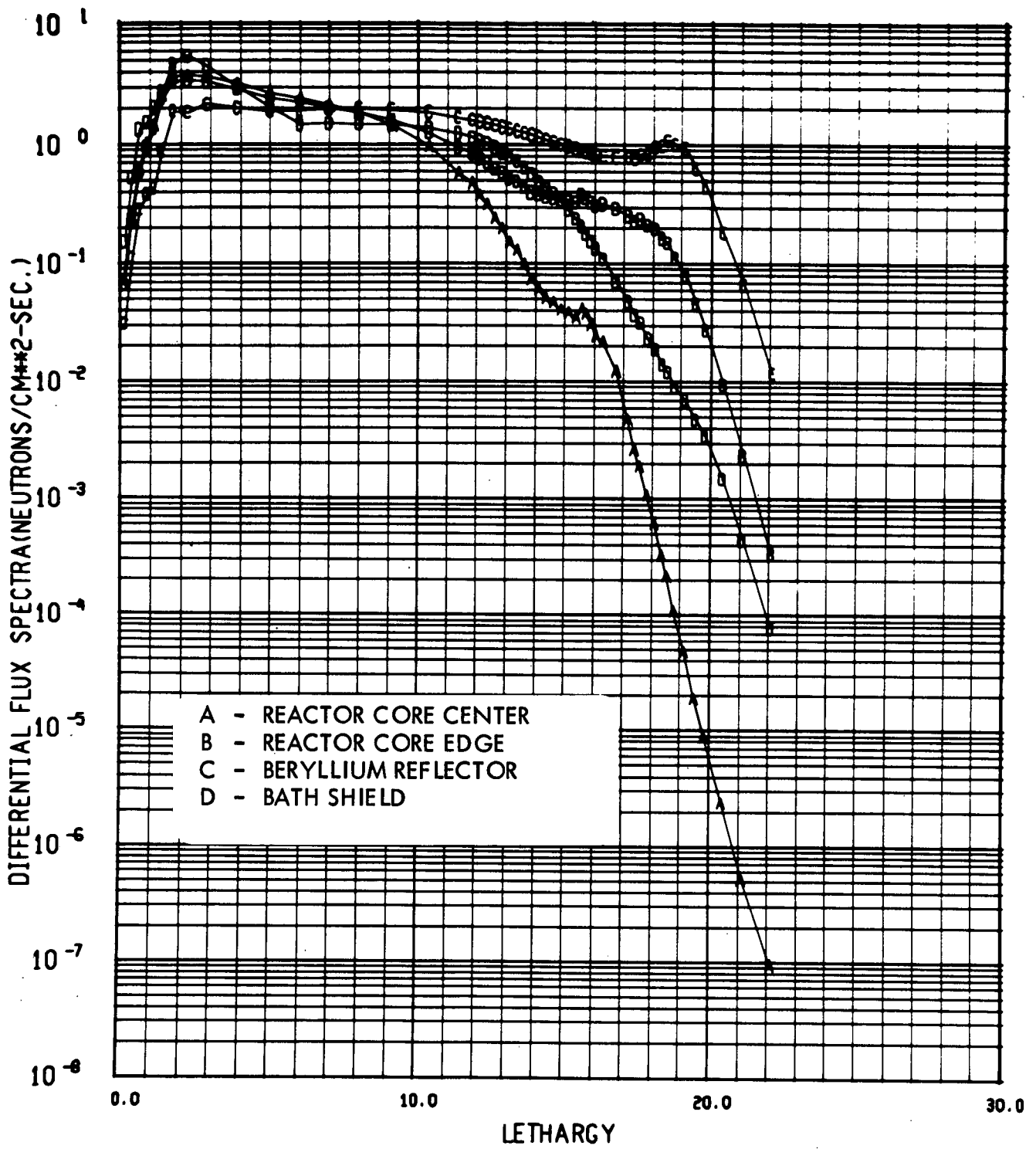


FIGURE 6-2. NEUTRON CROSS SECTION WEIGHTING SPECTRA

TABLE 6-1

SUMMARY OF MASTER LIBRARIES

<u>Master Library Library No.</u>	<u>Description</u>
1	Microscopic, 52 Group, Transport Corrected, Neutron Cross Section Sets for Use in the APPROPOS, ANISN-W, DOT-IIW Codes
2	Microscopic, 52 Group, P_l ($l \leq 3$), Neutron Cross Section Sets for Use in the APPROPOS, ANISN-W, and DOT-IIW Codes
3	Microscopic, 52 Group, Neutron Reaction Rate Cross Section Sets for Use in the APPROPOS Code
4	Microscopic, 13 Group, P_l ($l \leq 9$), Gamma Ray Cross Section Sets for Use in the APPROPOS, ANISN-W, and DOT-IIW Codes
5	Pair-Production and Photo-Electric, Pointwise, Photon Cross Sections for Use in the GAMLEG-W, KAP-VI, SCAP, MAP, and LHAP Codes
6	Photon Production Data Due to Neutron Radiative Capture and Inelastic Scatter, Selected Element or Isotope Nuclear Parameters, and Other Related Data

TABLE 6-2

TRANSPORT CORRECTED NEUTRON CROSS SECTIONS SETS IN MASTER LIBRARY 1

SET NO.	IDENTIFICATION NO.	SET DESCRIPTION	TYPE	SPECTRUM
1	119	ALUMINUM	TRC	CORE CENTER
2	129	ALUMINUM	TRC	CORE EDGE
3	139	ALUMINUM	TRC	REFLECTOR
4	149	ALUMINUM	TRC	SHIELD
5	219	BERYLLIUM, 296 DEG. K	TRC	CORE CENTER
6	229	BERYLLIUM, 296 DEG. K	TRC	CORE EDGE
7	239	BERYLLIUM, 296 DEG. K	TRC	REFLECTOR
8	249	BERYLLIUM, 296 DEG. K	TRC	SHIELD
9	319	BORON	TRC	CORE CENTER
10	329	BORON	TRC	CORE EDGE
11	339	BORON	TRC	REFLECTOR
12	349	BORON	TRC	SHIELD
13	419	BORON-10	TRC	CORE CENTER
14	429	BORON-10	TRC	CORE EDGE
15	439	BORON-10	TRC	REFLECTOR
16	449	BORON-10	TRC	SHIELD
17	519	CADMIUM	TRC	CORE CENTER
18	529	CADMIUM	TRC	CORE EDGE
19	539	CADMIUM	TRC	REFLECTOR
20	549	CADMIUM	TRC	SHIELD
21	619	CARBON, 296 DEG. K	TRC	CORE CENTER
22	629	CARBON, 296 DEG. K	TRC	CORE EDGE
23	639	CARBON, 296 DEG. K	TRC	REFLECTOR
24	649	CARBON, 296 DEG. K	TRC	SHIELD
25	719	CHROMIUM	TRC	CORE CENTER
26	729	CHROMIUM	TRC	CORE EDGE
27	739	CHROMIUM	TRC	REFLECTOR
28	749	CHROMIUM	TRC	SHIELD
29	819	COBALT	TRC	CORE CENTER
30	829	COBALT	TRC	CORE EDGE

TABLE 6-2 (CONT)

TRANSPORT CORRECTED NEUTRON CROSS SECTIONS SETS IN MASTER LIBRARY 1

SET NO.	IDENTIFICATION NO.	SET DESCRIPTION	TYPE	SPECTRUM
31	839	COBALT	TRC	REFLECTOR
32	849	COBALT	TRC	SHIELD
33	919	COPPER	TRC	CORE CENTER
34	929	COPPER	TRC	CORE EDGE
35	939	COPPER	TRC	REFLECTOR
36	949	COPPER	TRC	SHIELD
37	1019	GADOLINIUM	TRC	CORE CENTER
38	1029	GADOLINIUM	TRC	CORE EDGE
39	1039	GADOLINIUM	TRC	REFLECTOR
40	1049	GADOLINIUM	TRC	SHIELD
41	1119	GOLD	TRC	CORE CENTER
42	1129	GOLD	TRC	CORE EDGE
43	1139	GOLD	TRC	REFLECTOR
44	1149	GOLD	TRC	SHIELD
45	1219	HYDROGEN, PARA, 20.4 DEG.	TRC	CORE CENTER
46	1229	HYDROGEN, PARA, 20.4 DEG.	TRC	CORE EDGE
47	1239	HYDROGEN, PARA, 20.4 DEG.	TRC	REFLECTOR
48	1249	HYDROGEN, PARA, 20.4 DEG.	TRC	SHIELD
49	1319	HYDROGEN, ORTHO, 20.4 DEG.	TRC	CORE CENTER
50	1329	HYDROGEN, ORTHO, 20.4 DEG.	TRC	CORE EDGE
51	1339	HYDROGEN, ORTHO, 20.4 DEG.	TRC	REFLECTOR
52	1349	HYDROGEN, ORTHO, 20.4 DEG.	TRC	SHIELD
53	1419	HYDROGEN, PARA, 300 DEG.	TRC	CORE CENTER
54	1429	HYDROGEN, PARA, 300 DEG.	TRC	CORE EDGE
55	1439	HYDROGEN, PARA, 300 DEG.	TRC	REFLECTOR
56	1449	HYDROGEN, PARA, 300 DEG.	TRC	SHIELD
57	1519	HYDROGEN, ORTHO, 300 DEG.	TRC	CORE CENTER
58	1529	HYDROGEN, ORTHO, 300 DEG.	TRC	CORE EDGE
59	1539	HYDROGEN, ORTHO, 300 DEG.	TRC	REFLECTOR
60	1549	HYDROGEN, ORTHO, 300 DEG.	TRC	SHIELD

TABLE 6-2 (CONT)

TRANSPORT CORRECTED NEUTRON CROSS SECTIONS SETS IN MASTER LIBRARY 1

SET NO.	IDENTIFICATION NO.	SET DESCRIPTION	TYPE	SPECTRUM
61	1619	HYDROGEN, GAS, 2500 DEG. K	TRC	CORE CENTER
62	1629	HYDROGEN, GAS, 2500 DEG. K	TRC	CORE EDGE
63	1639	HYDROGEN, GAS, 2500 DEG. K	TRC	REFLECTOR
64	1649	HYDROGEN, GAS, 2500 DEG. K	TRC	SHIELD
65	1719	INDIUM-115	TRC	CORE CENTER
66	1729	INDIUM-115	TRC	CORE EDGE
67	1739	INDIUM-115	TRC	REFLECTOR
68	1749	INDIUM-115	TRC	SHIELD
69	1819	IRON	TRC	CORE CENTER
70	1829	IRON	TRC	CORE EDGE
71	1839	IRON	TRC	REFLECTOR
72	1849	IRON	TRC	SHIELD
73	1919	LEAD	TRC	CORE CENTER
74	1929	LEAD	TRC	CORE EDGE
75	1939	LEAD	TRC	REFLECTOR
76	1949	LEAD	TRC	SHIELD
77	2019	LITHIUM	TRC	CORE CENTER
78	2029	LITHIUM	TRC	CORE EDGE
79	2039	LITHIUM	TRC	REFLECTOR
80	2049	LITHIUM	TRC	SHIELD
81	2119	LITHIUM-6	TRC	CORE CENTER
82	2129	LITHIUM-6	TRC	CORE EDGE
83	2139	LITHIUM-6	TRC	REFLECTOR
84	2149	LITHIUM-6	TRC	SHIELD
85	2219	LITHIUM-7	TRC	CORE CENTER
86	2229	LITHIUM-7	TRC	CORE EDGE
87	2239	LITHIUM-7	TRC	REFLECTOR
88	2249	LITHIUM-7	TRC	SHIELD
89	2319	MAGNESIUM	TRC	CORE CENTER
90	2329	MAGNESIUM	TRC	CORE EDGE

TABLE 6-2(CONT)

TRANSPORT CORRECTED NEUTRON CROSS SECTIONS SETS IN MASTER LIBRARY 1

SET NO.	IDENTIFICATION NO.	SET DESCRIPTION	TYPE	SPECTRUM
91	2339	MAGNESIUM	TRC	REFLECTOR
92	2349	MAGNESIUM	TRC	SHIELD
93	2419	MANGANESE	TRC	CORE CENTER
94	2429	MANGANESE	TRC	CORE EDGE
95	2449	MANGANESE	TRC	SHIELD
96	2519	MOLYBDENUM	TRC	CORE CENTER
97	2529	MOLYBDENUM	TRC	CORE EDGE
98	2539	MOLYBDENUM	TRC	REFLECTOR
99	2549	MOLYBDENUM	TRC	SHIELD
100	2619	NICKEL	TRC	CORE CENTER
101	2629	NICKEL	TRC	CORE EDGE
102	2639	NICKEL	TRC	REFLECTOR
103	2649	NICKEL	TRC	SHIELD
104	2719	NIObIUM	TRC	CORE CENTER
105	2729	NIObIUM	TRC	CORE EDGE
106	2739	NIObIUM	TRC	REFLECTOR
107	2749	NIObIUM	TRC	SHIELD
108	2819	NITROGEN	TRC	CORE CENTER
109	2829	NITROGEN	TRC	CORE EDGE
110	2839	NITROGEN	TRC	REFLECTOR
111	2849	NITROGEN	TRC	SHIELD
112	2919	OXYGEN	TRC	CORE CENTER
113	2929	OXYGEN	TRC	CORE EDGE
114	2939	OXYGEN	TRC	REFLECTOR
115	2949	OXYGEN	TRC	SHIELD
116	3019	SILICON	TRC	CORE CENTER
117	3029	SILICON	TRC	CORE EDGE
118	3039	SILICON	TRC	REFLECTOR
119	3049	SILICON	TRC	SHIELD
120	3219	TANTALUM	TRC	CORE CENTER

TABLE 6-2 (CONT)

TRANSPORT CORRECTED NEUTRON CROSS SECTIONS SETS IN MASTER LIBRARY 1

SET NO.	IDENTIFICATION NO.	SET DESCRIPTION	TYPE	SPECTRUM
121	3229	TANTALUM	TRC	CORE EDGE
122	3319	TITANIUM	TRC	CORE CENTER
123	3329	TITANIUM	TRC	CORE EDGE
124	3339	TITANIUM	TRC	REFLECTOR
125	3349	TITANIUM	TRC	SHIELD
126	3449	TUNGSTEN	TRC	SHIELD
127	3519	URANIUM-235	TRC	CORE CENTER
128	3529	URANIUM-235	TRC	CORE EDGE
129	3619	URANIUM-238	TRC	CORE CENTER
130	3629	URANIUM-238	TRC	CORE EDGE
131	3719	ZIRCONIUM	TRC	CORE CENTER
132	3729	ZIRCONIUM	TRC	CORE EDGE
133	3739	ZIRCONIUM	TRC	REFLECTOR
134	3749	ZIRCONIUM	TRC	SHIELD
135	3839	RING VANE PRESCRIPTION	TRC	REFLECTOR
136	3919	HYDROGEN, GAS, 150 DEG.	TRC	CORE CENTER
137	3929	HYDROGEN, GAS, 150 DEG.	TRC	CORE EDGE
138	3939	HYDROGEN, GAS, 150 DEG.	TRC	REFLECTOR
139	3949	HYDROGEN, GAS, 150 DEG.	TRC	SHIELD
140	4019	HYDROGEN, GAS, 275 DEG.	TRC	CORE CENTER
141	4029	HYDROGEN, GAS, 275 DEG.	TRC	CORE EDGE
142	4039	HYDROGEN, GAS, 275 DEG.	TRC	REFLECTOR
143	4049	HYDROGEN, GAS, 275 DEG.	TRC	SHIELD

TABLE 6-3

P(L) NEUTRON CROSS SECTION SETS IN MASTER LIBRARY 2

SET NO.	IDENTIFICATION NO.	SET DESCRIPTION	TYPE	SPECTRUM
1	110	ALUMINUM	P0	CORE CENTER
2	111	ALUMINUM	P1	CORE CENTER
3	112	ALUMINUM	P2	1/E SPECTRUM
4	113	ALUMINUM	P3	1/E SPECTRUM
5	120	ALUMINUM	P0	CORE EDGE
6	121	ALUMINUM	P1	CORE EDGE
7	122	ALUMINUM	P2	1/E SPECTRUM
8	123	ALUMINUM	P3	1/E SPECTRUM
9	130	ALUMINUM	P0	REFLECTOR
10	131	ALUMINUM	P1	REFLECTOR
11	132	ALUMINUM	P2	1/E SPECTRUM
12	133	ALUMINUM	P3	1/E SPECTRUM
13	140	ALUMINUM	P0	SHIELD
14	141	ALUMINUM	P1	SHIELD
15	142	ALUMINUM	P2	1/E SPECTRUM
16	143	ALUMINUM	P3	1/E SPECTRUM
17	210	BERYLLIUM, 296 DEG. K	P0	CORE CENTER
18	211	BERYLLIUM, 296 DEG. K	P1	CORE CENTER
19	212	BERYLLIUM	P2	1/E SPECTRUM
20	213	BERYLLIUM	P3	1/E SPECTRUM
21	220	BERYLLIUM, 296 DEG. K	P0	CORE EDGE
22	221	BERYLLIUM, 296 DEG. K	P1	CORE EDGE
23	222	BERYLLIUM	P2	1/E SPECTRUM
24	223	BERYLLIUM	P3	1/E SPECTRUM
25	230	BERYLLIUM, 296 DEG. K	P0	REFLECTOR
26	231	BERYLLIUM, 296 DEG. K	P1	REFLECTOR
27	232	BERYLLIUM	P2	1/E SPECTRUM
28	233	BERYLLIUM	P3	1/E SPECTRUM
29	240	BERYLLIUM, 296 DEG. K	P0	SHIELD
30	241	BERYLLIUM, 296 DEG. K	P1	SHIELD

TABLE 6-3(CONT)

P(L) NEUTRON CROSS SECTION SETS IN MASTER LIBRARY 2

SET NO.	IDENTIFICATION NO.	SET DESCRIPTION	TYPE	SPECTRUM
31	242	BERYLLIUM	P2	1/E SPECTRUM
32	243	BERYLLIUM	P3	1/E SPECTRUM
33	310	BORON	P0	CORE CENTER
34	311	BORON	P1	CORE CENTER
35	312	BORON	P2	1/E SPECTRUM
36	313	BORON	P3	1/E SPECTRUM
37	320	BORON	P0	CORE EDGE
38	321	BORON	P1	CORE EDGE
39	322	BORON	P2	1/E SPECTRUM
40	323	BORON	P3	1/E SPECTRUM
41	330	BORON	P0	REFLECTOR
42	331	BORON	P1	REFLECTOR
43	332	BORON	P2	1/E SPECTRUM
44	333	BORON	P3	1/E SPECTRUM
45	340	BORON	P0	SHIELD
46	341	BORON	P1	SHIELD
47	342	BORON	P2	1/E SPECTRUM
48	343	BORON	P3	1/E SPECTRUM
49	410	BORON-10	P0	CORE CENTER
50	411	BORON-10	P1	CORE CENTER
51	420	BORON-10	P0	CORE EDGE
52	421	BORON-10	P1	CORE EDGE
53	430	BORON-10	P0	REFLECTOR
54	431	BORON-10	P1	REFLECTOR
55	440	BORON-10	P0	SHIELD
56	441	BORON-10	P1	SHIELD
57	510	CADMIUM	P0	CORE CENTER
58	511	CADMIUM	P1	CORE CENTER
59	520	CADMIUM	P0	CORE EDGE
60	521	CADMIUM	P1	CORE EDGE

TABLE 6-3 (CONT)

P(L) NEUTRON CROSS SECTION SETS IN MASTER LIBRARY 2

SET NO.	IDENTIFICATION NO.	SET DESCRIPTION	TYPE	SPECTRUM
61	530	CADMIUM	P0	REFLECTOR
62	531	CADMIUM	P1	REFLECTOR
63	540	CADMIUM	P0	SHIELD
64	541	CADMIUM	P1	SHIELD
65	610	CARBON, 296 DEG. K	P0	CORE CENTER
66	611	CARBON, 296 DEG. K	P1	CORE CENTER
67	612	CARBON	P2	1/E SPECTRUM
68	613	CARBON	P3	1/E SPECTRUM
69	620	CARBON, 296 DEG. K	P0	CORE EDGE
70	621	CARBON, 296 DEG. K	P1	CORE EDGE
71	622	CARBON	P2	1/E SPECTRUM
72	623	CARBON	P3	1/E SPECTRUM
73	630	CARBON, 296 DEG. K	P0	REFLECTOR
74	631	CARBON, 296 DEG. K	P1	REFLECTOR
75	632	CARBON	P2	1/E SPECTRUM
76	633	CARBON	P3	1/E SPECTRUM
77	640	CARBON, 296 DEG. K	P0	SHIELD
78	641	CARBON, 296 DEG. K	P1	SHIELD
79	642	CARBON	P2	1/E SPECTRUM
80	643	CARBON	P3	1/E SPECTRUM
81	710	CHROMIUM	P0	CORE CENTER
82	711	CHROMIUM	P1	CORE CENTER
83	712	CHROMIUM	P2	1/E SPECTRUM
84	713	CHROMIUM	P3	1/E SPECTRUM
85	720	CHROMIUM	P0	CORE EDGE
86	721	CHROMIUM	P1	CORE EDGE
87	722	CHROMIUM	P2	1/E SPECTRUM
88	723	CHROMIUM	P3	1/E SPECTRUM
89	730	CHROMIUM	P0	REFLECTOR
90	731	CHROMIUM	P1	REFLECTOR

TABLE 6-3(CONT)

P(L) NEUTRON CROSS SECTION SETS IN MASTER LIBRARY 2

SET NO.	IDENTIFICATION NO.	SET DESCRIPTION	TYPE	SPECTRUM
91	732	CHROMIUM	P2	1/E SPECTRUM
92	733	CHROMIUM	P3	1/E SPECTRUM
93	740	CHROMIUM	P0	SHIELD
94	741	CHROMIUM	P1	SHIELD
95	742	CHROMIUM	P2	1/E SPECTRUM
96	743	CHROMIUM	P3	1/E SPECTRUM
97	810	COBALT	P0	CORE CENTER
98	811	COBALT	P1	CORE CENTER
99	820	COBALT	P0	CORE EDGE
100	821	COBALT	P1	CORE EDGE
101	830	COBALT	P0	REFLECTOR
102	831	COBALT	P1	REFLECTOR
103	840	COBALT	P0	SHIELD
104	841	COBALT	P1	SHIELD
105	910	COPPER	P0	CORE CENTER
106	911	COPPER	P1	CORE CENTER
107	912	COPPER	P2	1/E SPECTRUM
108	913	COPPER	P3	1/E SPECTRUM
109	920	COPPER	P0	CORE EDGE
110	921	COPPER	P1	CORE EDGE
111	922	COPPER	P2	1/E SPECTRUM
112	923	COPPER	P3	1/E SPECTRUM
113	930	COPPER	P0	REFLECTOR
114	931	COPPER	P1	REFLECTOR
115	932	COPPER	P2	1/E SPECTRUM
116	933	COPPER	P3	1/E SPECTRUM
117	940	COPPER	P0	SHIELD
118	941	COPPER	P1	SHIELD
119	942	COPPER	P2	1/E SPECTRUM
120	943	COPPER	P3	1/E SPECTRUM

TABLE 6-3 (CONT)

P(L) NEUTRON CROSS SECTION SETS IN MASTER LIBRARY 2

SET NO.	IDENTIFICATION NO.	SET DESCRIPTION	TYPE	SPECTRUM
121	1010	GADOLINIUM	P0	CORE CENTER
122	1011	GADOLINIUM	P1	CORE CENTER
123	1020	GADOLINIUM	P0	CORE EDGE
124	1021	GADOLINIUM	P1	CORE EDGE
125	1030	GADOLINIUM	P0	REFLECTOR
126	1031	GADOLINIUM	P1	REFLECTOR
127	1040	GADOLINIUM	P0	SHIELD
128	1041	GADOLINIUM	P1	SHIELD
129	1110	GOLD	P0	CORE CENTER
130	1111	GOLD	P1	CORE CENTER
131	1120	GOLD	P0	CORE EDGE
132	1121	GOLD	P1	CORE EDGE
133	1130	GOLD	P0	REFLECTOR
134	1131	GOLD	P1	REFLECTOR
135	1140	GOLD	P0	SHIELD
136	1141	GOLD	P1	SHIELD
137	1210	HYDROGEN, PARA, 20.4 DEG.	P0	CORE CENTER
138	1211	HYDROGEN, PARA, 20.4 DEG.	P1	CORE CENTER
139	1212	HYDROGEN	P2	1/E SPECTRUM
140	1213	HYDROGEN	P3	1/E SPECTRUM
141	1220	HYDROGEN, PARA, 20.4 DEG.	P0	CORE EDGE
142	1221	HYDROGEN, PARA, 20.4 DEG.	P1	CORE EDGE
143	1222	HYDROGEN	P2	1/E SPECTRUM
144	1223	HYDROGEN	P3	1/E SPECTRUM
145	1230	HYDROGEN, PARA, 20.4 DEG.	P0	REFLECTOR
146	1231	HYDROGEN, PARA, 20.4 DEG.	P1	REFLECTOR
147	1232	HYDROGEN	P2	1/E SPECTRUM
148	1233	HYDROGEN	P3	1/E SPECTRUM
149	1240	HYDROGEN, PARA, 20.4 DEG.	P0	SHIELD
150	1241	HYDROGEN, PARA, 20.4 DEG.	P1	SHIELD

TABLE 6-3(CONT)

P(L) NEUTRON CROSS SECTION SETS IN MASTER LIBRARY 2

SET NO.	IDENTIFICATION NO.	SET DESCRIPTION	TYPE	SPECTRUM
151	1242	HYDROGEN	P2	1/E SPECTRUM
152	1243	HYDROGEN	P3	1/E SPECTRUM
153	1310	HYDROGEN, ORTHO, 20.4 DEG.	P0	CORE CENTER
154	1311	HYDROGEN, ORTHO, 20.4 DEG.	P1	CORE CENTER
155	1312	HYDROGEN	P2	1/E SPECTRUM
156	1313	HYDROGEN	P3	1/E SPECTRUM
157	1320	HYDROGEN, ORTHO, 20.4 DEG.	P0	CORE EDGE
158	1321	HYDROGEN, ORTHO, 20.4 DEG.	P1	CORE EDGE
159	1322	HYDROGEN	P2	1/E SPECTRUM
160	1323	HYDROGEN	P3	1/E SPECTRUM
161	1330	HYDROGEN, ORTHO, 20.4 DEG.	P0	REFLECTOR
162	1331	HYDROGEN, ORTHO, 20.4 DEG.	P1	REFLECTOR
163	1332	HYDROGEN	P2	1/E SPECTRUM
164	1333	HYDROGEN	P3	1/E SPECTRUM
165	1340	HYDROGEN, ORTHO, 20.4 DEG.	P0	SHIELD
166	1341	HYDROGEN, ORTHO, 20.4 DEG.	P1	SHIELD
167	1342	HYDROGEN	P2	1/E SPECTRUM
168	1343	HYDROGEN	P3	1/E SPECTRUM
169	1410	HYDROGEN, PARA, 300 DEG.	P0	CORE CENTER
170	1411	HYDROGEN, PARA, 300 DEG.	P1	CORE CENTER
171	1412	HYDROGEN	P2	1/E SPECTRUM
172	1413	HYDROGEN	P3	1/E SPECTRUM
173	1420	HYDROGEN, PARA, 300 DEG.	P0	CORE EDGE
174	1421	HYDROGEN, PARA, 300 DEG.	P1	CORE EDGE
175	1422	HYDROGEN	P2	1/E SPECTRUM
176	1423	HYDROGEN	P3	1/E SPECTRUM
177	1430	HYDROGEN, PARA, 300 DEG.	P0	REFLECTOR
178	1431	HYDROGEN, PARA, 300 DEG.	P1	REFLECTOR
179	1432	HYDROGEN	P2	1/E SPECTRUM
180	1433	HYDROGEN	P3	1/E SPECTRUM

TABLE 6-3(CONT)

P(L) NEUTRON CROSS SECTION SETS IN MASTER LIBRARY 2

SET NO.	IDENTIFICATION NO.	SET DESCRIPTION	TYPE	SPECTRUM
181	1440	HYDROGEN, PARA, 300 DEG. K	P0	SHIELD
182	1441	HYDROGEN, PARA, 300 DEG. K	P1	SHIELD
183	1442	HYDROGEN	P2	1/E SPECTRUM
184	1443	HYDROGEN	P3	1/E SPECTRUM
185	1510	HYDROGEN, ORTHO, 300 DEG. K	P0	CORE CENTER
186	1511	HYDROGEN, ORTHO, 300 DEG. K	P1	CORE CENTER
187	1512	HYDROGEN	P2	1/E SPECTRUM
188	1513	HYDROGEN	P3	1/E SPECTRUM
189	1520	HYDROGEN, ORTHO, 300 DEG. K	P0	CORE EDGE
190	1521	HYDROGEN, ORTHO, 300 DEG. K	P1	CORE EDGE
191	1522	HYDROGEN	P2	1/E SPECTRUM
192	1523	HYDROGEN	P3	1/E SPECTRUM
193	1530	HYDROGEN, ORTHO, 300 DEG. K	P0	REFLECTOR
194	1531	HYDROGEN, ORTHO, 300 DEG. K	P1	REFLECTOR
195	1532	HYDROGEN	P2	1/E SPECTRUM
196	1533	HYDROGEN	P3	1/E SPECTRUM
197	1540	HYDROGEN, ORTHO, 300 DEG. K	P0	SHIELD
198	1541	HYDROGEN, ORTHO, 300 DEG. K	P1	SHIELD
199	1542	HYDROGEN	P2	1/E SPECTRUM
200	1543	HYDROGEN	P3	1/E SPECTRUM
201	1610	HYDROGEN, GAS, 2500 DEG. K	P0	CORE CENTER
202	1611	HYDROGEN, GAS, 2500 DEG. K	P1	CORE CENTER
203	1612	HYDROGEN	P2	1/E SPECTRUM
204	1613	HYDROGEN	P3	1/E SPECTRUM
205	1620	HYDROGEN, GAS, 2500 DEG. K	P0	CORE EDGE
206	1621	HYDROGEN, GAS, 2500 DEG. K	P1	CORE EDGE
207	1622	HYDROGEN	P2	1/E SPECTRUM
208	1623	HYDROGEN	P3	1/E SPECTRUM
209	1630	HYDROGEN, GAS, 2500 DEG. K	P0	REFLECTOR
210	1631	HYDROGEN, GAS, 2500 DEG. K	P1	REFLECTOR

TABLE 6-3(CONT)

P(L) NEUTRON CROSS SECTION SETS IN MASTER LIBRARY 2

SET NO.	IDENTIFICATION NO.	SET DESCRIPTION	TYPE	SPECTRUM
211	1632	HYDROGEN	P2	1/E SPECTRUM
212	1633	HYDROGEN	P3	1/E SPECTRUM
213	1640	HYDROGEN, GAS, 2500 DEG. K	P0	SHIELD
214	1641	HYDROGEN, GAS, 2500 DEG. K	P1	SHIELD
215	1642	HYDROGEN	P2	1/E SPECTRUM
216	1643	HYDROGEN	P3	1/E SPECTRUM
217	1710	INDIUM-115	P0	CORE CENTER
218	1711	INDIUM-115	P1	CORE CENTER
219	1720	INDIUM-115	P0	CORE EDGE
220	1721	INDIUM-115	P1	CORE EDGE
221	1730	INDIUM-115	P0	REFLECTOR
222	1731	INDIUM-115	P1	REFLECTOR
223	1740	INDIUM-115	P0	SHIELD
224	1741	INDIUM-115	P1	SHIELD
225	1810	IRON	P0	CORE CENTER
226	1811	IRON	P1	CORE CENTER
227	1812	IRON	P2	1/E SPECTRUM
228	1813	IRON	P3	1/E SPECTRUM
229	1820	IRON	P0	CORE EDGE
230	1821	IRON	P1	CORE EDGE
231	1822	IRON	P2	1/E SPECTRUM
232	1823	IRON	P3	1/E SPECTRUM
233	1830	IRON	P0	REFLECTOR
234	1831	IRON	P1	REFLECTOR
235	1832	IRON	P2	1/E SPECTRUM
236	1833	IRON	P3	1/E SPECTRUM
237	1840	IRON	P0	SHIELD
238	1841	IRON	P1	SHIELD
239	1842	IRON	P2	1/E SPECTRUM
240	1843	IRON	P3	1/E SPECTRUM

TABLE 6-3(CONT)

P(L) NEUTRON CROSS SECTION SETS IN MASTER LIBRARY 2

SET NO.	IDENTIFICATION NO.	SET DESCRIPTION	TYPE	SPECTRUM
241	1910	LEAD	P0	CORE CENTER
242	1911	LEAD	P1	CORE CENTER
243	1920	LEAD	P0	CORE EDGE
244	1921	LEAD	P1	CORE EDGE
245	1930	LEAD	P0	REFLECTOR
246	1931	LEAD	P1	REFLECTOR
247	1940	LEAD	P0	SHIELD
248	1941	LEAD	P1	SHIELD
249	2010	LITHIUM	P0	CORE CENTER
250	2011	LITHIUM	P1	CORE CENTER
251	2020	LITHIUM	P0	CORE EDGE
252	2021	LITHIUM	P1	CORE EDGE
253	2030	LITHIUM	P0	REFLECTOR
254	2031	LITHIUM	P1	REFLECTOR
255	2040	LITHIUM	P0	SHIELD
256	2041	LITHIUM	P1	SHIELD
257	2110	LITHIUM-6	P0	CORE CENTER
258	2111	LITHIUM-6	P1	CORE CENTER
259	2120	LITHIUM-6	P0	CORE EDGE
260	2121	LITHIUM-6	P1	CORE EDGE
261	2130	LITHIUM-6	P0	REFLECTOR
262	2131	LITHIUM-6	P1	REFLECTOR
263	2140	LITHIUM-6	P0	SHIELD
264	2141	LITHIUM-6	P1	SHIELD
265	2210	LITHIUM-7	P0	CORE CENTER
266	2211	LITHIUM-7	P1	CORE CENTER
267	2220	LITHIUM-7	P0	CORE EDGE
268	2221	LITHIUM-7	P1	CORE EDGE
269	2230	LITHIUM-7	P0	REFLECTOR
270	2231	LITHIUM-7	P1	REFLECTOR

TABLE 6-3 (CONT)
P(L) NEUTRON CROSS SECTION SETS IN MASTER LIBRARY 2

SET NO.	IDENTIFICATION NO.	SET DESCRIPTION	TYPE	SPECTRUM
271	2240	LITHIUM-7	P0	SHIELD
272	2241	LITHIUM-7	P1	SHIELD
273	2310	MAGNESIUM	P0	CORE CENTER
274	2311	MAGNESIUM	P1	CORE CENTER
275	2320	MAGNESIUM	P0	CORE EDGE
276	2321	MAGNESIUM	P1	CORE EDGE
277	2330	MAGNESIUM	P0	REFLECTOR
278	2331	MAGNESIUM	P1	REFLECTOR
279	2340	MAGNESIUM	P0	SHIELD
280	2341	MAGNESIUM	P1	SHIELD
281	2410	MANGANESE	P0	CORE CENTER
282	2411	MANGANESE	P1	CORE CENTER
283	2412	MANGANESE	P2	1/E SPECTRUM
284	2413	MANGANESE	P3	1/E SPECTRUM
285	2420	MANGANESE	P0	CORE EDGE
286	2421	MANGANESE	P1	CORE EDGE
287	2422	MANGANESE	P2	1/E SPECTRUM
288	2423	MANGANESE	P3	1/E SPECTRUM
289	2440	MANGANESE	P0	SHIELD
290	2441	MANGANESE	P1	SHIELD
291	2442	MANGANESE	P2	1/E SPECTRUM
292	2443	MANGANESE	P3	1/E SPECTRUM
293	2510	MOLYBDENUM	P0	CORE CENTER
294	2511	MOLYBDENUM	P1	CORE CENTER
295	2512	MOLYBDENUM	P2	1/E SPECTRUM
296	2513	MOLYBDENUM	P3	1/E SPECTRUM
297	2520	MOLYBDENUM	P0	CORE EDGE
298	2521	MOLYBDENUM	P1	CORE EDGE
299	2522	MOLYBDENUM	P2	1/E SPECTRUM
300	2523	MOLYBDENUM	P3	1/E SPECTRUM

TABLE 6-3(CONT)

P(L) NEUTRON CROSS SECTION SETS IN MASTER LIBRARY 2

SET NO.	IDENTIFICATION NO.	SET DESCRIPTION	TYPE	SPECTRUM
301	2530	MOLYBDENUM	P0	REFLECTOR
302	2531	MOLYBDENUM	P1	REFLECTOR
303	2532	MOLYBDENUM	P2	1/E SPECTRUM
304	2533	MOLYBDENUM	P3	1/E SPECTRUM
305	2540	MOLYBDENUM	P0	SHIELD
306	2541	MOLYBDENUM	P1	SHIELD
307	2542	MOLYBDENUM	P2	1/E SPECTRUM
308	2543	MOLYBDENUM	P3	1/E SPECTRUM
309	2610	NICKEL	P0	CORE CENTER
310	2611	NICKEL	P1	CORE CENTER
311	2612	NICKEL	P2	1/E SPECTRUM
312	2613	NICKEL	P3	1/E SPECTRUM
313	2620	NICKEL	P0	CORE EDGE
314	2621	NICKEL	P1	CORE EDGE
315	2622	NICKEL	P2	1/E SPECTRUM
316	2623	NICKEL	P3	1/E SPECTRUM
317	2630	NICKEL	P0	REFLECTOR
318	2631	NICKEL	P1	REFLECTOR
319	2632	NICKEL	P2	1/E SPECTRUM
320	2633	NICKEL	P3	1/E SPECTRUM
321	2640	NICKEL	P0	SHIELD
322	2641	NICKEL	P1	SHIELD
323	2642	NICKEL	P2	1/E SPECTRUM
324	2643	NICKEL	P3	1/E SPECTRUM
325	2710	NIObIUM	P0	CORE CENTER
326	2711	NIObIUM	P1	CORE CENTER
327	2712	NIObIUM	P2	1/E SPECTRUM
328	2713	NIObIUM	P3	1/E SPECTRUM
329	2720	NIObIUM	P0	CORE EDGE
330	2721	NIObIUM	P1	CORE EDGE

TABLE 6-3(CONT)

P(L) NEUTRON CROSS SECTION SETS IN MASTER LIBRARY 2

SET NO.	IDENTIFICATION NO.	SET DESCRIPTION	TYPE	SPECTRUM
331	2722	NIObIUM	P2	1/E SPECTRUM
332	2723	NIObIUM	P3	1/E SPECTRUM
333	2730	NIObIUM	P0	REFLECTOR
334	2731	NIObIUM	P1	REFLECTOR
335	2732	NIObIUM	P2	1/E SPECTRUM
336	2733	NIObIUM	P3	1/E SPECTRUM
337	2740	NIObIUM	P0	SHIELD
338	2741	NIObIUM	P1	SHIELD
339	2742	NIObIUM	P2	1/E SPECTRUM
340	2743	NIObIUM	P3	1/E SPECTRUM
341	2810	NITROGEN	P0	CORE CENTER
342	2811	NITROGEN	P1	CORE CENTER
343	2820	NITROGEN	P0	CORE EDGE
344	2821	NITROGEN	P1	CORE EDGE
345	2830	NITROGEN	P0	CORE EDGE
346	2831	NITROGEN	P1	REFLECTOR
347	2840	NITROGEN	P0	REFLECTOR
348	2841	NITROGEN	P1	SHIELD
349	2910	OXYGEN	P1	SHIELD
350	2911	OXYGEN	P0	CORE CENTER
351	2920	OXYGEN	P1	CORE CENTER
352	2921	OXYGEN	P0	CORE EDGE
353	2930	OXYGEN	P1	CORE EDGE
354	2931	OXYGEN	P0	CORE EDGE
355	2940	OXYGEN	P1	REFLECTOR
356	2941	OXYGEN	P0	REFLECTOR
357	3010	SILICON	P1	SHIELD
358	3011	SILICON	P0	SHIELD
359	3020	SILICON	P1	CORE CENTER
360	3021	SILICON	P0	CORE CENTER
			P1	CORE EDGE
			P1	CORE EDGE

TABLE 6-3(CONT)

P(L) NEUTRON CROSS SECTION SETS IN MASTER LIBRARY 2

SET NO.	IDENTIFICATION NO.	SET DESCRIPTION	TYPE	SPECTRUM
361	3030	SILICON	P0	REFLECTOR
362	3031	SILICON	P1	REFLECTOR
363	3040	SILICON	P0	SHIELD
364	3041	SILICON	P1	SHIELD
365	3210	TANTALUM	P0	CORE CENTER
366	3211	TANTALUM	P1	CORE CENTER
367	3220	TANTALUM	P0	CORE EDGE
368	3221	TANTALUM	P1	CORE EDGE
369	3310	TITANIUM	P0	CORE CENTER
370	3311	TITANIUM	P1	CORE CENTER
371	3312	TITANIUM	P2	1/E SPECTRUM
372	3313	TITANIUM	P3	1/E SPECTRUM
373	3320	TITANIUM	P0	CORE EDGE
374	3321	TITANIUM	P1	CORE EDGE
375	3322	TITANIUM	P2	1/E SPECTRUM
376	3323	TITANIUM	P3	1/E SPECTRUM
377	3330	TITANIUM	P0	REFLECTOR
378	3331	TITANIUM	P1	REFLECTOR
379	3332	TITANIUM	P2	1/E SPECTRUM
380	3333	TITANIUM	P3	1/E SPECTRUM
381	3340	TITANIUM	P0	SHIELD
382	3341	TITANIUM	P1	SHIELD
383	3342	TITANIUM	P2	1/E SPECTRUM
384	3343	TITANIUM	P3	1/E SPECTRUM
385	3440	TUNGSTEN	P0	SHIELD
386	3441	TUNGSTEN	P1	SHIELD
387	3442	TUNGSTEN	P2	1/E SPECTRUM
388	3443	TUNGSTEN	P3	1/E SPECTRUM
389	3510	URANIUM-235	P0	CORE CENTER
390	3511	URANIUM-235	P1	CORE CENTER

TABLE 6-3(CONT)

P(L) NEUTRON CROSS SECTION SETS IN MASTER LIBRARY 2

SET NO.	IDENTIFICATION NO.	SET DESCRIPTION	TYPE	SPECTRUM
391	3512	URANIUM-235	P2	1/E SPECTRUM
392	3513	URANIUM-235	P3	1/E SPECTRUM
393	3520	URANIUM-235	P0	CORE EDGE
394	3521	URANIUM-235	P1	CORE EDGE
395	3522	URANIUM-235	P2	1/E SPECTRUM
396	3523	URANIUM-235	P3	1/E SPECTRUM
397	3610	URANIUM-238	P0	CORE CENTER
398	3611	URANIUM-238	P1	CORE CENTER
399	3612	URANIUM-238	P2	1/E SPECTRUM
400	3613	URANIUM-238	P3	1/E SPECTRUM
401	3620	URANIUM-238	P0	CORE EDGE
402	3621	URANIUM-238	P1	CORE EDGE
403	3622	URANIUM-238	P2	1/E SPECTRUM
404	3623	URANIUM-238	P3	1/E SPECTRUM
405	3710	ZIRCONIUM	P0	CORE CENTER
406	3711	ZIRCONIUM	P1	CORE CENTER
407	3720	ZIRCONIUM	P0	CORE EDGE
408	3721	ZIRCONIUM	P1	CORE EDGE
409	3730	ZIRCONIUM	P0	REFLECTOR
410	3731	ZIRCONIUM	P1	REFLECTOR
411	3740	ZIRCONIUM	P0	SHIELD
412	3741	ZIRCONIUM	P1	SHIELD
413	3839	RING VANE PRESCRIPTION	TRC	REFLECTOR
414	3910	HYDROGEN, GAS, 150 DEG.	P0	CORE CENTER
415	3911	HYDROGEN, GAS, 150 DEG.	P1	CORE CENTER
416	3912	HYDROGEN	P2	1/E SPECTRUM
417	3913	HYDROGEN	P3	1/E SPECTRUM
418	3920	HYDROGEN, GAS, 150 DEG.	P0	COREEDGE
419	3921	HYDROGEN, GAS, 150 DEG.	P1	CORE EDGE
420	3922	HYDROGEN	P2	1/E SPECTRUM

TABLE 6-3(CONT)

P(L) NEUTRON CROSS SECTION SETS IN MASTER LIBRARY 2

SET NO.	IDENTIFICATION NO.	SET DESCRIPTION	TYPE	SPECTRUM
421	3923	HYDROGEN	P3	1/E SPECTRUM
422	3930	HYDROGEN, GAS, 150 DEG. K	P0	REFLECTOR
423	3931	HYDROGEN, GAS, 150 DEG. K	P1	REFLECTOR
424	3932	HYDROGEN	P2	1/E SPECTRUM
425	3933	HYDROGEN	P3	1/E SPECTRUM
426	3940	HYDROGEN, GAS, 150 DEG. K	P0	SHIELD
427	3941	HYDROGEN, GAS, 150 DEG. K	P1	SHIELD
428	3942	HYDROGEN	P2	1/E SPECTRUM
429	3943	HYDROGEN	P3	1/E SPECTRUM
430	4010	HYDROGEN, GAS, 275 DEG. K	P0	CORE CENTER
431	4011	HYDROGEN, GAS, 275 DEG. K	P1	CORE CENTER
432	4012	HYDROGEN	P2	1/E SPECTRUM
433	4013	HYDROGEN	P3	1/E SPECTRUM
434	4020	HYDROGEN, GAS, 275 DEG. K	P0	COREEDGE
435	4021	HYDROGEN, GAS, 275 DEG. K	P1	CORE EDGE
436	4022	HYDROGEN	P2	1/E SPECTRUM
437	4023	HYDROGEN	P3	1/E SPECTRUM
438	4030	HYDROGEN, GAS, 275 DEG. K	P0	REFLECTOR
439	4031	HYDROGEN, GAS, 275 DEG. K	P1	REFLECTOR
440	4032	HYDROGEN	P2	1/E SPECTRUM
441	4033	HYDROGEN	P3	1/E SPECTRUM
442	4040	HYDROGEN, GAS, 275 DEG. K	P0	SHIELD
443	4041	HYDROGEN, GAS, 275 DEG. K	P1	SHIELD
444	4042	HYDROGEN	P2	1/E SPECTRUM
445	4043	HYDROGEN	P3	1/E SPECTRUM

TABLE 6-4

THERMAL NEUTRON CAPTURE GAMMA PRODUCTION SPECTRA
FOR APPROPOS-NAGS (MEV/CAPTURE)

GAMMA ENERGY GROUP BOUNDS (MEV)	ELEMENT OR ISOTOPE					U-238
	HYDROGEN	BERYLLIUM	BORON(NAT)	CARBON	U-235	
9.50- 7.50	.0000000	.0000000	.0000000	.0000000	.0004800	.0000000
7.50- 7.00	.0000000	.0000000	.0000000	.0000000	.0003500	.0000000
7.00- 6.00	.0000000	4.2830000	.0000000	.0000000	.0189000	.0000000
6.00- 5.00	.0000000	.1200000	.0000000	.0000000	.0702000	.0000000
5.00- 4.00	.0000000	.0000000	.0000000	3.3760000	.2130000	.1120000
4.00- 3.00	.0000000	1.5680000	.0000000	1.1930000	.5060000	.4500000
3.00- 2.60	.0000000	.0000000	.0000000	.0000000	.3250000	.1040000
2.60- 2.20	2.2230000	.6260000	.0000000	.0000000	.4710000	.2990000
2.20- 1.80	.0000000	.0000000	.0000000	.0000000	.6040000	.6340000
1.80- 1.35	.0000000	.0000000	.0000000	.0000000	.8570000	.7160000
1.35- 0.90	.0000000	.0000000	.0000000	.3750000	1.1080000	.6190000
0.90- 0.40	.0000000	.2170000	.4780000	.0000000	1.7100000	1.0690000
0.40- 0.10	.0000000	.0000000	.0000000	.0000000	.7250000	.6260000
TOTAL ENERGY RELEASED	2.2230000	6.8140000	.4780000	4.9440000	6.6089300	4.6290000

TABLE 6-4 (CONT)
 THERMAL NEUTRON CAPTURE GAMMA PRODUCTION SPECTRA
 FOR APPROPRIATE NAGS (MEV/CAPTURE)

GAMMA ENERGY GROUP BOUNDS (MEV)	ELEMENT OR ISOTOPE						
	NITROGEN	OXYGEN	MAGNESIUM	ALUMINUM	SILICON	CHROMIUM	
9.50 - 7.50	2.1170000	.0058540	.5650000	2.6010000	.1740000	4.8930000	
7.50 - 7.00	.6930000	.3563000	.1660000	.2390000	.5110000	.9770000	
7.00 - 6.00	1.2320000	4.2260000	.7390000	.6850000	.8790000	.8770000	
6.00 - 5.00	3.8410000	.0000000	.5870000	.4470000	.2330000	.7080000	
5.00 - 4.00	.7070000	.0000000	.2940000	1.6860000	3.1660000	.2160000	
4.00 - 3.00	.9540000	.0000000	3.4940000	.9460000	2.9520000	.3630000	
3.00 - 2.60	.0000000	.0244100	1.4900000	.4250000	.0480000	.0950000	
2.60 - 2.20	.3390000	.0000000	.0810000	.2700000	.1420000	.4560000	
2.20 - 1.80	.7260000	.0006448	.9080000	.1730000	.5160000	.1490000	
1.80 - 1.35	.1000000	.0019300	.3350000	.1120000	.0000000	.1730000	
1.35 - 0.90	.0000000	.0000000	.1470000	.0550000	.0320000	.0110000	
0.90 - 0.40	.0850000	.0000000	.2470000	.0490000	.0250000	.3580000	
0.40 - 0.10	.0370000	.0000000	.0420000	.0390000	.0200000	.0000000	
TOTAL ENERGY RELEASED	10.8310000	4.6151388	9.0950000	7.7270000	8.6980000	9.2760000	

TABLE 6-4 (CONT)

THERMAL NEUTRON CAPTURE GAMMA PRODUCTION SPECTRA
FOR APPROPRIOS-NAGS (MEV/CAPTURE)

GAMMA ENERGY GROUP BOUNDS (MEV)	ELEMENT OR ISOTOPE						
	MANGANESE	IRON	COBALT	NICKEL	COPPER	ZIRCONIUM	
9.50- 7.50	.0000000	4.0930000	.0000000	6.2640000	3.8810000	.1390000	
7.50- 7.00	2.7240000	.5210000	.9840000	.0120000	1.1030000	.0530000	
7.00- 6.00	.7120000	.9120000	2.3590000	1.1420000	1.0670000	1.3350000	
6.00- 5.00	1.6660000	.7090000	2.0290000	.4210000	.5430000	.7910000	
5.00- 4.00	.7920000	.5180000	.6610000	.1710000	.4000000	1.0620000	
4.00- 3.00	.5430000	.4330000	.2750000	.1280000	.2210000	1.5560000	
3.00- 2.60	.1220000	.1340000	.0216000	.0710000	.0630000	.7050000	
2.60- 2.20	.2640000	.0790000	.0000000	.0520000	.0470000	.6770000	
2.20- 1.80	.2940000	.0520000	.1940000	.0890000	.0380000	.9360000	
1.80- 1.35	.0940000	.1910000	.2360000	.0120000	.0400000	.5140000	
1.35- 0.90	.0070000	.0660000	.1950000	.0360000	.0310000	.4570000	
0.90- 0.40	.0130000	.0870000	.3390000	.1070000	.1500000	.0920000	
0.40- 0.10	.0380000	.0520000	.1960000	.0240000	.1570000	.0560000	
TOTAL ENERGY RELEASED	7.2690000	7.8470000	7.4896000	8.5290000	7.7490000	8.3730000	

TABLE 6-4 (CONT)
 THERMAL NEUTRON CAPTURE GAMMA PRODUCTION SPECTRA
 FOR APPROPOS-NAGS (MEV/CAPTURE)

GAMMA ENERGY GROUP BOUNDS (MEV)	ELEMENT OR ISOTOPE						
	MOLYBDENUM	SILVER	INDIUM	CADMIUM	GADOLINIUM	LEAD	
9.50- 7.50	.2030000	.0500000	.0000000	.2080000	.0360000	.0000000	.0000000
7.50- 7.00	.0980000	.1310000	.0000000	.0690000	.0300000	6.9300000	.0000000
7.00- 6.00	.7020000	.3900000	.0890400	.3580000	.3730000	.3390000	.0000000
6.00- 5.00	.8590000	1.0860000	.8727000	1.3130000	.6720000	.0000000	.0000000
5.00- 4.00	1.2410000	1.1680000	.8679000	1.3330000	1.0180000	.0000000	.0000000
4.00- 3.00	1.6030000	1.5240000	.4400000	1.9140000	1.7820000	.0000000	.0000000
3.00- 2.60	.8470000	.8000000	.1167000	1.1210000	1.0870000	.0000000	.0000000
2.60- 2.20	.8030000	.8150000	.1286000	.9680000	1.0320000	.0000000	.0000000
2.20- 1.80	.8280000	.6160000	1.2830000	.5180000	.6740000	.0000000	.0000000
1.80- 1.35	.7160000	.1520000	.3279000	.4540000	.4250000	.0000000	.0000000
1.35- 0.90	.2630000	.0310000	1.8740000	.0680000	.7410000	.0000000	.0000000
0.90- 0.40	.5690000	.0470000	.5049000	.6610000	.1340000	.0000000	.0000000
0.40- 0.10	.0180000	.0990000	.2205000	.0550000	.0150000	.0000000	.0000000
TOTAL ENERGY RELEASED	8.7500000	6.9090000	6.7252400	9.0400000	8.0190000	7.2690000	7.2690000

TABLE 6-4 (CONT)

THERMAL NEUTRON CAPTURE GAMMA PRODUCTION SPECTRA
FOR APPROPOS-NAGS (MEV/CAPTURE)

GAMMA ENERGY GROUP BOUNDS (MEV)	ELEMENT OR ISOTOPE					
	NIObIUM	TITANIUM	TANTALUM	LITHIUM-6	LITHIUM-7	BORON-10
9.50- 7.50	.0470000	.0150000	.0270000	.0000000	.0000000	.0000000
7.50- 7.00	.1200000	.0220000	.0250000	2.5410000	.0000000	.0000000
7.00- 6.00	.3180000	5.6410000	.0740000	1.9660000	.0000000	.0000000
6.00- 5.00	1.1880000	.1330000	.3400000	.0000000	.0000000	.0000000
5.00- 4.00	1.2320000	.5390000	.9030000	1.6700000	.0000000	.0000000
4.00- 3.00	1.4820000	.4310000	1.4130000	.0000000	.0000000	.0000000
3.00- 2.60	.6720000	.0770000	.8080000	.9400000	.0000000	.0000000
2.60- 2.20	.6990000	.0490000	.8720000	.0000000	.0000000	.0000000
2.20- 1.80	.6970000	.0940000	.8290000	.0000000	1.6160000	.0000000
1.80- 1.35	.4000000	1.1310000	.4760000	.0000000	.0000000	.0000000
1.35- 0.90	.1440000	.0310000	.1190000	.0000000	.4040000	.0000000
0.90- 0.40	.0930000	.0130000	.1390000	.1390000	.0000000	.4780000
0.40- 0.10	.1200000	.0920000	.0400000	.0000000	.0000000	.0000000
TOTAL ENERGY RELEASED	7.2120000	8.2680000	6.0650000	7.2560000	2.0200000	.4780000

TABLE 6-4 (CONT)
 THERMAL NEUTRON CAPTURE GAMMA PRODUCTION SPECTRA
 FOR APPROPRIOS-NAGS (MEV/CAPTURE)

GAMMA ENERGY GROUP BOUNDS (MEV)	ELEMENT OR ISOTOPE					
	W-182	W-183A	W-183B	W-184	W-186	SULFUR
9.50- 7.50	.5860000	.5060000	.5060000	.4120000	.4710000	.5020000
7.50- 7.00	.5860000	.5060000	.5060000	.4120000	.4170000	.1190000
7.00- 6.00	.5860000	.5060000	.5060000	.4120000	.4170000	.0544000
6.00- 5.00	.5860000	.5060000	.5060000	.4120000	.4170000	3.4490000
5.00- 4.00	.5860000	.5060000	.5060000	.4120000	.4170000	.8450000
4.00- 3.00	.5860000	.5060000	.5060000	.4120000	.4170000	1.0770000
3.00- 2.60	.5860000	.5060000	.5060000	.4120000	.4170000	.6940000
2.60- 2.20	.8930000	1.6600000	1.6600000	1.2260000	1.0880000	1.1440000
2.20- 1.80	.5370000	.9990000	.9990000	.7380000	.6550000	.0608000
1.80- 1.35	.4040000	.7520000	.7520000	.5560000	.4910000	.0442000
1.35- 0.90	.2300000	.4260000	.4260000	.3170000	.2810000	.0037400
0.90- 0.40	.0210000	.0390000	.0390000	.0290000	.0260000	.5040000
0.40- 0.10	.0000000	.0000000	.0000000	.0000000	.0000000	.0000000
TOTAL ENERGY RELEASED	6.1870000	7.4180000	7.4180000	5.7500000	5.5140000	8.4971400

TABLE 6-4 (CONT)

THERMAL NEUTRON CAPTURE GAMMA PRODUCTION SPECTRA
FOR APPROPOS-NAGS (MEV/CAPTURE)

GAMMA ENERGY GROUP BOUNDS (MEV)	ELEMENT OR ISOTOPE				
	LITHIUM	TUNGSTEN	SODIUM	GOLD	HAFNIUM
9.50- 7.50	.0000000	.0400000	.0000000	.0270000	.0290000
7.50- 7.00	.1885000	.0890000	.0000000	.0220000	.0230000
7.00- 6.00	.1458000	.6080000	1.4340000	1.1590000	.1040000
6.00- 5.00	.0000000	.7210000	.3510000	1.2300000	.4660000
5.00- 4.00	.1239000	.8580000	.1400000	1.2300000	.6340000
4.00- 3.00	.0000000	1.1780000	2.3520000	.7520000	1.3250000
3.00- 2.60	.0697000	.6360000	.5910000	.4980000	.8580000
2.60- 2.20	.0000000	.6900000	.6900000	.6980000	.9230000
2.20- 1.80	1.4960000	.5380000	.6560000	.4090000	1.0030000
1.80- 1.35	.0000000	.2210000	.1590000	.1710000	1.4330000
1.35- 0.90	.3740000	.0600000	.0350000	.1610000	.3240000
0.90- 0.40	.0103000	.0830000	.5510000	.0660000	.0100000
0.40- 0.10	.0000000	.0270000	.0000000	.0900000	.0700000
TOTAL ENERGY RELEASED	2.4082000	5.7490000	6.9590000	6.5130000	7.2020000

TABLE 6-5
**BASIC DATA SOURCE FOR THERMAL NEUTRON CAPTURE
PHOTON PRODUCTION SPECTRA DATA**

<u>Element</u>	<u>Data Source</u>	<u>Element</u>	<u>Data Source</u>
Hydrogen	1	Cadmium	1
Beryllium	1	Gadolinium	1
Boron (Natural)	4	Lead	1
Carbon	1	Niobium	1
Uranium-235	5	Titanium	1
Uranium-238	4	Tantalum	1
Nitrogen	1	Lithium-6	3
Oxygen	5	Lithium-7	3
Magnesium	1	Boron-10	4
Aluminum	1	Tungsten-182	4
Silicon	2	Tungsten-183A	4
Chromium	2	Tungsten-183B	4
Manganese	1	Tungsten-184	4
Iron	1	Tungsten-186	4
Cobalt	5	Sulphur	5
Nickel	1	Lithium	3
Copper	1	Tungsten	1
Zirconium	2	Sodium	1
Molybdenum	1	Gold	1
Silver	1	Hafnium	1
Indium	3		

TABLE 6-5 (CONT)

Data Source References

- 1 - WANL-TME-2713, "Some New Thermal Neutron Capture Gamma Yields for the WANL POINT Library", S. A. Fody, July 1970.
- 2 - Revised data from WANL-TME-2713 normalized to Binding Energy from Nuclear Data Sheets.
- 3 - Nuclear Data Sheets - A3, 1967, Part I and Nuclear Data Sheets - A5, 1969, Parts II and III, "Compendium of Thermal Neutron Capture Gamma Ray Measurements", G. A. Bartholemew, et. al.
- 4 - WANL Internal Communication, "POINT Library", R. N. Nassano and R. G. Soltesz, September 1969.
- 5 - POPOP-4 Library Data, April 1969.

TABLE 6-6

NEUTRON INELASTIC SCATTER PHOTON PRODUCTION SPECTRA

BERYLLIUM - (N,NPRIME,GAMMA) REACTION-GAMMA PRODUCTION SPECTRUM-52 GRP.
 DATA SOURCE--UNC-5139 P. 20
 POPOP-4 I.O. NO. 04000301

GAMMA ENERGY GROUP BOUNDS (MEV)	10.000-	2.870	2.870-	1.350	1.350-	0.821	0.821-	0.388	0.388-	0.111	0.111-	0.015
	NEUTRON ENERGY BOUNDS (MEV)											
9.50- 7.50	0.	0.	0.	0.	0.	0.	0.	0.	0.	0.	0.	0.
7.50- 7.00	0.	0.	0.	0.	0.	0.	0.	0.	0.	0.	0.	0.
7.00- 6.00	0.	0.	0.	0.	0.	0.	0.	0.	0.	0.	0.	0.
6.00- 5.00	0.	0.	0.	0.	0.	0.	0.	0.	0.	0.	0.	0.
5.00- 4.00	0.	0.	0.	0.	0.	0.	0.	0.	0.	0.	0.	0.
4.00- 3.00	0.	0.	0.	0.	0.	0.	0.	0.	0.	0.	0.	0.
3.00- 2.60	0.	0.	0.	0.	0.	0.	0.	0.	0.	0.	0.	0.
2.60- 2.20	0.	0.	0.	0.	0.	0.	0.	0.	0.	0.	0.	0.
2.20- 1.80	0.	0.	0.	0.	0.	0.	0.	0.	0.	0.	0.	0.
1.80- 1.35	0.	0.	0.	0.	0.	0.	0.	0.	0.	0.	0.	0.
1.35- .90	0.	0.	0.	0.	0.	0.	0.	0.	0.	0.	0.	0.
.90- .40	0.	0.	0.	0.	0.	0.	0.	0.	0.	0.	0.	0.
.40- .10	0.	0.	0.	0.	0.	0.	0.	0.	0.	0.	0.	0.
TOTAL ENERGY RELEASED	0.	0.	0.	0.	0.	0.	0.	0.	0.	0.	0.	0.

TABLE 6-6 (CONT)

NEUTRON INELASTIC SCATTER PHOTON PRODUCTION SPECTRA

CARBON ---- (N,PRIME,GAMMA) REACTION-GAMMA PRODUCTION SPECTRUM-52 GRP.
 DATA SOURCE--UNC-5140
 POPP-4 I.O. NO. 06000301

GAMMA ENERGY GROUP BOUNDS (MEV)	NEUTRON ENERGY BOUNDS (MEV)											
	10.000-	2.870	2.870-	1.350	1.350-	0.821	0.821-	0.388	0.388-	0.111	0.111-	0.015
9.50- 7.50	0.	0.	0.	0.	0.	0.	0.	0.	0.	0.	0.	0.
7.50- 7.00	0.	0.	0.	0.	0.	0.	0.	0.	0.	0.	0.	0.
7.00- 6.00	0.	0.	0.	0.	0.	0.	0.	0.	0.	0.	0.	0.
6.00- 5.00	0.	0.	0.	0.	0.	0.	0.	0.	0.	0.	0.	0.
5.00- 4.00	4.284E+00	0.	0.	0.	0.	0.	0.	0.	0.	0.	0.	0.
4.00- 3.00	0.	0.	0.	0.	0.	0.	0.	0.	0.	0.	0.	0.
3.00- 2.60	0.	0.	0.	0.	0.	0.	0.	0.	0.	0.	0.	0.
2.60- 2.20	0.	0.	0.	0.	0.	0.	0.	0.	0.	0.	0.	0.
2.20- 1.80	0.	0.	0.	0.	0.	0.	0.	0.	0.	0.	0.	0.
1.80- 1.35	0.	0.	0.	0.	0.	0.	0.	0.	0.	0.	0.	0.
1.35- .90	0.	0.	0.	0.	0.	0.	0.	0.	0.	0.	0.	0.
.90- .40	0.	0.	0.	0.	0.	0.	0.	0.	0.	0.	0.	0.
.40- .10	0.	0.	0.	0.	0.	0.	0.	0.	0.	0.	0.	0.
TOTAL ENERGY RELEASED	4.284E+00	0.	0.	0.	0.	0.	0.	0.	0.	0.	0.	0.

TABLE 6-6 (CONT)

NEUTRON INELASTIC SCATTER PHOTON PRODUCTION SPECTRA

U-238 ----- (N,PRIME,GAMMA) REACTION-GAMMA PRODUCTION SPECTRUM-52 GRP.
 DATA SOURCE--UNC-5140 P. 54
 POPOP-4 I.D. NO. 92380301

GAMMA ENERGY GROUP BOUNDS (MEV)	NEUTRON ENERGY ROUNDS (MEV)										
	10.000-	2.870	2.870-	1.350	1.350-	.821	.821-	.388	.388-	.111-	.015
9.50-	0.		0.		0.		0.		0.		0.
7.50-	0.		0.		0.		0.		0.		0.
7.00-	6.255E-03		0.		0.		0.		0.		0.
6.00-	1.418E-01		0.		0.		0.		0.		0.
5.00-	5.949E-01		0.		0.		0.		0.		0.
4.00-	3.746E-01		0.		0.		0.		0.		0.
3.00-	1.382E-01	1.469E-03	0.		0.		0.		0.		0.
2.60-	1.539E-01	1.316E-02	0.		0.		0.		0.		0.
2.20-	1.704E-01	4.084E-02	0.		0.		0.		0.		0.
1.80-	2.079E-01	1.045E-01	4.675E-03		0.		0.		0.		0.
1.35-	2.040E-01	1.705E-01	5.353E-02		2.441E-03		0.		0.		0.
.90-	2.537E-01	2.787E-01	2.406E-01		1.220E-01		1.635E-02		0.		0.
.40-	1.975E-01	2.193E-01	1.936E-01		2.032E-01		2.895E-02		0.		0.
TOTAL ENERGY RELEASED	2.443E+00	8.285E-01	4.924E-01	3.277E-01	4.529E-02						

TABLE 6-6 (CONT)

NEUTRON INELASTIC SCATTER PHOTON PRODUCTION SPECTRA

NITROGEN -- (N,PRIME,GAMMA) REACTION-GAMMA PRODUCTION SPECTRUM-52 GRP.
 DATA SOURCE--UNC-5139 P. 22 P0P0P-4 I.D. NO. 07000301

GAMMA ENERGY GROUP BOUNDS (MEV)	10.000-	2.870	2.870-	1.350	1.350-	.821	.821-	.388	.388-	.111	.111-	.015
	NEUTRON ENERGY BOUNDS (MEV)											
9.50-	7.50	1.214E-01	0.	0.	0.	0.	0.	0.	0.	0.	0.	0.
7.50-	7.00	5.272E-02	0.	0.	0.	0.	0.	0.	0.	0.	0.	0.
7.00-	6.00	5.070E-01	0.	0.	0.	0.	0.	0.	0.	0.	0.	0.
6.00-	5.00	7.673E-01	0.	0.	0.	0.	0.	0.	0.	0.	0.	0.
5.00-	4.00	8.402E-01	0.	0.	0.	0.	0.	0.	0.	0.	0.	0.
4.00-	3.00	1.838E-01	0.	0.	0.	0.	0.	0.	0.	0.	0.	0.
3.00-	2.60	8.512E-02	0.	0.	0.	0.	0.	0.	0.	0.	0.	0.
2.60-	2.20	3.477E+00	0.	0.	0.	0.	0.	0.	0.	0.	0.	0.
2.20-	1.80	7.419E+00	0.	0.	0.	0.	0.	0.	0.	0.	0.	0.
1.80-	1.35	4.680E-01	0.	0.	0.	0.	0.	0.	0.	0.	0.	0.
1.35-	.90	7.392E-04	0.	0.	0.	0.	0.	0.	0.	0.	0.	0.
.90-	.40	1.126E-04	0.	0.	0.	0.	0.	0.	0.	0.	0.	0.
.40-	.10	2.771E-05	0.	0.	0.	0.	0.	0.	0.	0.	0.	0.
TOTAL ENERGY RELEASED		8.922E+00	0.	0.	0.	0.	0.	0.	0.	0.	0.	0.

TABLE 6-6 (CONT)

NEUTRON INELASTIC SCATTER PHOTON PRODUCTION SPECTRA

OXYGEN ----- (N, PRIME, GAMMA) REACTION-GAMMA PRODUCTION SPECTRUM-52 GRP.
 DATA SOURCE--ORNL(E.A. STRAKERS DATA) POPOP-4 I.D. NO. 08160301

GAMMA ENERGY GROUP BOUNDS (MEV)	NEUTRON ENERGY BOUNDS (MEV)	NEUTRON ENERGY BOUNDS (MEV)	NEUTRON ENERGY BOUNDS (MEV)	NEUTRON ENERGY BOUNDS (MEV)	NEUTRON ENERGY BOUNDS (MEV)	NEUTRON ENERGY BOUNDS (MEV)	NEUTRON ENERGY BOUNDS (MEV)
9.50-7.50	10.000-2.870	2.870-1.350	1.350-0.821	0.821-0.388	0.388-0.111	0.111-0.015	0.015
7.50-7.00	1.072E-03	0.0	0.0	0.0	0.0	0.0	0.0
7.00-6.00	1.238E-01	0.0	0.0	0.0	0.0	0.0	0.0
6.00-5.00	5.281E+00	0.0	0.0	0.0	0.0	0.0	0.0
5.00-4.00	0.0	0.0	0.0	0.0	0.0	0.0	0.0
4.00-3.00	0.0	0.0	0.0	0.0	0.0	0.0	0.0
3.00-2.60	4.960E-03	0.0	0.0	0.0	0.0	0.0	0.0
2.60-2.20	0.0	0.0	0.0	0.0	0.0	0.0	0.0
2.20-1.80	9.655E-04	0.0	0.0	0.0	0.0	0.0	0.0
1.80-1.35	0.0	0.0	0.0	0.0	0.0	0.0	0.0
1.35-.90	0.0	0.0	0.0	0.0	0.0	0.0	0.0
.90-.40	0.0	0.0	0.0	0.0	0.0	0.0	0.0
.40-.10	0.0	0.0	0.0	0.0	0.0	0.0	0.0
TOTAL ENERGY RELEASED	5.411E+00	0.0	0.0	0.0	0.0	0.0	0.0

TABLE 6-6 (CONT)

NEUTRON INELASTIC SCATTER PHOTON PRODUCTION SPECTRA

MAGNESIUM - (N,NPPIMF,GAMMA) REACTION-GAMMA PROD. CROSS SECTION-52 GRP.
 DATA SOURCE--NDL-TR-89-111(DRAKE) P. 74-89 P0POP-4 I.D. NO. 12000301

GAMMA ENERGY GROUP BOUNDS (MEV)	NEUTRON ENERGY BOUNDS (MEV)											
	10.000-	2.870	2.870-	1.350	1.350-	0.821	0.821-	0.388	0.388-	0.111	0.111-	0.015
9.50- 7.50	0.		0.		0.		0.		0.		0.	
7.50- 7.00	0.		0.		0.		0.		0.		0.	
7.00- 6.00	0.		0.		0.		0.		0.		0.	
6.00- 5.00	3.913F-04		0.		0.		0.		0.		0.	
5.00- 4.00	1.548E-01		0.		0.		0.		0.		0.	
4.00- 3.00	2.988E-02		0.		0.		0.		0.		0.	
3.00- 2.60	1.122E-01		0.		0.		0.		0.		0.	
2.60- 2.20	3.395E-05		0.		0.		0.		0.		0.	
2.20- 1.80	1.058E-01		2.282E-01		0.		0.		0.		0.	
1.80- 1.35	1.015F+00		2.369E+00		0.		0.		0.		0.	
1.35- .90	1.975E-02		6.863E-02		3.786E-01		0.		0.		0.	
.90- .40	8.849E-03		7.189F-02		5.745E-01		0.		0.		0.	
.40- .10	2.209F-03		2.141E-02		6.156E-02		0.		0.		0.	
TOTAL ENERGY RELEASED	1.449E+00		2.759E+00		1.015F+00		0.		0.		0.	

TABLE 6-6 (CONT)

NEUTRON INELASTIC SCATTER PHOTON PRODUCTION SPECTRA

ALUMINUM -- (N,NPRIME,GAMMA) REACTION-GAMMA PRODUCTION SPECTRUM-52 GRP.
 DATA SOURCE--UNC-5139 P. 75
 POPPP-4 I.D. NO. 13000301

GAMMA ENERGY GROUP BOUNDS (MEV)	NEUTRON ENERGY BOUNDS (MEV)					
	10.000-	2.870	2.870-	1.350	1.350-	0.015
9.50- 7.50	4.012E-03	0.	0.	0.	0.	0.
7.50- 7.00	3.241E-03	0.	0.	0.	0.	0.
7.00- 6.00	2.351E-02	0.	0.	0.	0.	0.
6.00- 5.00	7.183F-02	0.	0.	0.	0.	0.
5.00- 4.00	1.662F-01	0.	0.	0.	0.	0.
4.00- 3.00	2.179F-01	0.	0.	0.	0.	0.
3.00- 2.60	2.187F-01	0.	0.	0.	0.	0.
2.60- 2.20	5.267E-01	1.286E-01	0.	0.	0.	0.
2.20- 1.80	4.435E-01	8.506E-02	0.	0.	0.	0.
1.80- 1.35	3.643E-01	2.814E-01	1.576E-01	0.	0.	0.
1.35- .90	3.211E-01	5.460E-01	3.594E-01	0.	0.	0.
.90- .40	6.637E-02	8.795E-02	1.924E-01	0.	0.	0.
.40- .10	1.632F-02	2.164E-02	4.734E-02	0.	0.	0.
TOTAL ENFRGY RELEASED	2.444E+00	1.151E+00	7.567E-01	0.	0.	0.

TABLE 6-6 (CONT)

NEUTRON INELASTIC SCATTERPHOTON PRODUCTION SPECTRA

SILICON --- (N,PRIME,GAMMA) REACTION-GAMMA PRODUCTION SPECTRUM-52 GRP.
 DATA SOURCE--UNC.-5139 P.101
 POPOP-4 I.D. NO. 14000302

GAMMA ENERGY GROUP BOUNDS (MEV)	NEUTRON ENERGY BOUNDS (MEV)			
	10.000-	2.870	2.870- 1.350	1.350- 0.000
9.50- 7.50	0.	0.	0.	0.
7.50- 7.00	9.046E-03	0.	0.	0.
7.00- 6.00	2.095E-02	0.	0.	0.
6.00- 5.00	2.777E-02	0.	0.	0.
5.00- 4.00	3.258E-02	0.	0.	0.
4.00- 3.00	6.725E-02	0.	0.	0.
3.00- 2.60	6.561E-02	0.	0.	0.
2.60- 2.20	1.483E-01	8.184E-02	0.	0.
2.20- 1.80	7.206E-01	7.233E-01	0.	0.
1.80- 1.35	8.383E-01	9.019E-01	0.	0.
1.35- .90	7.162E-03	4.477E-02	0.	0.
.90- .40	3.889E-03	0.	0.	0.
.40- .10	9.568E-04	0.	0.	0.
TOTAL ENERGY RELEASED	1.942E+00	1.752E+00	0.	0.

TABLE 6-6 (CONT)

NEUTRON INELASTIC SCATTER PHOTON PRODUCTION SPECTRA

CHROMIUM -- (N,PRIME,GAMMA) REACTION--GAMMA PRODUCTION SPECTRUM-52 GRP.
 DATA SOURCE--UNC-5140 P. 32
 POPOP-4 I.D. NO. 24000301

GAMMA ENERGY GROUP BOUNDS (MEV)	NEUTRON ENERGY BOUNDS (MEV)					
	10.000-	2.870	2.870-	1.350	1.350-	0.000
9.50- 7.50	5.418E-02	0.	0.	0.	0.	0.
7.50- 7.00	1.339E-02	0.	0.	0.	0.	0.
7.00- 6.00	7.656E-02	0.	0.	0.	0.	0.
6.00- 5.00	1.155E-01	0.	0.	0.	0.	0.
5.00- 4.00	3.100E-01	0.	0.	0.	0.	0.
4.00- 3.00	3.284E-01	0.	0.	0.	0.	0.
3.00- 2.60	1.100E-01	0.	0.	0.	0.	0.
2.60- 2.20	8.639E-02	0.	0.	0.	0.	0.
2.20- 1.80	1.205E-01	0.	0.	0.	0.	0.
1.80- 1.35	3.234E-01	0.	0.	0.	0.	0.
1.35- .90	4.833E-01	0.	0.	0.	0.	0.
.90- .40	2.764E-01	0.	0.	0.	0.	0.
.40- .10	1.164E-01	0.	0.	0.	0.	0.
TOTAL ENERGY RELEASED	2.414E+00	0.	0.	0.	0.	0.

TABLE 6-6 (CONT)

NEUTRON INELASTIC SCATTERPHOTON PRODUCTION SPECTRA

IRON ----- (N,PRIME,GAMMA) REACTION-GAMMA PRODUCTION SPECTRUM-5? GRP.
 DATA SOURCE--UNC-5140 P. 35
 POPCP-4 I.D. NO. 26000301

GAMMA ENERGY GROUP BOUNDS (MEV)	NEUTRON ENERGY BOUNDS (MEV)					
	10.000-	2.870	2.870-	1.350	1.350-	0.821
9.50-	6.630E-03	0.	0.	0.	0.	0.
7.50-	3.489E-03	0.	0.	0.	0.	0.
7.00-	1.683F-02	0.	0.	0.	0.	0.
6.00-	6.865E-02	0.	0.	0.	0.	0.
5.00-	1.026F-01	0.	0.	0.	0.	0.
4.00-	5.815F-01	0.	0.	0.	0.	0.
3.00-	4.406E-01	7.121E-04	0.	0.	0.	0.
2.60-	3.777E-01	6.104E-04	0.	0.	0.	0.
2.20-	4.102E-01	3.402E-02	0.	0.	0.	0.
1.80-	4.569E-01	6.296E-02	0.	0.	0.	0.
1.35-	4.084E-01	2.522F-01	2.387E-01	0.	0.	0.
.90-	3.030E-01	2.648E-01	2.719E-01	0.	0.	0.
.40-	7.454E-02	6.515E-02	6.688E-02	0.	0.	0.
TOTAL ENERGY RELEASED	3.251F+00	6.805F-01	5.774E-01	0.	0.	0.

TABLE 6-6 (CONT)

NEUTRON INELASTIC SCATTER PHOTON PRODUCTION SPECTRA

NICKEL ---- (N,PRIME,GAMMA) REACTION-GAMMA PRODUCTION SPECTRUM-52 GPP.
 DATA SOURCE--UNC-5140 P. 38
 POPPP-4 I.D. NO. 29000301

GAMMA ENERGY GROUP BOUNDS (MEV)	NEUTRON ENERGY ROUNDS (MEV)					
	10.000-	2.870	2.870-	1.350	1.350-	0.015
9.50-	2.580E-03	0.	0.	0.	0.	0.
7.50-	1.418E-03	0.	0.	0.	0.	0.
7.00-	1.697E-02	0.	0.	0.	0.	0.
6.00-	5.161E-02	0.	0.	0.	0.	0.
5.00-	1.308E-01	0.	0.	0.	0.	0.
4.00-	2.283E-01	0.	0.	0.	0.	0.
3.00-	1.384E-01	0.	0.	0.	0.	0.
2.60-	1.483E-01	1.603E-03	0.	0.	0.	0.
2.20-	1.380E-01	1.153E-02	0.	0.	0.	0.
1.80-	1.332E+00	1.247E+00	0.	0.	0.	0.
1.35-	3.864E-01	2.927E-01	0.	0.	0.	0.
.90-	2.285E-01	1.037E-02	0.	0.	0.	0.
.40-	7.639E-02	0.	0.	0.	0.	0.
TOTAL ENERGY RELEASED	2.880E+00	1.563E+00	0.	0.	0.	0.

TABLE 6-6 (CONT)

NEUTRON INELASTIC SCATTER PHOTON PRODUCTION SPECTRA

ZIRCONIUM - (N, PRIME, GAMMA) REACTION-GAMMA PRODUCTION SPECTRUM-52 GRP.
 DATA SOURCE--UNC-5140 P. 39 PCPOP-4 I.D. NO. 40000101

GAMMA ENERGY GROUP BOUNDS (MEV)	NEUTRON ENERGY BOUNDS (MEV)					
	10.000-	2.870	2.870-	1.350	1.350-	.821
9.50-	0.	0.	0.	0.	0.	0.
7.50-	0.	0.	0.	0.	0.	0.
7.00-	2.340F-02	0.	0.	0.	0.	0.
6.00-	1.177E-01	0.	0.	0.	0.	0.
5.00-	2.921E-01	0.	0.	0.	0.	0.
4.00-	5.190E-01	0.	0.	0.	0.	0.
3.00-	2.330E-01	0.	0.	0.	0.	0.
2.60-	3.565E-01	1.829E-01	0.	0.	0.	0.
2.20-	3.443F-01	2.076E-01	0.	0.	0.	0.
1.80-	3.178F-01	2.719E-01	1.435E-01	0.	0.	0.
1.35-	2.481E-01	3.398E-01	3.398E-01	0.	0.	0.
.90-	1.593F-01	2.181E-01	2.181E-01	0.	0.	0.
.40-	3.919F-02	5.366E-02	5.366E-02	0.	0.	0.
TOTAL ENERGY RELEASED	2.651E+00	1.274F+00	7.551E-01	0.	0.	0.

TABLE 6-6 (CONT)

NEUTRON INELASTIC SCATTER PHOTON PRODUCTION SPECTRA

LEAD ----- (N, PRIME, GAMMA) REACTION-GAMMA PRODUCTION SPECTRUM-52 GRP.
 DATA SOURCE--UNC-5099 P.174 POPOP-4 I.D. NO. 82000301

GAMMA ENERGY GROUP BOUNDS (MEV)	10.000-	2.870	2.870-	1.350	1.350-	.821	.821-	.388	.388-	.111	.111-	.015
	NEUTRON ENERGY BOUNDS (MEV)											
9.50-	0.		0.		0.		0.		0.		0.	
7.50-	6.922E-03		0.		0.		0.		0.		0.	
7.00-	5.097E-02		0.		0.		0.		0.		0.	
6.00-	3.921E-02		0.		0.		0.		0.		0.	
5.00-	2.768E-01		0.		0.		0.		0.		0.	
4.00-	3.291E-01		0.		0.		0.		0.		0.	
3.00-	7.357E-01		6.554E-02		0.		0.		0.		0.	
2.60-	2.032E-01		1.492E-02		0.		0.		0.		0.	
2.20-	1.473E-01		3.536E-02		0.		0.		0.		0.	
1.80-	2.177E-01		6.559E-02		0.		0.		0.		0.	
1.35-	2.221E-01		2.412E-01		1.381E-01		0.		0.		0.	
.90-	3.534E-01		6.000E-01		4.070E-01		0.		0.		0.	
.40-	4.036E-03		0.		0.		0.		0.		0.	
TOTAL ENERGY RELEASED	2.586E+00		1.023E+00		5.451E-01		0.		0.		0.	

TABLE 6-6 (CONT)

NEUTRON INELASTIC SCATTER PHOTON PRODUCTION SPECTRA

NIORIUM---- (N,NPRIME,GAMMA) REACTION--GAMMA PRODUCTION SPECTRUM
 DATA SOURCE--APPROPOS LIBRARY

GAMMA ENERGY GROUP BOUNDS (MEV)	NEUTRON ENERGY BOUNDS (MEV)			
	10.000-	2.870	2.870-	0.015
9.50- 7.50	0.0	0.0	0.0	0.0
7.50- 7.00	0.0	0.0	0.0	0.0
7.00- 6.00	0.0	0.0	0.0	0.0
6.00- 5.00	0.0	0.0	0.0	0.0
5.00- 4.00	0.0	0.0	0.0	0.0
4.00- 3.00	0.0	0.0	0.0	0.0
3.00- 2.60	0.0	0.0	0.0	0.0
2.60- 2.20	0.0	0.0	0.0	0.0
2.20- 1.80	1.92	1.92	0.0	0.0
1.80- 1.35	0.0	0.0	0.0	0.0
1.35- 0.90	0.0	0.0	1.08	0.0
0.90- 0.40	0.0	0.0	0.0	0.0
0.40- 0.10	0.0	0.0	0.0	0.0
TOTAL ENERGY RELEASED	0.0	0.0	0.0	0.0

TABLE 6-6 (CONT)

NEUTRON INELASTIC SCATTER PHOTON PRODUCTION SPECTRA

TITANIUM -- (N,NPRIME,GAMMA) REACTION--GAMMA PROD. CROSS SECTION--52 GRP.
 DATA SOURCE--UNC-5002 P. 31
 PCPOP-4 I.D. NO. 22000302

GAMMA ENERGY GROUP BOUNDS (MEV)	10.000-	2.870	2.870-	1.350	1.350-	.821	.821-	.388	.388-	.111	.111-	.015
	NEUTRON ENERGY BOUNDS (MEV)											
9.50- 7.50			0.		0.				0.			0.
7.50- 7.00			0.		0.				0.			0.
7.00- 6.00			0.		0.				0.			0.
6.00- 5.00			0.		0.				0.			0.
5.00- 4.00			0.		0.				0.			0.
4.00- 3.00			0.		0.				0.			0.
3.00- 2.60			0.		0.				0.			0.
2.60- 2.20			0.		0.				0.			0.
2.20- 1.80			0.		0.				0.			0.
1.80- 1.35			5.768E-02		0.				0.			0.
1.35- .90			1.051E+00		1.169E+00				0.			0.
.90- .40			0.		0.				0.			0.
.40- .10			0.		0.				0.			0.
TOTAL ENERGY RELEASED	2.421	1.10868	1.169	0.	0.	0.	0.	0.	0.	0.	0.	0.

TABLE 6-6 (CONT)

NEUTRON INELASTIC SCATTER PHOTON PRODUCTION SPECTRA (Cont.)

LITHIUM-7-- (N,NPRIME,GAMMA) REACTION-GAMMA PRODUCTION SPECTRUM DATA SOURCE--APPROPOS LIBRARY		NEUTRON ENERGY BOUNDS (MEV)					
GAMMA ENERGY GROUP BOUNDS (MEV)	10.000- 2.870	2.870- 1.350	1.350- 0.821	0.821- 0.388	0.388- 0.111	0.111- 0.015	
9.50- 7.50	1.95 E-01	1.95 E-01	1.95 E-01	4.87 E-01	0.0	0.0	0.0
7.50- 7.00	0.0	0.0	0.0	0.0	0.0	0.0	0.0
7.00- 6.00	0.0	0.0	0.0	0.0	0.0	0.0	0.0
6.00- 5.00	0.0	0.0	0.0	0.0	0.0	0.0	0.0
5.00- 4.00	0.0	0.0	0.0	0.0	0.0	0.0	0.0
4.00- 3.00	0.0	0.0	0.0	0.0	0.0	0.0	0.0
3.00- 2.60	0.0	0.0	0.0	0.0	0.0	0.0	0.0
2.60- 2.20	0.0	0.0	0.0	0.0	0.0	0.0	0.0
2.20- 1.80	0.0	0.0	0.0	0.0	0.0	0.0	0.0
1.80- 1.35	0.0	0.0	0.0	0.0	0.0	0.0	0.0
1.35- 0.90	2.70	2.70	2.70	0.0	0.0	0.0	0.0
0.90- 0.40	4.35	4.35	4.35	0.0	0.0	0.0	0.0
0.40- 0.10	0.0	0.0	0.0	0.0	0.0	0.0	0.0
TOTAL ENERGY RELEASED	7.245	7.245	7.245	4.87 E-01	0.0	0.0	0.0

TABLE 6-6 (CONT)

NEUTRON INELASTIC SCATTER PHOTON PRODUCTION SPECTRA (Cont.)

TUNGSTEN -- (N, PRIME, GAMMA) REACTION--GAMMA PRODUCTION SPECTRUM--52 GRP.
 DATA SOURCE--UNC-5140 P. 42
 POPPOP-4 I.O. NO. 74000301

GAMMA ENERGY GROUP BOUNDS (MEV)	NEUTRON ENERGY BOUNDS (MEV)											
	10.000-	2.870	2.870-	1.350	1.350-	.821	.821-	.388	.388-	.111	.111-	.015
9.50- 7.50	0.		0.		0.		0.		0.		0.	
7.50- 7.00	0.		0.		0.		0.		0.		0.	
7.00- 6.00	0.		0.		0.		0.		0.		0.	
6.00- 5.00	3.464E-02		0.		0.		0.		0.		0.	
5.00- 4.00	1.040E-01		0.		0.		0.		0.		0.	
4.00- 3.00	3.214E-01		0.		0.		0.		0.		0.	
3.00- 2.60	1.467E-01		0.		0.		0.		0.		0.	
2.60- 2.20	4.293E-01		2.135E-02		0.		0.		0.		0.	
2.20- 1.80	7.691E-01		2.177E-01		0.		0.		0.		0.	
1.80- 1.35	1.037E+00		4.182E-01		1.145E-02		1.077E-03		0.		0.	
1.35- .90	1.337E+00		8.053E-01		1.701E-01		1.601E-02		0.		0.	
.90- .40	6.224E-01		4.182E-01		2.254E-01		1.988E-01		1.886E-01		0.	
.40- .10	4.743E-02		5.846E-02		1.071E-01		1.328E-01		1.303E-01		0.	
TOTAL ENERGY RELEASED	4.848E+00		1.939E+00		5.141E-01		3.487E-01		3.189E-01		0.	

7.0 REFERENCES

1. Radiation and Shielding Design Group, "Synthesis of Computational Methods for the Design and Analysis of Radiation Shields for Nuclear Rocket Systems", Volumes 1-9, WANL-PR(LL)-010, June 1967.
2. Radiation and Shielding Design Group, "Computer Code Symposium, Synthesis of Computational Methods for the Design and Analysis of Radiation Shields for Nuclear Rocket Systems", Volumes I-IX, WANL-PR(LL)-014, December 1967.
3. L. D. Stephenson, R. G. Soltesz, R. K. Disney, and S. L. Zeigler, "Synthesis of Computational Methods for the Design and Analysis of Radiation Shields for Nuclear Rocket System" - "Analysis of Measurements in a Nuclear Rocket Propellant Tank Mockup Using Simulated Liquid Hydrogen", WANL-PR(LL)-022, Volume II, September 1968.
4. R. G. Soltesz, R. K. Disney, et al, "Nuclear Rocket Shielding Methods, Modification, Updating, and Input Data Preparation", WANL-PR(LL)-034, August 1970.

Volume 1, "Synopsis of Methods and Results of Analysis".

Volume 2, "Compilation of Neutron and Photon Cross Section Data".

Volume 3, "Cross Section Generation and Data Processing Techniques".

Volume 4, "One-Dimensional, Discrete Ordinates Transport Technique".

Volume 5, "Two-Dimensional, Discrete Ordinates Transport Technique".

Volume 6, "Point Kernel Techniques".
5. Aerojet Nuclear Systems Company, "Final Report of Shield System Trade Study", S054-023, Volume 1, July 1970.
6. MacDonnell Douglas Company, "Nuclear Shuttle System Definition Study", Phase III, Final Report, MDC G 2134.
7. Radiation and Shielding Design Group, "Radiation and Shielding Analysis Report - Nuclear Subsystem", Volumes 1 and 2, WANL-TME-2757, February 1971.

8. E. A. Warman, "Full-Flow Flight-Engine Common Radiation-Analysis Model", RN-S-0551, March 1970.
9. W. W. Engle, Jr., "A User's Manual for ANISN", K-1693, March 1967.
10. K. D. Lathrop, "Ray Effects in Discrete Ordinates Equations", Nuclear Science and Engineering, Volume 32, 357-369, 1968.

APPENDIX A

CHEAPER CODE

A.1 COMPUTER CODE SYNOPSIS

1. Name: CHEAPER
2. Computer: The code is operational on the MSFC UNIVAC-1108 computer system and uses the MSFC SC 4020 plotting package.
3. Nature of Physical Problem Solved: CHEAPER performs several useful operations on DOT scalar flux tapes, such as linking two flux tapes, modifying the flux tapes so that they may be used as flux guesses in problems of differing geometry, adding two tapes together, etc. CHEAPER also calculates flux-response data as traverses internal to the geometry and plots these data on a SC 4020 plotter. Scalar flux and response data may also be calculated at discrete R, Z or R, θ points.
4. Restrictions on the Complexity of the Problem: The CHEAPER code uses complete flexible dimensioning to facilitate dynamic core storage allocation at job execution time. Because of the use of a flexible dimensioning technique for each array, no size restriction is imposed for a given array. The only restriction is that the size of the sum of all data array storage must be less than 31000_{10} for a field length of 57000_{10} . The required storage size for a given problem may be exactly computed as indicated in the documentation.
5. Typical Running Time: Most CHEAPER problems will run in less than 60 seconds of Central Processor Unit (CPU) time.
6. Unusual Features of the Code: The code employs variable dimensioning as described in Item 4 above.

7. Related or Auxiliary Codes: The current version of the CHEAPER code is used primarily for reducing output from or preparing input for the DOT-IIW⁽¹⁾ Discrete Ordinates Transport Code.
8. Status: The code is operational on the MSFC UNIVAC-1108 computer system.
9. References:
 1. WANL-PR(LL)-034, "Nuclear Rocket Shielding Methods, Modification, Updating, and Input Data Preparation, Two Dimensional Discrete Ordinates Transport Technique", Volume 4, August 1970.
 2. WANL-TME-1982, "User's Manual for the DOT-IIW Discrete Ordinates Transport Computer Code", R. G. Soltesz, R. K. Disney, and G. Collier, December 1969.
 3. Internal WANL Memorandum, "User's Instructions for the AICRTW and AICRT 4 (Revised) General Purpose Plotting Subroutines", R. K. Disney, and G. A. Long, December 23, 1970.
10. Machine Requirements: The source program requires 26000₁₀ core memory locations with additional core storage required for data. The current version requires an input disc, an output disc, a punch disc, a plot tape, two input data tapes and one output data tape.
11. Programming Language Used: The code is written in standard FORTRAN-IV with the exception of the plotting routines.
12. Operating System Under Which Program is Executed: The CHEAPER code is operational in the MSFC UNIVAC-1108 computer system.
13. Other Programming or Operating Information or Restrictions: CHEAPER uses the MSFC SC 4020 plotting package.

14. Name and Establishment of Authors:

A. H. Fero and R. K. Disney
 Westinghouse Astronuclear Laboratory
 Post Office Box 10864
 Pittsburgh, Pennsylvania 15236

A.2 INPUT DATA INSTRUCTIONS

A.2.1 Input Format

All input data for the CHEAPER code are entered in a fixed, FORTRAN format for each card. Integer data are entered in 12 fields per card where each field contains 6 columns. Integer data must be entered as right adjusted within each field. Floating point data are entered in 6 fields per card where each field contains 12 columns, and may be written with or without an exponent and with or without a decimal point.

A.2.2 Input Data Instructions

This section is to be used as a guide in preparing problem input data (Table A-1) for the CHEAPER code. Other sections present a more detailed description of the data presented here.

A.3 DETAILED INPUT DATA INSTRUCTIONS

A.3.1 Problem Size Determination

To determine the number of data locations required for a given problem (and therefore, the value required for the parameter, ISIZE on card 1 each of the expressions should be evaluated and summed.

$$x(1) = 3 * (IM + JM) + 4 * (INU + JNU) + 5 + \text{MAX} (IM, JM)$$

$$x(2) = (IM * JM) + 2 * ((\text{MAX} (IM, INU) * \text{MAX} (JM, JNU)))$$

$$x(3) = (IGM * \text{MAX} (IM, JM) * (NZ + NR)) + NZ + NR$$

$$x(4) = \text{NACT} * \text{MAX} (IM, JM) * \text{MAX} (NZ, NR)$$

$$x(5) = \text{NACT} * (IGM + 12)$$

$$x(6) = \text{NP} * (IGM + \text{NACT} + 2)$$

$$ISIZE = \sum_{I=1}^6 X(I)$$

A.3.2 Discussion of Calculation Options

DOT Scalar Flux Tape Linkage (IND = 0)

Two DOT scalar flux tapes having the same number of energy groups and having the same radial mesh may be combined in the axial direction to form one tape. For example, the following values input on card 6 would produce a flux tape with 50 radial mesh and 92 axial mesh.

JMR = 53	LPTR2 = 40
JMS = 52	LPTS1 = 1
LPTR1 = 1	LPTS2 = 52

The flux tape generated would contain the first 40 of 53 total axial mesh from tape 10 and all 52 axial mesh from tape 11. As the above example indicates any portion of the two tapes may be used to produce the final tape.

In addition the values input for IM, INU, JM, JNU, R, and Z must describe the final linked tape. In the above example, IM = INU = 50, JM = JNU = 92. The input values R and Z describe the mesh for the output tape.

Generate A DOT Flux Guess (IND = 1)

A good flux guess is an essential requirement for an eigenvalue solution to minimize computer time. The best flux guess is from a similar DOT calculation where the number of mesh and energy groups are the same. Even if minor perturbations in material composition or mesh spacing occur, these data constitute a very good flux guess.

If, however, the new DOT geometry differs in the number of mesh, two CHEAPER options are available to modify an existing DOT flux to conform to the desired mesh.

For the first option ($IND = 1$, $SCHEME = 1$), the user specifies the mesh line coordinates of the original or input flux solution as well as the mesh line coordinates defining the desired output mesh. CHEAPER then linearly interpolates or logarithmically extrapolates the input flux as necessary to obtain the flux for the desired output mesh.

The second option ($IND = 1$, $SCHEME = 2$) allows the user to specify the type of modification to be used for each mesh cell in the radial and axial directions. This is accomplished with the arrays IC and JC which are input in addition to the mesh coordinate data.

DOT Scalar Flux Tape Inversion ($IND = 2$)

When running a fixed boundary source, coupled geometry DOT calculation, one geometry may be inverted in the Z direction with respect to the other geometry.

To facilitate further flux processing, this CHEAPER option is often employed to generate flux tapes with the same axial orientation. Specifically, CHEAPER reads a DOT scalar flux tape and writes a tape with the row order inverted (i.e., row 1 becomes row JM, row 2 becomes row (JM-1), etc.). This option also punches an inverted Z vector on cards.

DOT Scalar Flux Tape Addition and Inversion ($IND = 3$)

This option is similar to option 2 except that it reads two DOT scalar flux tapes from identical geometries, adds the fluxes together, and then inverts the result as described above. This option also punches an inverted Z vector.

Traverse Flux Calculation ($IND = 4$)

Scalar fluxes for each energy group in the problem may be calculated as traverses at any radius or axial location internal to, or on the surfaces of, the DOT geometry. Axial traverse data are calculated for each axial mesh cell at a specified radius. Radial traverse data are calculated for each radial mesh cell at a specified Z. Traverses internal to the DOT geometry are calculated by linear interpolation of the scalar flux, with logarithmic extrapolation being used to obtain those traverses which are beyond the last mesh midpoint in the geometry. The traverse flux data are printed by setting $NPRIN1 = 1$.

Traverse Flux Calculation with Response Functions (IND = 5)

Groupwise traverse flux data are calculated as described above. These fluxes are multiplied by input response functions and then summed over the energy groups. The resultant traverse responses may be plotted by setting IPLOT = 1 and inputting the necessary title cards. As in the case above the traverse flux data are printed by setting NPRINT = 1.

Discrete Point Flux - Response Calculation (IND = 6)

Pointwise scalar flux data may be calculated at any arbitrary set of R, Z coordinates within, or on the surfaces of, the DOT geometry. These fluxes are multiplied by the input response functions and then summed over the energy groups.

The R, Z point coordinates may be input in two ways. First, the coordinate sets may be in metric units, relative to the DOT geometry origin (0, 0), with the following quantities also input; ICON = 0, and ZREF = 0.0. The alternative method of point coordinate input is in English units with the Z coordinate in terms of reactor station in inches. These point coordinate data will be converted to metric units as follows:

$$PR_m = 2.54 * PR_e$$

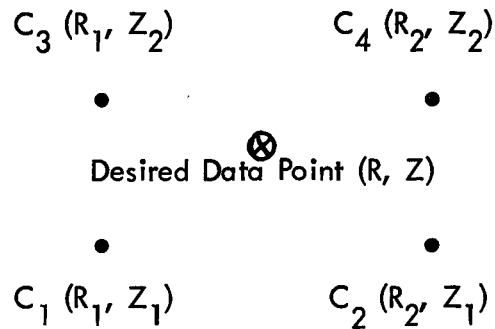
$$PZ_m = 2.54 * (ZREF - PZ_e)$$

where the subscripts m and e refer to metric and English units respectively.

ZREF = The distance, in inches, from reactor station zero to the DOT geometry origin.

If the point coordinate input is in English units, set ICON = 1.

The groupwise scalar flux at a discrete (R, Z) point is calculated in the following manner. For points internal to the flux geometry the flux will be calculated by interpolation of adjacent values.



- C_i = Calculated Scalar flux at center of DOT mesh cell
 R_i = Radial location of the center of DOT mesh cell
 Z_i = Axial location of the center of DOT mesh cell

First, the values C_1 and C_2 are interpolated radially to obtain a value at R, Z_1 . Second, the values C_3 and C_4 are interpolated radially to obtain a value at R, Z_2 . Finally, the two values just calculated are interpolated axially to obtain the flux at the R, Z point of interest. All interpolation is linear. If the desired R, Z data point lies beyond the DOT data in either radial, axial, or both directions, logarithmic extrapolation of the last two DOT scalar flux values replaces the linear interpolation of data in the above calculation.

The calculated pointwise response data are punched in the following order; all responses, point 1; all responses, point 2; etc. Each point begins a new card and the point number is punched in card columns 73 - 80.

DOT Scalar Flux Collapse (IND = 7)

CHEAPER is capable of collapsing the DOT scalar flux in the radial and/or axial direction. The collapsing of mesh cells is done in a manner to conserve mesh cell fluxes in the redefined mesh cells. This procedure is restricted to the deletion of mesh lines internal to the problem geometry. The user specifies in the general problem input data, the mesh line coordinates of the original or input flux solution, the radial mesh line coordinates of the collapsed mesh (only if the mesh is collapsed radially), the axial mesh line coordinates of the collapsed mesh (only if the mesh is collapsed axially), as well as the mesh cell coordinate identification numbers which will comprise the new (or redefined) mesh cell description (IC and JC arrays).

The average particle flux, ϕ_{l_i} , in each group in each new (redefined) radial mesh cell is computed as:

$$\phi_{l_i} = \frac{\sum_{i=i_s}^{i_f} \phi_{i_i} \cdot \Delta A_i}{\sum_{i=i_s}^{i_f} \Delta A_i}$$

where ϕ_{l_i} is the centered average flux in the redefined radial mesh cell, l , for each axial mesh cell, j . The quantities i_s and i_f are the input flux mesh cell coordinate indices which form the left and right boundaries of the new or redefined radial mesh cell, l . The quantity, ΔA_i is the cross sectional area, $\pi (R_{i+1}^2 - R_i^2)$, of the mesh cell, i . The computed average flux data, ϕ_{l_i} , is placed at the radial midpoint of the new mesh cell, $R_l = 1/2 (R_{i_s} + R_{i_f})$.

In a similar fashion, the average flux, ϕ_{l_j} , in each new axial mesh cell is obtained as:

$$\phi_{l_j} = \frac{\sum_{i=i_s}^{i_f} \phi_{l_i} \cdot \Delta Z_i}{\sum_{i=i_s}^{i_f} \Delta Z_i}$$

where ϕ_{l_j} is the centered average flux in each group in the redefined mesh cell, (l, j) and ϕ_{l_i} is the centered average flux previously computed in the redefined radial mesh cell, l , for each axial mesh cell, j . The quantities, i_s and i_f , are the input flux mesh cell coordinate indices which form the bottom and top boundaries of the new (or redefined) axial mesh cell

J. The quantity, ΔZ_j , is the height of each axial mesh cell, j . The computed average flux data, ϕ_{1j} , is placed at the axial midpoint of the redefined mesh cell, $Z_j = 1/2 (Z_{i_s} + Z_{i_f})$.

A.3.3 Other Useful Information

Input DOT Scalar Flux Tape

The flux tape is written in the binary mode and contains one logical record for each energy group. The first $IM * JM$ words in the record contain the scalar flux in the order (1, 1), (2, 1), . . ., (IM, 1), (1, 2), (2, 2), . . ., (IM, 2), . . ., (IM, JM). The remaining data on the flux tape is not read by CHEAPER.

DOT Geometry Type

The foregoing discussion of CHEAPER calculation options has referred to scalar fluxes resulting from R, Z geometry DOT calculations. It should be noted that all options are equally correct for R, θ geometry DOT calculations. One suggestion, however, is in order. If azimuthal traverses are to be plotted, the resulting plots would be more meaningful if the user converted the DOT 2* array from revolutions to either radians or degrees before inputting the data to CHEAPER (card 9).

Input Value of PNORM

PNORM is used in the following manner. CHEAPER takes the absolute value of the input scalar flux values and multiplies each by PNORM.

A.4 PROBLEM SETUP INFORMATION

A.4.1 Tape Assignments

A maximum of six magnetic tapes or disc devices are required in the current version of the CHEAPER code. The files required are as follows:

- Tape 5 Input Disc
- Tape 6 Printed Output Disc
- Tape 7 Punched Output Disc
- Tape 10 Input Magnetic Tape from DOT-IIW or CHEAPER
- Tape 11 Input Magnetic Tape from DOT-IIW or CHEAPER
- Tape 12 Output Magnetic Tape (Contains Calculated Scalar Fluxes in the DOT-IIW Format)

A.4.2 Running Time

Most CHEAPER problems will run in less than 60 seconds of Central Processor Unit (CPU) Time.

A.4.3 Core Storage Requirements

The CHEAPER program requires 26000₁₀ core locations. The user is referred to Section 3.1 for the number of locations required for problem data.

A.4.4 Error Messages

The following error messages or program stops may be encountered in running a CHEAPER problem.

<u>Message</u>	<u>Description or Explanation</u>
STOP 1	The number of data storage locations required by CHEAPER is greater than the input quantity ISIZE (refer to Section A.3).
STOP 2	IND = 1 and an incorrect value has been input for SCHEME.
STOP 3	R array not in ascending order, check card 7 input.
STOP 4	RNU array not in ascending order, check card 8 input.
STOP 5	Z array not in ascending order, check card 9 input.
STOP 6	ZNU array not in ascending order, check card 10 input.
STOP 7	Card 6 input is not consistent with the input quantity JM.
STOP 10	"One of the arrays is identically equal to zero, check X and Y." Either the X or f(x) array to be plotted contains all zeros, check <u>all</u> input.

A.5 DESCRIPTION OF OUTPUT

Computer output from a CHEAPER calculation consists of printed output and, depending on the options selected, punched output, SC 4020 hardcopy plots, and a binary tape.

A.5.1 Printout

The first part of the printed output is an edit of the input data. The following quantities are printed out.

1. The title card at the top of the page
2. The input quantities IND through FRAM with a brief description of each
3. If $IND = 0$, the input quantities JMR through LPTS2 and descriptions
4. The number of variable dimension data storage locations needed for the problem and the value input for ISIZE.
5. The radial interval data. These are printed in eight columns across the page.
 - a. The interval number
 - b. The input R array
 - c. The calculated interval midpoint
 - d. The calculated interval area
 - e. The input RNU array
 - f. The calculated interval midpoint
 - g. The calculated interval area
 - h. The input IC array
6. The axial interval data. These are printed in eight columns across the page.
 - a. The interval number
 - b. The input Z array
 - c. The calculated interval midpoint

- d. The calculated interval area
 - e. The input ZNU array
 - f. The calculated interval midpoint
 - g. The calculated interval area
 - h. The input JC array
7. IF IND = 4, 5, or 6 the traverse and point coordinate data are printed. These data include the radii at which the axial traverses are to be calculated, the Z's at which radial traverses are to be calculated, also, the point coordinates as input (R, Z).
 8. If ICON = 1 the converted point coordinates are printed
 9. If NACT is greater than zero, the input response functions are printed, followed by the titles input for each response.

The second part of the printed output consists of the results of the calculations performed.

1. If IND = 0, 1, 2, 3, or 7 the scalar flux calculated by CHEAPER, for the option selected, is printed. The flux is printed by mesh point and energy group.
2. If IND = 4 the descriptive titles for the traverses are printed.
3. If IND = 4 or 5 and NPRIN1 = 1 the scalar fluxes calculated on the desired traverses are printed by traverse, mesh point, and energy group.
4. If IND = 5 the calculated traverse - response data are printed, followed by the descriptive titles.
5. If IND = 6 and NPRIN2 = 1 the scalar fluxes calculated at each discrete point are printed by energy group and point.
6. If IND = 6 the pointwise response data are printed by point and activity.

A.5.2 Punched Output

The punched output is discussed in Section A.3.2.

A.5.3 Output Flux Tape

The scalar flux resulting from options 0, 1, 2, 3 and 7 is written on tape in the binary mode and contains one logical record per group. Each record contains INU* JNU words in the order (1, 1), (2, 1), . . ., (INU, 1), (1, 2), (2, 2), . . ., (INU, 2), . . ., (INU, JNU).

TABLE A-1

INPUT INSTRUCTIONS FOR THE CHEAPER CODE

<u>CARD NO.</u>	<u>FORMAT</u>	<u>CARD COLUMN</u>	<u>VARIABLE</u>	<u>DESCRIPTION</u>
1	I6	1-6	ISIZE	Maximum number of core locations available for CHEAPER data (ISIZE = 30500 for a field length of 150000 _g on the job card)
2	12A6	1-72	TITLE	Title card describing the overall CHEAPER problem
3	12I6	1-6	IND	Type of calculation to be performed: IND = 0 Link two DOT scalar flux tapes axially. Card 6 is required input. Input IR1 and IR2 as 0. IND = 1 Modify an existing DOT scalar flux tape to use as a flux guess for DOT. The method of modification is determined by SCHEME. IND = 2 Invert the row order of the input DOT scalar flux tape. IND = 3 Add two DOT scalar flux tapes together and invert the row order of the result. IND = 4 Calculate the scalar flux on selected axial and/or radial traverses. IND = 5 Calculate the traverse flux as in option 4 and multiply the traverse fluxes by input response functions. IND = 6 Calculate the scalar flux at discrete R-Z points and multiply the calculated fluxes by input response functions.

TABLE A-1 (CONT)

<u>CARD NO.</u>	<u>FORMAT</u>	<u>CARD COLUMN</u>	<u>VARIABLE</u>	<u>DESCRIPTION</u>
			IND = 7	Collapse the input DOT scalar fluxes radially and/or axially.
7-12			SCHEME	Method of flux shape modification
			SCHEME = 1	The modified flux is calculated by interpolating and/or extrapolating the input flux to the desired mesh.
			SCHEME = 2	Modification is controlled by the input quantities IC and JC.
			IF IND \neq 1, SCHEME = 0	
13-18			IR1	Read new radial mesh line coordinates
			IR1 = 0	No.
			IR1 = 1	Yes; Card 8 required input
			IF IND = 0, 4, 5, or 6; IR1 = 0.	
19-24			IR2	Read new axial mesh line coordinates
			IR2 = 0	No.
			IR2 = 1	Yes. Card 10 required input.
			IF IND = 0, 4, 5, or 6; IR2 = 0.	
25-30			NZ	Number of axial traverses to be calculated.
31-36			NR	Number of radial traverses to be calculated.
37-42			NP	Number of discrete points at which flux and response data are to be calculated.
			IF IND \neq 6, NP = 0.	

TABLE A-1 (CONT)

<u>CARD NO.</u>	<u>FORMAT</u>	<u>CARD COLUMN</u>	<u>VARIABLE</u>	<u>DESCRIPTION</u>
		43-48	NACT	Number of sets of response functions to be read. If IND = 5 or 6; NACT must be at least 1.
		49-54	IPLØT	Plot traverse responses IPLØT = 0 No. IPLØT = 1 Yes.
		55-60	NPRIN1	Print the calculated traverse fluxes NPRIN1 = 0 No. NPRIN1 = 1 Yes. If IND = 4; NPRIN1 must = 1.
		61-66	NPRIN2	Print the calculated point fluxes NPRIN2 = 0 No. NPRIN2 = 1 Yes.
		67-72	ICØN	Units for input point coordinates ICØN = 0 The point coordinates are in metric units relative to the DOT geometry origin (0, 0). ICØN = 1 The point coordinates are in English units, radius in inches and Z in reactor station in inches. The radius will be converted to centimeters and the Z will be converted to centimeters in the DOT geometry coordinate system relative to the input quantity ZREF.
4	516	1-6	IM	If IND ≠ 6, ICØN = 0 Number of radial mesh intervals in the input DOT scalar flux.

TABLE A-1 (CONT)

<u>CARD NO.</u>	<u>FORMAT</u>	<u>CARD COLUMN</u>	<u>VARIABLE</u>	<u>DESCRIPTION</u>
		7-12	INU	Number of radial mesh intervals in the desired output scalar flux.
		13-18	JM	If IND = 0, or 2 thru 6; input INU = IM. Number of axial mesh intervals in the input DOT scalar flux.
		19-24	JNU	If IND = 0, input JM as the total number of axial mesh intervals in the final linked output tape. Number of axial mesh intervals in the desired output scalar flux.
		25-30	IGM	If IND = 0, or 2 thru 6; input JNU = JM. Number of energy groups in problem.
5	3 E 12.5	1-12	PNØRM	Flux normalization factor, PNØRM usually = 1.0.
		13-24	ZREF	Reference Plane distance, in inches, from DOT geometry origin (Z = 0.0 cm) If ICØN = 0; ZREF = 0.0
		25-36	FRAM	If ICØN = 1; ZREF is input as the distance from the DOT geometry origin to reactor station 0.0 inches. Not required input.

TABLE A-1 (CONT)

<u>CARD NO.</u>	<u>FORMAT</u>	<u>CARD COLUMN</u>	<u>VARIABLE</u>	<u>DESCRIPTION</u>
Card 6 is input only if IND = 0				
6	6I6	1-6	JMR	Number of axial mesh for tape 10 input.
		7-12	JMS	Number of axial mesh for tape 11 input.
		13-18	LPTR1	First axial mesh cell to be used from tape 10.
		19-24	LPTR2	Last axial mesh cell to be used from tape 10.
		25-30	LPTS1	First axial mesh cell to be used from tape 11.
		31-36	LPTS2	Last axial mesh cell to be used from tape 11.
7	6 E 12.5	1-12, 13-24, Etc.	R	Radial mesh line coordinates for the input DOT scalar flux (IM + 1 entries required)
Card 8 is input only if IR1 = 1				
8	6 E 12.5	1-12, 13-24, etc.	RNU	Radial mesh line coordinates for the desired scalar flux output (INU + 1 entries required)
9	6 E 12.5	1-12, 13-24, etc.	Z	Axial mesh line coordinates for the input DOT scalar flux (JM + 1 entries required)
Card 10 is input only if IR2 = 1				
10	6 E 12.5	1-12, 13-24, etc.	ZNU	Axial mesh line coordinates for the desired scalar flux output (JNU + 1 entries required)
Card 11 is input only if SCHEME = 2 and IR1 = 1.				
11	12I6	1-6, 7-12, etc.	IC	Method of radial flux modification IC(1) = 0 Interpolate/extrapolate the input scalar flux to obtain the output flux for the I th radial mesh cell.

TABLE A-1 (CONT)

<u>CARD NO.</u>	<u>FORMAT</u>	<u>CARD COLUMN</u>	<u>VARIABLE</u>	<u>DESCRIPTION</u>
				$IC(I) = N$ Use the input scalar flux, mesh cell N, for the I th radial mesh cell. (INU entries required)
				Method of axial flux modification
12	1216	1-6, 7-12, etc.	JC	$JC(J) = 0$ Interpolate/extrapolate the input scalar flux to obtain the output scalar flux for the J th axial mesh cell. $JC(J) = N$ Use the input scalar flux, mesh cell N, for the J th axial mesh cell. (JNU entries required)
				Card 12 is input only if SCHEME = 2 and IR2 = 1.
13	1216	1-6, 7-12, etc.	IC	Mesh line number of the right radial mesh line of each collapsed mesh cell (e.g., if no mesh collapsing is required, $IC = 2, 3, 4, 5, \dots (IM + 1)$; or, if a reduction of two mesh cells must be made, $IC = 2, 5, \dots (IM + 1)$, where 3 and 4 are removed. (INU entries required)
				Cards 13 and 14 are input only if IND = 7.
14	1216	1-6, 7-12, etc.	JC	Mesh line number of the top axial mesh line of each collapsed mesh cell. The discussion of IC is applicable to JC. (JNU entries required)
				Card 15 is input only if NZ > 0

TABLE A-1 (CONT)

CARD NO.	FORMAT	CARD COLUMN	VARIABLE	DESCRIPTION
15	6 E 12.5	1-12, 13-24, etc.	RTR	Radii at which axial traverses are to be calculated (NZ entries required)
Card 16 is input only if NR > 0				
16	6 E 12.5	1-12, 13-24, etc.	ZTR	Z' s at which radial traverses are to be calculated (NR entries required)
Card 17 is input only if NP > 0				
17	3(2 E 12.5)	1-12	PR	Radial coordinate of first discrete point at which the scalar flux is to be calculated.
		13-24	PZ	Axial coordinate of first discrete point at which the scalar flux is to be calculated.
(NP sets of point coordinates are required, entered three points per card)				
Cards 18 and 19 are input only if IND = 5 or 6.				
18	12A6	1-72	ACTTIT	Title for response function
19	6 E 12.5	1-12, 13-24, etc.	ACT	Response function (IGM entries required).
Cards 18 and 19 are repeated NACT times.				
The following cards are input only if IND = 4 or 5.				
20	7A10	1-70	PTITLE	Traverse description (appears as plot title)
21	5A10	1-50	XTITLE	X axis title
22	5A10	1-50	YTITLE	Y axis title

TABLE A-1 (CONT)

<u>CARD NO.</u>	<u>FORMAT</u>	<u>CARD COLUMN</u>	<u>VARIABLE</u>	<u>DESCRIPTION</u>
NOTE:				If IND = 4, input card 20 (NZ + NR) times, and omit cards 21 and 22. The order for the titles is: All axial traverses followed by all radial traverses.
				If IND = 5 and IPLOT = 0, input card 20 (NZ + NR) times, and omit cards 21 and 22. The order for the titles is: all axial traverses followed by all radial traverses.
				If IND = 5 and IPLOT = 1, input cards 20, 21, and 22 (NZ * NACT) + (NR * NACT) times. The order for the titles is: all axial traverses, response 1; all axial traverses, response 2; etc. The radial traverse titles follow in the same order.

APPENDIX B

LHAP CODE

B.1 COMPUTER CODE SYNOPSIS

1. Name: LHAP
2. Computer: The code is operational on the MSFC UNIVAC-1108 computer system under the EXEC 8 monitor system.
3. Nature of Physical Problem Solved: LHAP calculates the energy dependent gamma ray dose rate due to neutron captures in a complex geometry. The neutron radiation source is represented as an anisotropic point source (i.e., neutron flux levels as a function of polar angle on a meridian ring). The neutron capture events occur at the point of incidence of rays emanating from the point source on specified zones in the complex geometry. The uncollided flux, flux with buildup applied, and dose rate (Rads (carbon)/hr) are computed as a function of emanating ray angle, capture zone, and zone material. Geometry is describable by zone bounded by intersecting quadratic surfaces with a maximum of six boundary surfaces per zone.

No attenuation function is applied for the primary neutrons and the capture gamma ray attenuation function is an exponential function with a buildup factor approximation to account for multiple scatter between the capture site and the detector point.

4. Method of Solution: A point kernel method using an anisotropic point source representation is used. Inverse square spatial attenuation between the neutron source point and capture site is employed. Line-of-sight material attenuation and inverse square spatial attenuation between the capture source point and detector point is employed.

5. **Restrictions on the Complexity of the Problem:** The LHAP code is written in complete flexible dimensioning so that no restrictions are imposed on the number of energy groups, number of geometric zones, or point source representation. The complex geometry capability is limited to zones defined by a maximum of six boundary surfaces with each surface defined by a general quadratic equation or one of its degenerate forms. The only restriction in the code is that the total number of data entries must be less than the dimension of blank COMMON.
6. **Typical Running Time:** The LHAP code calculates approximately 50 neutron source point-capture source point-to detector point calculations per second on the UNIVAC-1108 computer. The running time is essentially independent of energy groups and is only dependent upon the complexity of the geometry calculation.
7. **Unusual Features of the Code:** The use of a method of determining the neutron capture site at the entry point into an absorbing zone of a complex geometry provides a flexible technique in evaluating the effect of the absorbing zone shape and position on the neutron capture gamma dose rates. The assumption that neutrons are absorbed at the entry point is generally a limitation but in the case of liquid hydrogen propellant tanks this is a reasonable approximation.
8. **Related or Auxiliary Codes:** Gamma absorption coefficients may be supplied by magnetic tape from the GAMLEG-W code. Neutron flux distributions at a meridian ring for use as an anisotropic energy dependent source can be supplied on punched cards from the KAP-VI⁽¹⁾ or MAP⁽³⁾ codes. The code is very similar to the SCAP⁽¹⁾ code.
9. **Status:** The code is in production use at the Marshall Space Flight Center (MSFC).

10. References:

1. R. K. Disney and S. L. Zeigler, WANL-PR(LL)-034, Volume 6, "Point Kernel Techniques", August 1970.
2. R. G. Soltesz, R. K. Disney and S. L. Zeigler, WANL-PR(LL)-034, Volume 3, "Cross Section Generation and Data Processing Techniques", August 1970.
3. R. G. Soltesz, R. K. Disney, S. L. Zeigler, and J. Jedruch, WANL-PR(LL)-034, Volume 5, "Two Dimensional Discrete Ordinates Transport Techniques", August 1970.

B.2 INPUT DATA DESCRIPTION

B.2.1 Input Format

The input data for the LHAP code are divided into the following three data sets:

1. Overall problem storage allocation
2. Overall problem title and parameters
3. Problem geometry, source, and detector data.

The first data set is entered on a single formatted card which is the first physical card of each problem deck. The second data set consists of the title card and five cards of integer and real data on formatted cards in data fields of 12 columns each. This set of data is always required as input to a LHAP problem and all input data must be entered in the correct field of each card since a fixed FORTRAN format is used to read all cards.

The remaining data set 3 of a LHAP problem input is input to one of three possible FORTRAN type formats. The integer data arrays (denoted by a dollar sign) must

always be input in the standard LHAP (FIDO)* format capability of six fields of 12 columns in each field. Each field in the standard format is subdivided into three subfields as shown in Figure B-1. Integer data must be entered as right adjusted** in the third subfield of each data field. Real data may be entered in the standard LHAP or one of two non-standard format capabilities.

The non-standard input formats which are shown in Figure B-1 are included for user convenience and can only be used for any real (floating point) data array. These non-standard formats cannot include any operation type (fill, skip, interpolate, repeat, etc.), but can include blank fields on a card that cause the input routine to ignore the rest of the card; i.e., if a data array should include 117 entries, the punched card input for the array would be 19 full cards (6 values/card) and a final card of three entries using the U format. LHAP, using this non-standard capability, would skip the last three fields of the last card and commence reading at the first data field of the next card.

In the standard LHAP format, the second subfield may include one of the data type or operation type code letters.

The following characters may be entered: &, *, U, V, R, I, T, S, F, A, +, -, Z, E, Q, N, M, W, X, or H.

\$ indicates the beginning of an integer (fixed point) array. The first subfield identifies the array.

* indicates the beginning of a real (floating point) array. The first subfield identifies the array.

*FIDO is a generalized input routine capable of performing operations to prepare data arrays. This routine is standardized through the DOT-IIW, ANISN-W, and MAP codes.

**"right adjusted" means that the least significant digit of an integer number is at the extreme right of the field.

- U indicates the beginning of a real (floating point) array in the non-standard format 6E12.5 and the data array beginning on the next physical card. The first subfield identifies the array.
- V indicates the beginning of a real (floating point) array in the non-standard format 4 (1X, E16.9, 1X). The first subfield identifies the array beginning on the next physical card.
- R indicates that the data contained in the third subfield are to be entered R times in succession. The first subfield defines the number of total successive entries or Repeats (i.e., a 16R 1.0 enters 16 1.0's).
- I indicates Interpolation between the data in the associated third subfield and the following third subfield. The first subfield defines the number of interpolations between the two data entries (i.e., 4I 0.0, 10.0 enters 0.0, 2.0, 4.0, 6.0, 8.0, 10.0).
- T indicates Termination of data reading for a particular subset of data. No further data reading for a subset of data is attempted and the program proceeds to the next subset and the next physical data card.
- S indicates Skip. The first subfield defines the number of entries to be skipped. The third subfield may contain the first entry following skips (i.e., 15S 1 enters a 1 in the 16th word of an array).
- F indicates that the remainder of the present array is to be Filled with the data entry in the third subfield. Any entry in the first subfield is ignored (i.e., F 1.0 will enter a 1.0 for all entries in an array).
- A indicates Address modification. The next non-blank data entry is entered in the Nth location of the present array where N is an integer entry in the third subfield associated with the A. Any entry in the first subfield is ignored.

- + or - indicates exponentiation. The data entry in the third subfield is multiplied by 10^{+N} where N is the entry in the first subfield. This option allows more significant digits if necessary.
- Z indicates the entry of Zeros. The integer entry in the first plus the third subfield indicates the number of successive zeros to be entered, (e.g., 10Z enters 10 zeros, Z 20 enters twenty zeros, and 10Z 20 enters 30 zeros).
- E indicates End array. This option skips to the end of an array without the need for specifying the number of skips.
- Q indicates sequence repeat. The integer entry in the first plus the third subfield indicates the number of previous entries to be repeated.
- N indicates inverted sequence repeat. This option is similar to the Q option except that the previous entries are repeated in reverse order (e.g., 0, 2, 4, 2N enters 0, 2, 4, 4, 2).
- M indicates inverted sequence repeat except that the signs of previous entries are reverse when they are repeated.
- W indicates the array identified by the first subfield will be read according to the format on the following card.
- X indicates the array identified by the first subfield will be read according to the last variable format read in. For example,

3W
(7E 10.3)
3X

Card 1 (remainder of card must be blank)
 Card 2 (contains format only)
 Card 3 (remainder of card must be blank)
 Card 4 through N (contain the data according to the specified format. No blank fields are allowed).

- H indicates the beginning of an alphanumeric descriptive title card array. Each card input in this manner is a separate 72 column title card.

The following restrictions must be observed when writing input data for
LHAP:

1. Floating point zeros must be written as 0. or 0.0; a.0 or -.0 in either the standard or non-standard format is not acceptable.
2. Blanks are ignored and the reading of data commences on the next physical card for the non-standard format and on the next field after the blank field for the standard formats.
3. If an I is specified in any data field, the third subfield of that field and the following third subfield of the next field cannot be blank. In addition, the second subfield of the field following a field containing an I cannot contain an A.
4. If the third subfield of a data field containing a \$ or a * contains an integer, N, the next data entry is assumed to be the (N + 1) th member of the array. Normally this third subfield is blank and is interpreted as zero.

Integer data in the third subfield must be right adjusted. Floating point data may be written with or without an exponent and with or without a decimal point. If the decimal point is not included, it is assumed to be at the extreme right of the nine column subfield.

B.2.2 Input Data Instructions

Table B-1 is to be used as a guide in preparing problem input data for the LHAP code. Other sections present a more detailed description of the data presented here. The quantity in slashes represents the array dimension, or the number of pieces of data required, and the expression in brackets is the condition requiring that array or set of arrays. Arrays or sets of arrays with the corresponding terminate (T) card which are not required should not be entered. If no condition is specified, the array is required. Note that a T card must follow the data entered in data set 3 and no T card is entered after data sets 1 and 2.

B.3 DETAILED INPUT DATA INFORMATION

The input data requirements for the LHAP code are very similar to the SCAP code described in Volume 6, WANL-PR(LL)-034. The input of geometry data is identical to the SCAP input as described in Section 3.3.1 of the SCAP user's manual and the only difference in input is the designation of an absorbing zone and the input of the neutron capture data as described in Table B-1.

B.4 PROBLEM SETUP INFORMATION

The setup of a LHAP code problem is described in this section. This section is intended to define the setup of a LHAP problem on the MSFC UNIVAC-1108 computer system. The MSFC version of the LHAP code resides on a production tape and is used by loading the code from tape with control cards preceding the input deck. The use of tape or disk files, running time, and error messages are described in the following sections.

B.4.1 Tape Assignments

The LHAP code requires a maximum of four magnetic tape or disk files for a specific problem. For a majority of problems only three files are required. The file assignments are as follows:

Tape 5	Input Disk
Tape 6	Output Disk
Tape 7	Punched Output Disk
Tape 11	Cross Section Library Input Tape / Required only if NL = 1/

The Tape 11 input tape is the tape produced by GAMLEG-W and contains the pair production and photoelectric pointwise cross section data for elements in the element/composition table specified as LHAP input.

B.4.2 Running Time

The required running time for a given LHAP problem on the MSFC UNIVAC-1108 computer is mainly dependent upon the number of source points and the number of capture points in the geometric zones. The estimate of the required CPU time is obtained by estimating the total number of source point-to-capture point-to-detector point calculations for each source point. The number of capture points in a geometric model is calculated internally based on the incidence of source rays on the absorber. The code performs approximately 50 capture point calculations per second in a geometry model.

The total running time for a LHAP problem is estimated as:

$$t(\text{CPU seconds}) = \frac{(NT + 1) * NR}{50}$$

where:

NT is the number (or order) of the azimuthal angle integration

NR is the number of polar angle source rays

B.4.3 Error Messages

A number of LHAP code generated error messages may be encountered in running a LHAP problem. These messages are primarily due to the incorrect problem input. The error messages are generally self-explanatory.

<u>Message</u>	<u>Explanation</u>
Data storage requirements and limits . . . x, y.	If $x > y$, the code terminates. This implies the problem is too large for available core storage or input value LIMIT is incorrect.
Geometry error - zone . . ., bnd . . . bnd number . . . equation number , coordinates $x = . . .$, $y = . . .$, $z = . . .$	A boundary equation number $NBE \leq 0$ or $NBE > 9$. Check NBZ, and NBD arrays for consistency.

<u>Message</u>	<u>Explanation</u>
Geometry error - zone . . . , boundary . . . , distance . . . , coordinates (x, y, z)	A boundary crossing on the line-of-sight cannot be found. Check location of the source point and detector point with relation to geometry description.
"Error, N entries required in (3*, for example) array, data edit continues"	Too many or too few pieces of data were input to the specified array.
"Warning, Interpolation used in the (9\$, for example) integer array, data edit continues"	The code is warning the user that integer interpolation, which involves computer integer arithmetic is being used. Computers, in performing integer arithmetic, drop any fractional remainder.
"Fill option ignored in (9\$, for example) array"	The code already has all the data it needs for the specified array.
"Warning, Address . . . is beyond the limits of (9\$, for example) array"	The user, in inputting data with the A format, has exceeded the storage area set aside for the specified array.

B.5 METHOD OF SOLUTION

The LHAP code is very similar to the SCAP code described in Volume 6, WANL-PR(LL)-034. The geometry calculation in LHAP is identical to SCAP and the only difference is the calculation of the neutron capture source in LHAP as compared to the scatter source in SCAP. The neutron capture source in LHAP is similar to the albedo source in SCAP except that an isotropic emission of photon energy is assumed at the neutron capture site. The reader is referred to the SCAP user's manual for a detailed description of the method of solution.

TABLE B-1
INPUT DATA INSTRUCTIONS FOR LHAP CODE

Data Set 1 - Overall Problem Data Storage Allocation

<u>Card No.</u>	<u>FORTTRAN Format</u>	<u>Card Column</u>	<u>Variable Name</u>	<u>Description</u>
1	6X, 16	7 - 12	LIM1	The number of locations available for core data storage. LIM1 = 4000 for a field length of 75,000g

Data Set 2 - Overall Problem Title and Parameters

1	12A6	1 - 72	TITLE	Descriptive title for problem
2	6112	-	-	Integer data
		1 - 12	NG	No. of energy groups of secondary gamma data in final results
		12 - 24	NS	Number of energy groups in neutron flux input data
		25 - 36	NA	Number of polar angles in source input data. If NA is negative, KAP input by energy and angle. If NA is positive, MAP input by angle and energy. NOTE: If data from previous case in stack is to be used, NA must be positive.
		37 - 48	NC	Number of energy points in gamma ray absorption cross section data
		49 - 60	NE	Number of elements in the zone composition-element table.
		61 - 72	NM	Number of compositions in the zone composition-element table.

TABLE B-1 (CONT)

<u>Card No.</u>	<u>FORTRAN Format</u>	<u>Card Column</u>	<u>Variable Name</u>	<u>Description</u>
3	6112	1 - 12	NZ	Number of zones in problem
		13 - 24	NB	Number of boundary surfaces in problem
		25 - 36	NR	Number of initial source rays emanating in equal polar angle from neutron pseudo-source point.
		37 - 48	NT	Order of azimuthal integration (trapezoidal) for neutron pseudo-source point If NT = 1, the 2π symmetry condition for an on-axis source point and detector point is applied
		49 - 60	NSZO	Most probable zone which contains the neutron pseudo-source point
		61 - 72	NL	Library option 1 - use GAMLEG library data tape on unit 11 to generate absorption (photo-electric plus pair production) cross section data 0 - enter cross section data SIG(27*) and ZOM(26*) as input data
4	6E12.5	1 - 12	TH1	Lower limit of polar angle at which source rays originate
		13 - 24	TH2	Upper limit in polar angle at which source rays originate
		25 - 36	TT1	Lower limit of azimuthal angle integration
		37 - 48	TT2	Upper limit of azimuthal angle integration. NOTE: TT1, TT2 can be used to assign symmetry in the scatter calculation.

TABLE B-1 (CONT)

<u>Card No.</u>	<u>FORTRAN Format</u>	<u>Card Column</u>	<u>Variable Name</u>	<u>Description</u>
5	6E12.5	1 - 12	RM	Radius of meridian ring at which source data is defined
		13 - 24	DED	Electron path length (electrons/cm ² x 10 ⁻²⁴) per scatter point used to determine position of scatter points. Not required for LHAP input
		25 - 36	RP	Radius of pseudo-sphere which contains <u>all</u> scatter points in the problem
		37 - 48	TFR	Total flux to Fast Flux ratio to be applied to all flux calculations at each polar angle.

Data Set 3 - Problem Geometry, Source and Detector Data

<u>Data Array No.</u>	<u>Format Symbol</u>	<u>Card Columns</u>	<u>Variable Name</u>	<u>Description</u>
1	\$	6112	NBZ	Number of boundaries per zone. (If NBZ is negative, then the zone is an outside zone and no further geometry calculations beyond this zone to the detector are performed.)
2	\$	6112	NBD	Boundary numbers for each surface of a zone, 6 numbers per zone must be entered (one card per zone with boundaries not used specified as 0 (6 x NZ numbers). (Ambiguity indices for boundaries of zones <u>must</u> be assigned by user as + or - the boundary number.

TABLE B-1 (CONT)

<u>Data Array No.</u>	<u>Format Symbol</u>	<u>Card Columns</u>	<u>Variable Name</u>	<u>Description</u>
2 (Cont)				Ambiguity indices are assigned as negative for boundaries which are in a negative X direction in relation to the origin in relation to the ray leaving the zone and crossing the boundary or a negative Z direction to the ray leaving the zone and crossing the boundary.
3	\$	6112	NTR	Zone numbers entered upon crossing each boundary of a zone, 6 numbers per zone (one card per zone) correspond to the NBD numbers with numbers not used specified as 0 (6 x NZ numbers).
4	\$	6112	NBE	Equation number for each boundary surface. Boundary equations defined in Table B-2.
5	* or U		XO	Coefficients for boundary surface equations
6	* or U		YO	Coefficients for boundary surface equations
7	* or U		ZO	Coefficients for boundary surface equations
8	* or U		AO	Coefficients for boundary surface equations
9	* or U		BO	Coefficients for boundary surface equations
10	* or U		CO	Coefficients for boundary surface equations
11	* or U		DO	Coefficients for boundary surface equations
12	* or U		ENC	Energy values for cross section data (NC values)
13	* or U		ZOE	Electrons/atom for each element in composition table. (NE values)

TABLE B-1 (CONT)

<u>Data Array No.</u>	<u>Format Symbol</u>	<u>Card Columns</u>	<u>Variable Name</u>	<u>Description</u>
14	* or U		COM	Density (gm/cm^3) for each element in each composition by element and composition. (NE X NM values)
15	\$		NMZ	Number of composition in each zone. (NZ values). If NMZ for a zone is negative, then this composition is an absorber.
16	* or U		ENS	Energy values of meridian ring source data (NS values)
17	* or U		ENG	Energy values for capture gamma ray (NG values)
18	* or U		ANS	Polar angle of meridian ring data (NA values)
19	* or U		SOS	Source data by angle and group (NAXNS or NSXNA values)
20	* or U		XP	Pseudo-source point coordinates (X_p, Y_p, Z_p)
21	* or U		XD	Detector point coordinates (X_d, Y_d, Z_d)
NOTE: ZOM and SIG are required only if NL = 0				
26	* or U		ZOM	Electrons/ cm^3 for each composition by zone (NM values)
27	* or U		SIG	Gamma absorption cross section (σ_{pp} plus σ_{pe}) by group energy ENC and composition (NC x NM values)

TABLE B-1 (CONT)

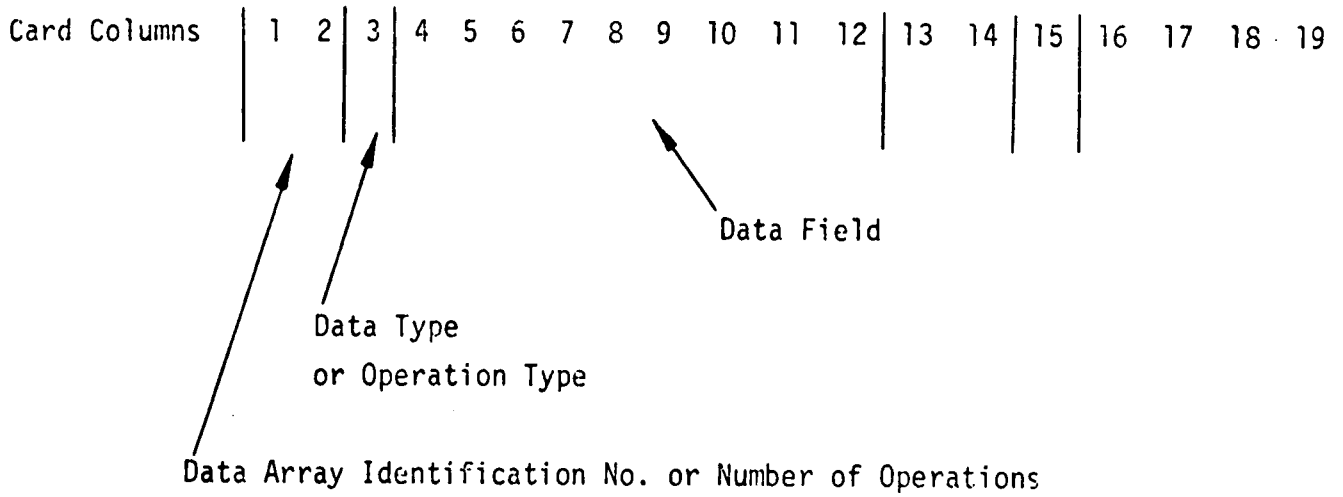
<u>Data Array No.</u>	<u>Format Symbol</u>	<u>Card Columns</u>	<u>Variable Name</u>	<u>Description</u>
28	* or U		ALB	Relative capture rate in capture zone per incident neutron as a function of polar angle and neutron energy group (NAXNS values)
29	* or U		ENP	Relative gamma energy release for each gamma group. $ENP \times ENG = \text{Mev/capture}$ (NG values)
T		3	-	Terminate card to end data reading

TABLE B-2
LHAP BOUNDARY EQUATION NUMBERS AND EQUATIONS

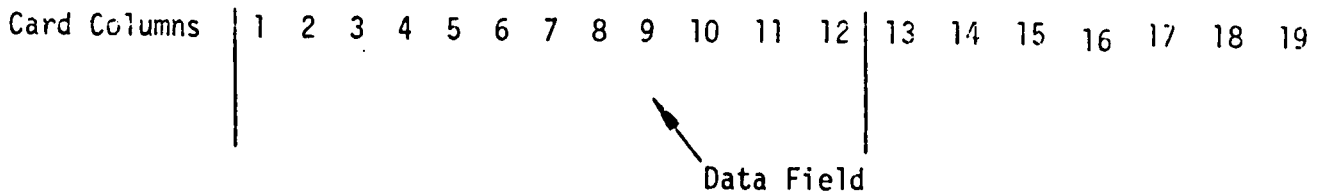
<u>Boundary Equation Number</u>	<u>Equation</u>
1	$AX^2 + XX_0 + BY^2 + YY_0 + CZ^2 + ZZ_0 = D_0$
2	$A(X-X_0)^2 + B(Y-Y_0)^2 + C(Z-Z_0)^2 = D_0$
3	$(X-X_0)^2 + (Y-Y_0)^2 = D_0$
4	$X = D_0$
5	$Y = D_0$
6	$Z = D_0$
7	$AX^2 + XX_0 + BY^2 + YY_0 + CZ^2 + ZZ_0 = D_0^2$
8	$A(X-X_0)^2 + B(Y-Y_0)^2 + C(Z-Z_0)^2 = D_0^2$
9	$(X-X_0)^2 + (Y-Y_0)^2 = D_0^2$

Input A, B, C, D, X₀, Y₀, Z₀, D₀ where required.

1. Standard: (6 (I2, A1, F9.0))



2. Non-Standard: (6E12.5), U Data Type



3. Non-Standard: (4(1X, E16.9, 1X)), V Data type or ODDK (FLOCOW)

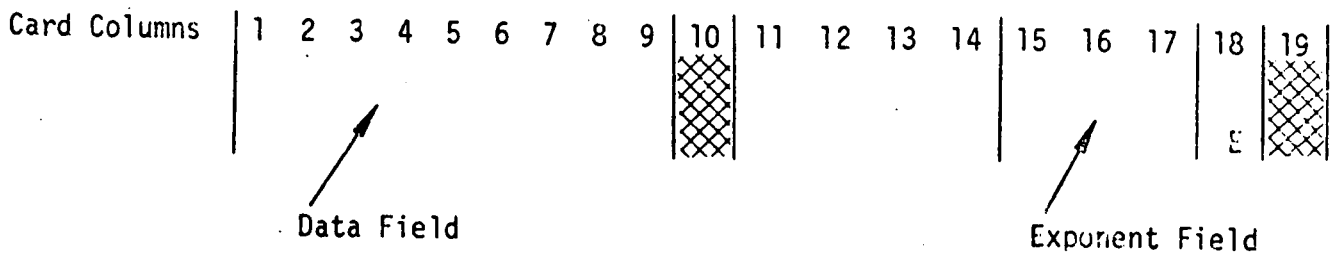


Figure B-1. LHAP Input Formats